Synthesis of Tetramic Acids and Investigation of their Biological Properties

Zur Erlangung des akademischen Grades eines
Doktors der Naturwissenschaften
vom Fachbereich Chemie der
Universität Dortmund
angenommen

DISSERTATION

von
Diplom-Chemikerin
Catherine P. Katzka
aus Mountain View (Kalifornien)

Eidesstattliche Erklärung

Hiermit erkläre ich an Eides Statt, dass ich diese Arbeit selbständig und nur mit den angegebenen Hilfsmitteln angefertigt habe.

Dortmund, Mai 2006

_____

To my family

_____

_____

Table of Contents

_____

_____

_____

_____

1   Preface

When Paul Ehrlich discovered that methylene blue selectively stains neuronal cells, he revealed that small molecules have specific biological targets.[1] Since then, small molecules have become an increasingly important tool for studying biological systems. The use of such chemical probes instead of genetic alterations to establish a link between gene-products and their functions is called chemical genetics. Chemical genetics relies on a collection of compounds that are able to modulate different proteins. Natural products are known to bind to proteins and may therefore serve as a fruitful source of inspiration for the synthesis of compound collections.

The tetramic acid natural product family is based on the 2,4-pyrrolidinedione core **1** (*Figure 1*) and is documented to affect a wide variety of biological targets.[2] The tetramic acid core is therefore an interesting scaffold for the design of a library of chemical probes to be used in chemical genetics.

1
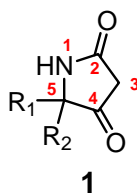
Figure 1: Structure of the 2,4-pyrrolidinedione (tetramic acid) **1** *scaffold.*

The aim of this dissertation was to synthesize a library of compounds based on the tetramic acid scaffold and use them to probe cellular and biochemical systems.

In the first part of this dissertation, the concepts of chemical genetics will be introduced and background will be provided to the tetramic acids as a natural product family. The goals of the thesis will then be laid out. Finally, the results of the synthetic and biological work will be presented and discussed.

_____

_____

# 2   Introduction

2.1   Linking Genes to Function

In 2004, the sequencing of the human genome was completed.[3] There were high hopes that this would accelerate the understanding of complex biological systems, thereby aiding in developing novel therapies for diseases. Alone though, the genetic information from the genome sequence is not enough to comprehend intricate biological mechanisms: the link between genes and their functions needs to be established. Modern genetic methods have made it possible to rapidly identify genes and their mutant alleles by simple database operations. Gene cloning and knockout techniques allow the overexpression or silencing of proteins in lower organisms such as fruit flies (*Drosophila melanogaster*), zebra fish (*Danio rerio*) and mice (*Mus musculus*) to produce observable phenotypical effects. Complementarily, human cell-based models can also be engineered using molecular biological methods. Although developments in genetics have advanced the understanding of biological processes, there are still some limitations: the study of essential genes is prevented because organisms with mutations in such genes are not viable. Furthermore, genetic approaches are not well suited to studying dynamical cell biological processes that occur on a time scale of minutes or seconds. A small molecule approach can complement gene-based methods.

2.1.1   Chemical Genetics

An alternative method to linking genes and proteins to their function and phenotypes is termed chemical genetics, and uses small molecules to perturb protein networks of biological systems.[4] It is a multiple step approach that generally begins with the assembly of a collection of small molecules, then with the screening of the compounds in a developed assay and finally the identification of the modulated target molecule. Like in classical genetics, this approach attempts to uncover the specific macromolecules (usual proteins) that act as regulators of cellular processes. Their functions are subsequently defined using protein biochemistry, molecular cell biology and synthetic chemistry.

_____

_____

Chemical genetics can be divided into two differing approaches: forward and reverse chemical genetics (*Figure 2*). These approaches will be briefly described in the following sections and will be illustrated with notable examples.
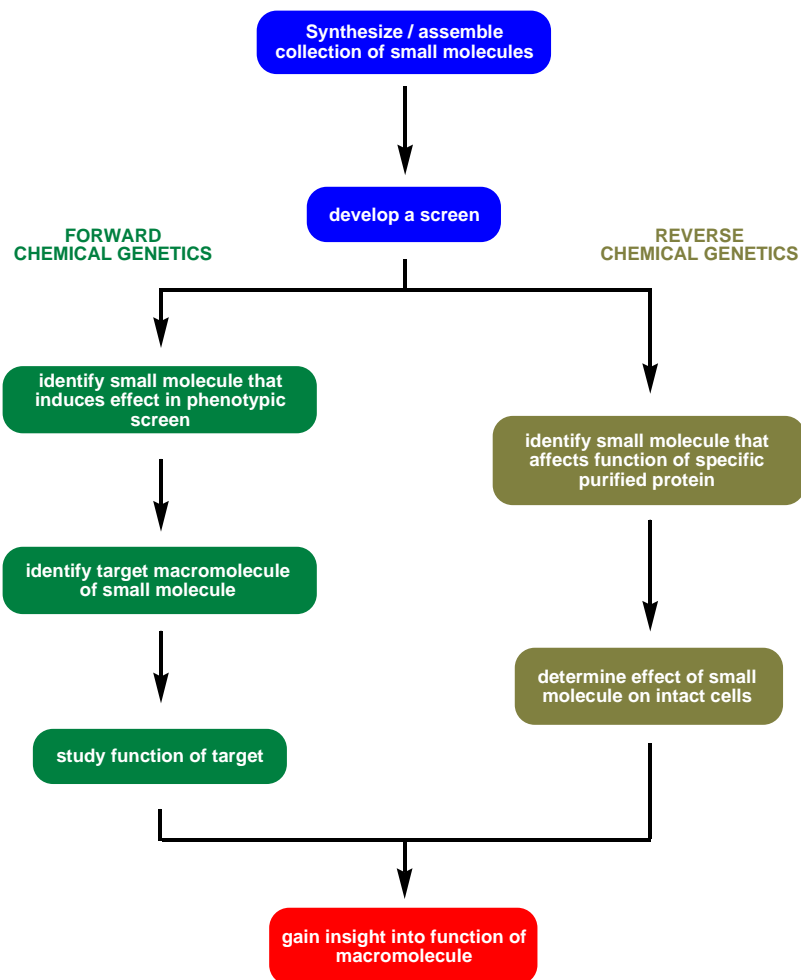
Figure 2: Summary of forward and reverse chemical genetics approach to understanding biological systems.

Forward chemical genetics involves the use of small molecules to screen for a desired phenotypical effect on the biological system under investigation. Once a small molecule has been identified, its molecular target needs to be revealed. This can be achieved by using molecular cell biology and protein biochemistry.

Mayer et al. used a combination of two phenotypical assays to screen a 16,320 member compound library for compounds that affect mitosis.[5] One synthetic small

_____ 3

_____

molecule, monastrol (**2**), provoked the reorganization of the mitotic spindle (*Figure 3*).
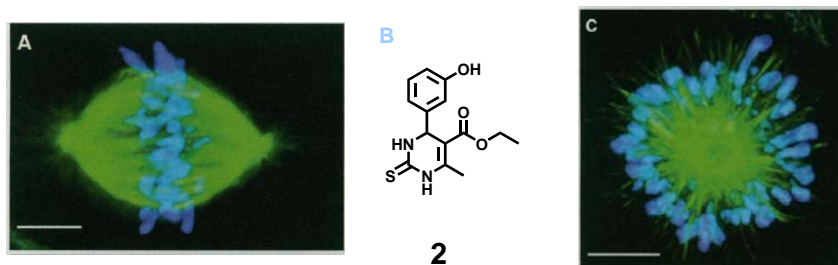
*Figure 3: (A) cell with normal mitotic bipolar spindle; (B) chemical structure of monastrol (**2**); (C) reorganization of mitotic spindle visualized by microscopy.*[5]

The phenotype induced by monastrol had been observed before on inhibition of the mitotic kinesin protein Eg5 using anti-Eg5 antibodies.[6;7] Biochemical investigations revealed that monastrol inhibits microtubule motility by binding Eg5.[5] The effect of monastrol is reversible: washing the compound out allows cells to move out of mitotic arrest and complete mitosis normally. This property was used to study the function of Eg5. This protein is now an established cancer target.[8]

In reverse chemical genetics, a small molecule is used against a purified protein. This molecule is then used to "knockout" the protein in question on a cellular level.
This approach was used to screen a library of compounds to find a small molecule that binds and inactivates the protein MEK1, an enzyme whose activity is needed for cell division.[9] A potent and selective MEK inhibitor PD184352 (**3**, *Figure 4*) was identified (50% inhibitory concentration, IC$_{50}$ 17 nM).
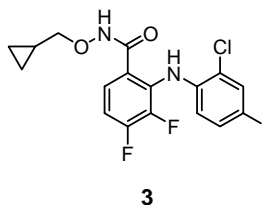
*Figure 4: Chemical Structure of PD184352 (**3**).*

Subsequent studies in vivo on mice with colon carcinomas of mouse and human origin demonstrated that tumor growth was inhibited by up to 80% upon treatment

_____ 4

_____

with PD184352. The low toxicity, high potency and selectivity made this compound promising for the treatment of colon cancer.

Some advantages of chemical genetics over classical genetics are that temporal control is possible as small molecules can be added to the studied systems at any time point of the experiment. The effects are also reversible as the compounds can be removed metabolically or by washing. To achieve reversibility in a genetic system, conditional alleles need to be introduced; these are difficult to generate and control. Another advantage is that small molecules have rapid effects as they are mostly diffusion limited. They can therefore be used to observe immediate effects. Furthermore, they can be used to study critical genes in developmental stages: whereas a cell knockout may not be viable, it may still possible to study the effects of a knockout gene product. However, the main disadvantage is that chemical genetics cannot be applied generally. Any gene, in principle, can be specifically manipulated by genetics; chemical genetics still needs selective small molecules. Moreover, the protein-targets still need to be uncovered, which at present is still a challenge.

The use of small molecules to study biological systems has had an impact on fields such as signaling,[10;11] cell morphogenesis,[12;13] and developmental biology.[14] In this dissertation, the focus will lie on using small molecules to study the Ras signaling pathway, phosphatases and bacterial cell growth.

2.1.2   Application Areas for Chemical Genetics

Ras Signaling Pathway
Normal cellular behavior is tightly regulated by complex signaling networks. The study of these signaling networks is important because dysfunction often leads to diseases such as cancer. One interesting example of signaling is that of the Ras/MAPK signaling pathway.

The Ras proteins belong to a family of small GTPases and play a key role in the signal transduction from receptor tyrosine kinases to the cell nucleus for the regulation of cell-cycle progression, cell division, survival and apoptosis.[15;16] There are three isoforms of Ras in mammals: N-Ras, K-Ras and H-Ras. Ras acts as a molecular

_____

switch by alternating from the inactive GDP-bound form to the active GTP-bound form (*Figure 5*).
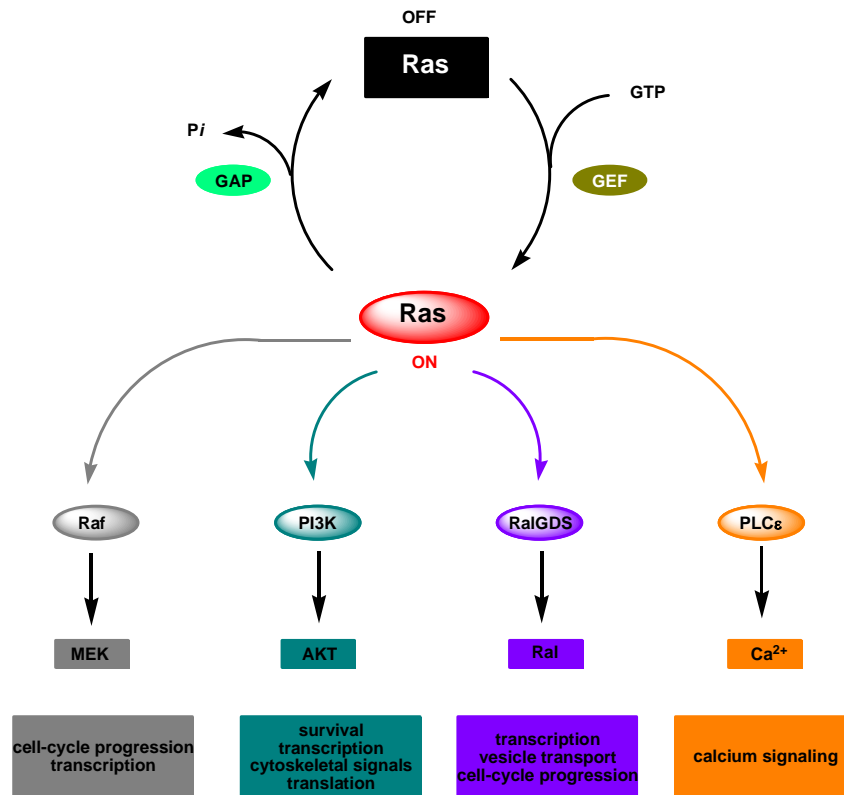

Figure 5: Cycling of the Ras molecular switch and downstream effectors of Ras and their activities.

The intrinsic GTPase activity in vitro is slow and nucleotide exchange from the mediums is slow as well due to the extremely high affinity of Ras to GDP. In the cell though, these processes are aided by GTPase activating proteins (GAPs) and guanine nucleotide exchange factors (GEFs), respectively. One of the best characterized GEFs is Sos (Son of Sevenless). Sos's GEF activity is mediated by its recruitment to the plasma membrane: this occurs via the activation and binding of receptor tyrosine kinases such as epidermal-growth-factor receptor (EGFR) to adaptor protein growth-factor-receptor-bound protein 2 (GRB2) that in turn binds to Sos. In its active, GTP-bound form, Ras is able to bind to and activate downstream effector proteins (*Figure 5*). Through these downstream effectors Ras is able to control cell proliferation, survival and other cellular processes. One of these effectors, serine-threonine kinase Raf, is the starting point of the much-studied mitogen-activated-protein kinase (MAPK) pathway.

_____

The phosphoinositide 3-kinases (PI3Ks), another family of Ras effectors, generate second messenger lipids such as phosphatidylinositol 3,4,5-triphosphate, that then activate numerous signaling proteins like the cell surving kinase AKT/PKB. Other Ras effectors include RalGDS, the GEF of Ral, that affects transcription factors, and phospholipase Cε (PLCε) that catalyzes the hydrolysis of phosphatidylinositol 4,5-diphosphate to diacylglycerol and inositol trisphosphate resulting in the activation of protein kinase C (PKC) and the mobilization of intracellular calcium stores.

A large percentage of human tumors occur as a result of aberrant signaling in the Ras signaling cascades. Mutations in the Ras genes that compromise GTPase activity, causing Ras to accumulate in the active form, occur frequently. GAP deletion,[17] overactivation of growth-factor receptors,[18] or mutations or amplification of Ras effectors[19] are also frequent causes of aberrant signaling. Particularly interesting is the role of the Ras signaling pathway in epithelial-mesenchymal transition (EMT, *Figure 6*).
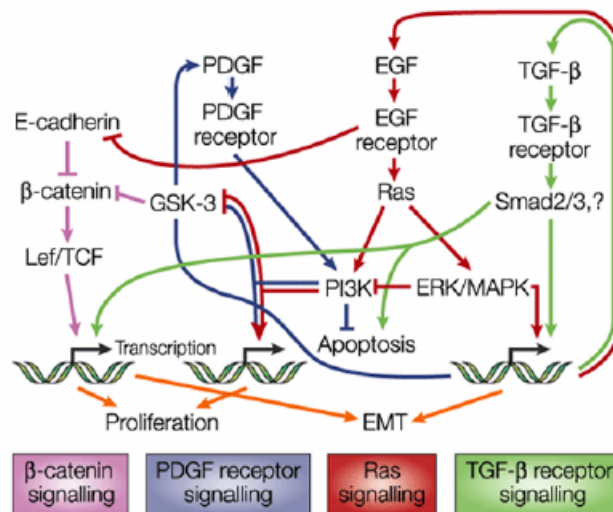
*Figure 6: Multiple signaling networks affecting EMT.[20]*

EMT is a process in which cells undergo a developmental switch from a polarized, epithelial phenotype to a highly motile fibroblastoid phenotype (*Figure 7*). It occurs as a key step during embryonic morphogenesis,[21] and has now been implicated in the progression of primary tumors towards metastasis.[22] It might therefore be attractive

_____ 7

to target pathways involved in EMT in order to regulate tumor cell proliferation, dedifferentiation and survival.

The transforming growth factor β (TGF-β) and Ras signaling pathways have been identified as key players in EMT and metastasis.[23] In fact, EMT requires a hyperactive Ras pathway along with TGF-β signaling.[24] The impact of these signaling pathways on epithelial plasticity was demonstrated using EpH4 cells transformed with Ha-Ras (EpRas cells). The EpRas cells underwent EMT after treatment with TGF-β. Reversal of EMT was achieved by inhibiting the Ras-Raf-MEK pathway with MEK-1 specific inhibitor PD98059 (**4**, *Figure 7*).
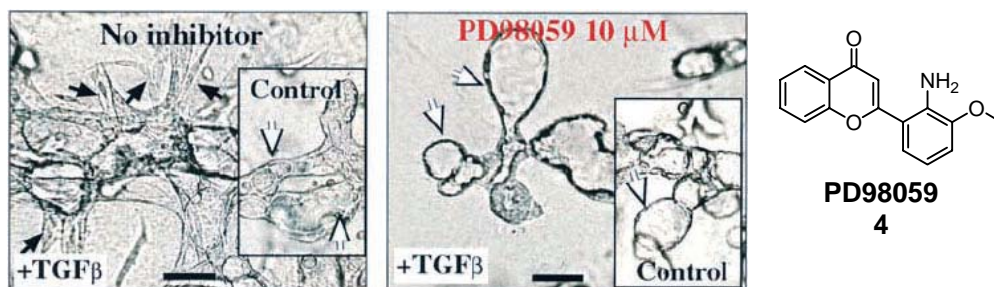

*Figure 7: Reversal of EMT by MEK-1 inhibitor PD98059 (**4**). EpRas cells seeded in collagen gels in the presence or absence (inset) of TGF-β and left untreated (left image) or treated with 10 µM PD98059 (right image).[24]*

These pathways are not alone in inducing EMT: Wnt/β-catenin signaling along with downstream effectors of Ras and TGF-β also promote EMT. For example, if E-cadherin is degraded or transcriptionally repressed, or if glycogen synthase kinase 3β (GSK-3β) activity is suppressed by activated PI3K (activated by upstream receptor tyrosine kinases [RTKs] or Ras), then the cytoplasmic amount of β-catenin increases and enhances transcription of T cell factor/lymphocyte enhancer factor (TCF/LEF) genes leading to cell proliferation and EMT (orange arrows in *Figure 6*, p.7).[25]

EMT-like cell behavior can be induced in epithelial cells by transforming them with oncogenic proteins such as Ras or Wnt.[26] Due to the resulting phenotypical change, these cells can be used in a forward chemical genetics approach to observe the effects of small molecules on activated signaling pathways.

_____

Phosphatases

Phosphorylation is employed by living organisms to regulate innumerable cellular processes such as cell mitosis, growth factor responses and insulin signaling. In fact, it is estimated that at least 30% of all cellular proteins are subject to phosphorylation at one or more residues.[27] The phosphorylation status of proteins is regulated by protein kinases, that catalyze the formation of phosphate ester bonds, and protein phosphatases, that catalyze the hydrolysis of phosphate ester bonds (*Scheme 1*). Due to the central role of phosphorylation /dephosphorylation in cellular signaling, many disease states involve perturbations in the balance between protein kinases and protein phosphatase activities.[28;29]
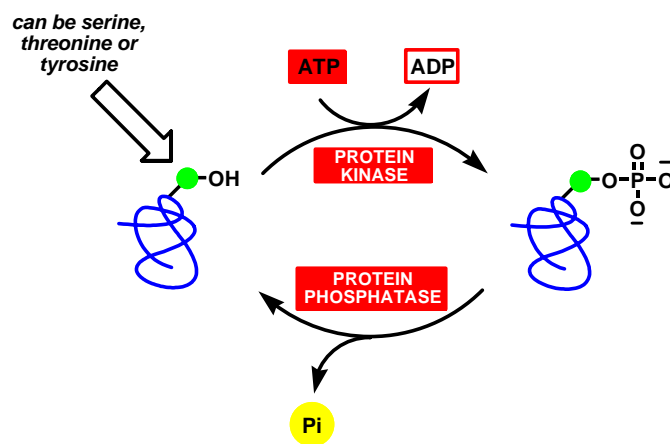
Scheme 1: Protein phosphorylation and dephosphorylation are catalyzed by kinases and phosphatases

Protein phosphatases are classified according to structure and substrate specificity into two families: the serine/threonine-specific protein phosphatases (PPs) and the protein tyrosine phosphatases (PTPs).

The serine/threonine phosphatases (PPs) are a large family of metalloprotein phosphatases that hydrolyze phosphate ester-modified serine or threonine residues.[30] They have extremely diverse functions in the cell. For example, PP1 is involved in regulating glycogen metabolism in response to insulin and adrenaline.[31] Structurally, the PPs consist of several subunits: a catalytic subunit with a metal ion at its core, and one or more regulatory subunits. It has been proposed that phosphate ester hydrolysis

_____

_____

involves the attack of the phosphorus atom by a metal-activated water molecule and proceeds without the formation of a phosphoenzyme intermediate.[32;33]

The second large family are the protein tyrosine phosphatases (PTPs). They play an important role in the regulation of signal transduction pathways. Unlike the PPs, the PTPs catalyze the hydrolysis of the phosphate ester of a tyrosine residue independently of a metal ion.[30] In a two-step process, the PTPs catalyze first the transfer of the phosphate to a catalytic cysteine residue then expel the dephosphorylated substrate from the active site using an acidic amino acid residue to protonate the tyrosine phenolic oxygen. PTP1B is the prototypical member of this family.[34] It has been implicated in oncogenesis, by being the major PTP that dephosphorylates and thus activates v-src in human breast cancer cell-lines,[35] and in the control of cell adhesion, via effects on integrin signaling and through regulation of the adhesive properties of cadherin-catenin complexes.[36] Additionally, it also plays a key role in the regulation of metabolic signaling: it has been shown to work as an insulin antagonist by dephosphorylating and thus inactivating the dimeric insulin receptor (IR).[37;38] Some bacteria, such as *Salmonella* and *Yersinia* bacteria, produce and employ PTPs for their pathogenicity.[39] *Mycobacterium tuberculosis* has two functional PTPs, MptpA and MptpB, that are secreted into the culture supernatant by the growing microbacterial cells.[40]

A subfamily of the PTPs are the dual-specificity phosphatases (DSPs) that hydrolyze the phosphate ester on both a tyrosine residue and either a serine or threonine residue located on the same protein. They have crucial roles in intracellular signaling pathways. VHR (for VH1-related) is mostly known for regulating mitogen activated protein kinase (MAPK) signaling pathway. It has been shown to dephosphorylate several members of the MAP kinase family including ERK1, ERK2 and JNK kinases.[38] The cell-cycle dependant-25 (Cdc25) family of phosphatases, present as 3 homologues in humans, function as key regulators of the cell cycle during normal eukaryotic cell division, promoting the dephosphorylation and thus activation of cyclin-dependant kinases (CDKs), propagating cell-cycle signal transduction.[41] The overexpression of Cdc25 is frequently associated with a wide variety of cancers and has been implicated in neurodegeneration.[42]

_____

_____

Although there is less than 5% sequence identity within the active sites of PTPs and DSPs, it has been shown that there is remarkable similarity in the overall structural fold of PTP1B, a PTP, and VHR, a DSP (*Figure 8*).[30]
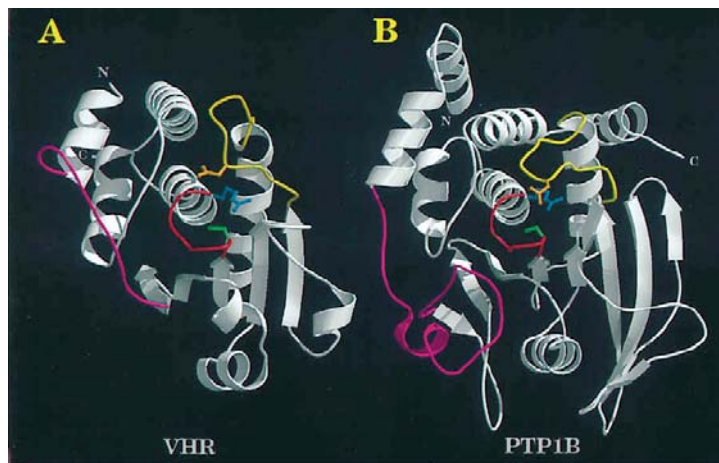
*Figure 8: Backbone representation of the catalytic domain of dual-specificity phosphatase VHR (**A**) and protein tyrosine phosphatase PTP1B (**B**).[30]*

The catalytic sites of the PTPs and DSPs share a characteristic highly conserved loop structure, $C(X)_5R$ (where C = cysteine, X = any amino acid, R = arginine), which interacts with the phosphate residue of the phosphotyrosine (shown in red in *Figure 8*). The major structural difference in the catalytic domains of the PTPs and DSP occurs at the insertion loop between the first α-helix (α1) and the first β-strand (β1, shown in magenta in *Figure 8*). This loop region contributes to the overall depth of the active-site pocket. In VHR, this loop was found to be 75% shorter than in PTP1B, with the consequence that a decrease in loop structure decreases the overall depth of the pocket.[43] It has been thus suggested that substrate specificity between PTPs and DSPs lies within the depth of the active-site pocket.[43]

It may therefore be possible to achieve selective inhibition of PTPs and DSPs by designing molecules that have a core structure that interacts with the conserved loop region instead of the phosphate of the substrate, and substituents that interact with the distinctive loop region between α1-β1. This design hypothesis was successfully tested with a library of tetronic acids, where 3-acyltetronic acids was used as the phosphate mimic (*Figure 9*).[44] By modulating the side-chain substituents, it was possible to tune the selectivity towards either PTPs or DSPs.
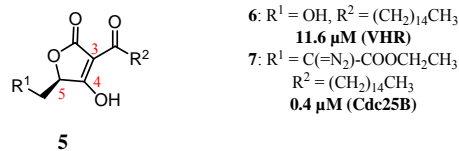
_____ 11

_____

6: R^1 = OH, R^2 = $(CH_2)_{14}CH_3$
11.6 μM (VHR)
7: R^1 = C(=N_2)-COOCH$_2$CH$_3$
R^2 = $(CH_2)_{14}CH_3$
0.4 μM (Cdc25B)

*Figure 9: Chemical structure of the tetronic acid core **5**.*

Moreover, PTP1B possesses a vicinal second aryl phosphate binding site which lies within a region that is not conserved among protein tyrosine phosphatases.[45] The presence of this structural feature suggests an effective strategy for the generation of potent and selective inhibitors: by tethering two small ligands, enhanced affinity and specificity ought to be achieved. Recently many industrial and academic groups have succeeded in generating such inhibitors.[46-48]

The central role of protein phosphatases in signaling make them particularly interesting targets to be studied with small molecules in a reverse chemical genetics approach.

Antibiotics

The optimism that accompanied the discovery of the first penicillin antibiotics to treat Staphylococcal infections in the 1940s has been tempered by the emergence of bacterial strains that are resistant to developed antibiotic treatment. Resistance to antibiotics has been monitored to develop rapidly, within one year to one decade of the introduction of the drug to clinical use.[49] Clinically relevant bacteria are not only characterized today by single drug resistance but also by multiple drug resistance, making them a significant public health threat.

Although antibiotics discovery is an example of the successful mining of natural products for therapeutic use, there is currently little advance in the discovery of novel lead structures. Many of the antibiotics in clinical use are second or third generation modifications of an older scaffold that still bind to the same protein. Therapeutic scaffolds have been developed via two alternate routes: from natural products or from synthetic sources. Some of the natural products have evolved to interact with and to be recognized by targets in pathogenic bacteria. They have successfully served as sources of inspiration to create some of the semi-synthetic variants of antibiotic

_____

_____

natural products currently being used in the clinic. Antibiotics from synthetic sources include the sulfa antibiotics that target folic acid synthesis and the fluoroquinolone family of compounds (Ciprofloxacin) that block DNA gyrase and topoisomerase IV. The latest structural class of antibiotics approved for use, the oxazolidinones (Linezolid), was introduced 40 years after the development of the fluoroquinolones class.

Mechanism of action	Antibiotic family
Inhibitors of bacterial-cell-wall biosynthesis	β-lactams (Penicillin, carbapenem antibiotics); cephalosporin; glycopeptides (Vancomycin)
Inhibitors of protein biosynthesis	Polyketides (tetracyclines); aminogylcosides; oxazolidinone (Linezolid); Ketolides (Erythromycin); macrolides; lincosamides
Inhibitors of DNA synthesis	Quinolones (Ciprofloxacin)
Inhibitors of folic acid synthesis	Sulfonamides

Table 1: Major families of antibiotics and their mechanism of action.

Not only does there appear to be an innovation gap in the generation of novel antibiotic scaffolds, there are currently only four molecular targets for the main classes of clinically-used antibiotics (*Table 1*): bacterial-cell-wall biosynthesis; bacterial protein biosynthesis; DNA replication; folate coenzyme synthesis. New targets may be less susceptible to existing mechanisms of bacterial resistance due to novel mechanisms of action.

2.1.3 Library Design for Chemical Genetics

To fully exploit the potentials of chemical genetics, it is necessary to have a compound library capable of modulating the function of many proteins. Additional properties of the ideal library include cell permeability and synthetic possibilities.

Not only is it currently impossible to generate a library that contains compounds that bind selectively to each protein, but for many proteins, small molecule ligands have not yet been identified. The composition of the library is of great importance, as it should increase the probability of finding interesting substances and effects. Fortunately, many natural products have been selected to interact with a wide assortment of proteins and other biological targets. For example, natural products

_____

have become effective drugs in a large range of therapeutic indications: a few prominent examples are vancomycin, an antibiotic, paclitaxel, a cytostatic drug used to treat cancer, and cyclosporine, an immunosuppressive agent. Natural products can be considered privileged structures for chemical genetics.[50]

Currently, there are multiple approaches to designing such libraries: libraries based on the general structural features of natural products, libraries based on core scaffolds of natural products and finally libraries based on specific substructures from classes of natural products. It should to be noted that these categories overlap to some extent, and that most synthesized libraries are designed to lie somewhere in between.

Libraries based on the general structural features of natural products

This approach seeks to exploit the structural characteristics of natural products in a high-throughput manner: the aims of this strategy are to generate compounds that are easy to access, that have plenty of chiral functional groups and are rich in stereochemical information, and are skeletally diverse.[51] In general, the compounds generated are used as probes for understanding cellular processes. In other words, the substances are not biased towards specific targets. This strategy was applied to generate a 1,3-dioxane based library to identify a novel function selective inhibitor of Ure2p, a yeast nutrient responsive signaling protein.[52]

Libraries based on core scaffolds of natural products

The second approach is used primarily to exploit the activity of parent natural products. Natural products can be used as biologically validated frameworks upon which to display diverse functionalities.

Waldmann and coworkers propose that protein domain cores with similar three dimensional structures can be clustered in so-called protein similarity clusters (PSSC)[53] and that this classification can be used as a guiding principle for the selection of biologically pre-validated starting points for compound library synthesis. According to this principle, ligands for one of the proteins of the cluster can be used as the starting point to obtain ligands for other members of the cluster. This approach was used to identify inhibitors of the dual-specificity phosphatase Cdc25A **8**, acetyl cholinesterase (AchE, **9**) and 11-β-hydroxysteroid dihydrogenase type 1 and 2 (11-β-HSD-1, **10**, and 11-β-HSD-2, **11**) from a library of butenolides (*Figure 10*).[53]
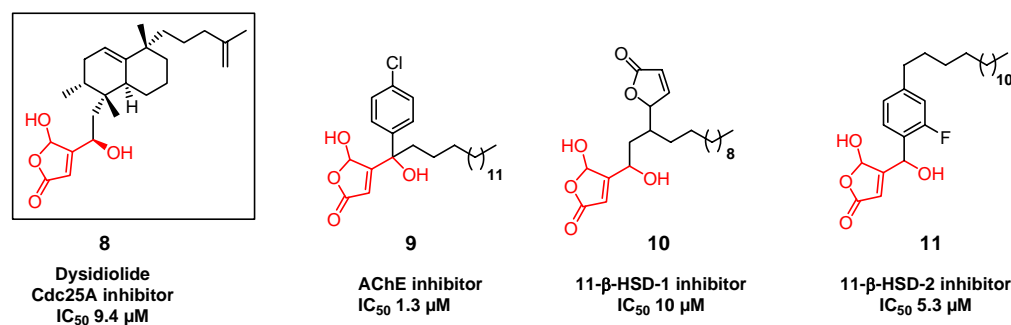
_____

Figure 10: Selected compounds from a butenolide library based on a core scaffold of the natural product Cdc25A inhibitor Dysidiolide (8).

Libraries based on specific substructures from classes of natural products

Similarly to the last described approach, here the substructures, which are generally found within a class of natural products and are also considered as biologically validated and privileged, are used as the starting point for library design. This approach offers the opportunity to generate structural diversity so that many targets can be used. One of the first examples of the application of this strategy was the synthesis of a 10,000-member library of 2,2-dimethylbenzopyrans (12),[54;55] a structural motif found in diverse natural products with many biological activities (*Figure 11*). Screening of this library in diverse assays, target identification and optimization of active compounds yielded inhibitors for NADH:ubiquinone oxidoreductase, 13,[56] anti-MRSA antibacterials, 14[57] and farnesoid-X reporter (FXR), 15.[58]
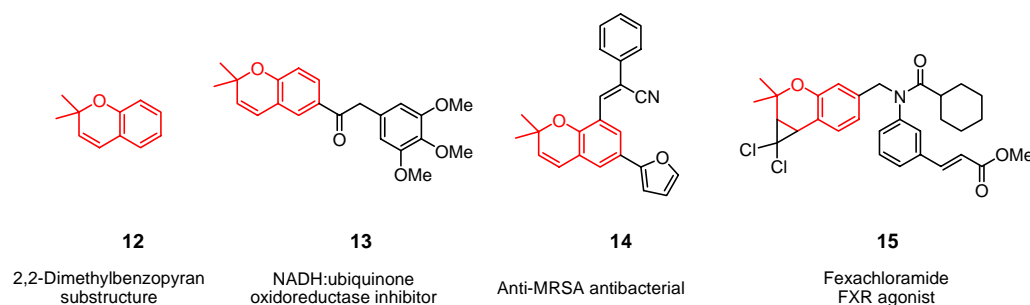

Figure 11: Library based on the specific substructure of 2,2-dimethylbenzopyran (12).

Another application of this approach made use of the structural classification of natural products (SCONP),[59] which is a structural classification of natural products

_____

_____

in a tree-like arrangement, providing a viable analysis and hypothesis-generating tool for the design of natural product-based libraries. SCONP was used as a guiding principle to generate libraries of 11-β-HSD-1 and 11-β-HSD-2 inhibitors.[59]

One class of natural products, the tetramic acids, have an interesting framework and also biological activity and are therefore good targets for a natural product-based compound collection for the chemical genetics study of their cellular and biological activity. The following sections will describe the biology, biosynthesis and chemistry of tetramic acids.

_____

2.2 Tetramic Acids

2.2.1 Tetramic Acid-Containing Natural Products

The tetramic acid (2,4-pyrrolidinedione, *Figure 12*) ring system was recognized in the sixties to be a reoccurring structural motif in a variety of isolated natural products (*Figure 12*).
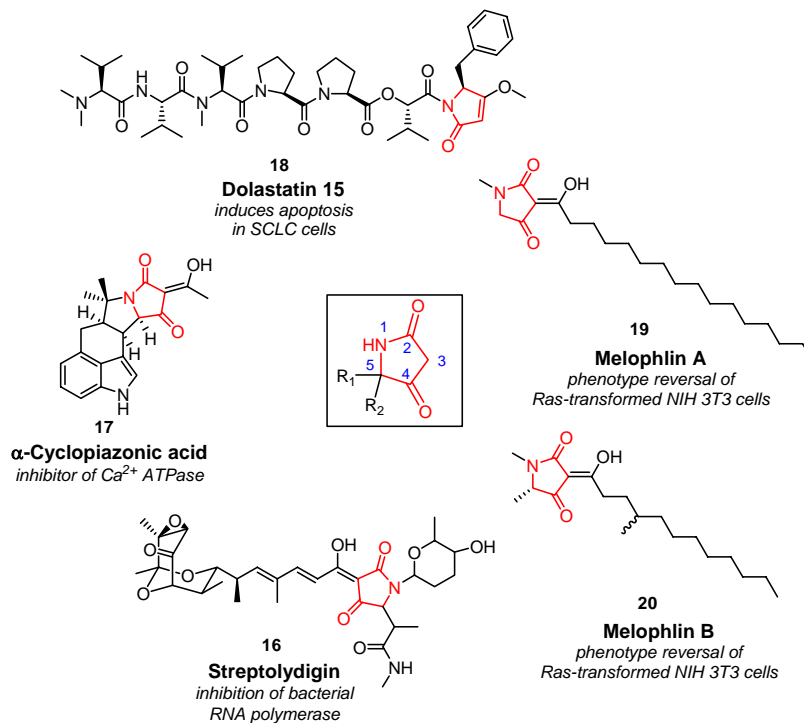
Figure 12: Representative natural products containing a tetramic acid motif.

This family of compounds has attracted significant attention in the past few years due to their synthetic challenge as well as their broad range of biological activities.[2] A steadily increasing number of tetramic acids are being isolated from natural sources ranging from marine species to fungi and terrestrial bacteria.[2] The biological activity is also remarkably varied, spanning from antibiotic and antiviral activity, cytotoxicity, mycotoxicity as well as inhibition of the cell cycle.

The tetramic acid antibiotic streptolydigin (**16**, *Figure 12*) inhibits initiation, elongation and pyrophosphorolysis in bacterial RNA polymerase (RNAP).[60] Streptolydigin does not inhibit eukaryotic RNAPI, RNAPII or RNAPIII because the

_____ 17

_____

proteins have low sequence identity with bacterial RNAP, though the proteins share high three-dimensional structural similarity. The target, mechanism and structural basis of inhibition were recently disclosed by Tuske et al.[60] and these results have implications in the design of novel bacterial RNAP-based antibiotics.

Cyclopiazonic acid (**17**, *Figure 12*) is a toxic indole tetramic acid produced by numerous Penicillium species.[61] It is an interesting mycotoxin as it is produced by numerous fungi that infect commodities though it is toxic only at higher concentrations (ingested LC_{50} ~30 mg/kg). Its toxicity appears to stem from its abitility to inhibit Ca^{2+} ATPase.[62]

The dolastatin family of natural products includes a series of linear and cyclic antineoplastic and/or cytostatic peptides. One of the most potent members of this family, dolastatin 15 (**18**, *Figure 12*) includes a tetramic acid at its terminal moiety. Dolastatin 15 induces apoptosis and is antiangiogenic. It binds weakly to tubulin but clearly disrupts microtubule formation.[63]

Melophlin A (**19**) and B (**20**), novel tetramic acids isolated from the marine sponge *Melophlus sarassinorum* from the Indonesian sea, possesses the ability to reverse Ras-transformed NIH3T3 cells as well as arrest NIH3T3 cells in the G1 phase of the cell cycle at a concentration of 1 µg. mL^{-1}.[64]

Tetramic acids are also found in the agrochemical field: they have been patented for fungicidal and herbicidal use.[65] Bayer CropScience has developed a series of insecticidal agents based on tetronic and tetramic acids. Spirotetr(o)amic acid **21** and **22** (*Figure 13*) appear to block acetyl-coenzyme A carboxylase,[66] a protein vital to the production of fatty acids in mites. As lipids are the principle source of energy in mite eggs, disruption of their lipid utilization impairs developmental processes.

21   **22**
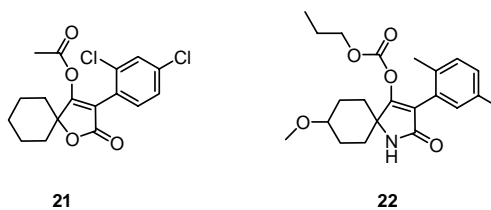
*Figure 13: Structure of insecticidal tetronic acid **21** and Spirotetramat **22**.*

_____

_____

The interesting biological and structural diversity of this class of substances makes it a particularly interesting template for the design of compound libraries in search of small molecules that affect cellular signalling pathways.

2.2.2   Biosynthesis of Tetramic Acids

The acyl tetramic acid group of metabolites that have been investigated biosynthetically possess a tetramic acid ring that is derived from an acetate unit and an amino acid.[2] The acyl group derives from a polyketide. However, the order in which these three entities are assembled is still subject to controversy.
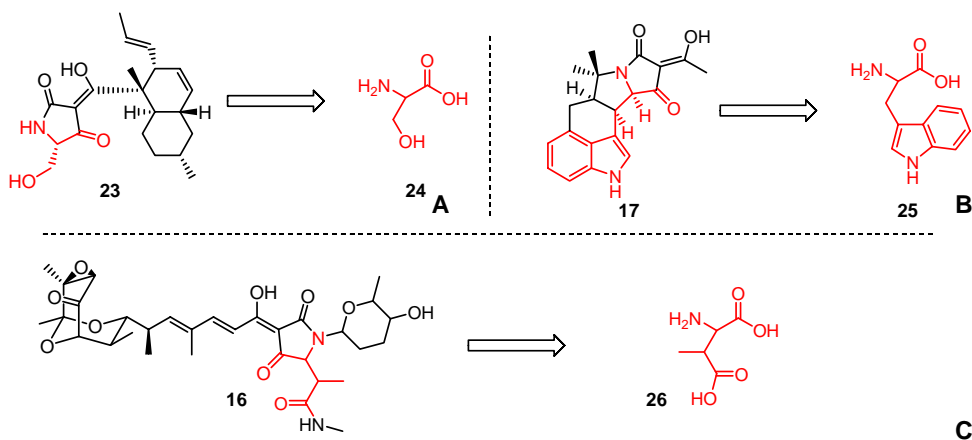
Figure 14: Biosynthetic precursors to equisetin (23, A), cyclopiazonic acid (17, B), and streptolydigin (16, C).

Thus, it is assumed that the pyrrolidine moieties in equisetin (**23**),[67] α-cyclopiazonic acid (**17**),[68;69] and streptolydigin (**16**)[70] are derived from serine (**24**), tryptophan (**25**), and methylaspartate (**26**), respectively (*Figure 14*).

Janda and co-workers[71] gave the biology of tetramic acids a different turn by proposing that tetramic acid **28** is formed non-enzymatically from *N*-acylhomoserine lactone, **27**, produced in Gram-negative bacteria by a Claisen-like intramolecular alkylation (*Scheme 2*).

_____

_____
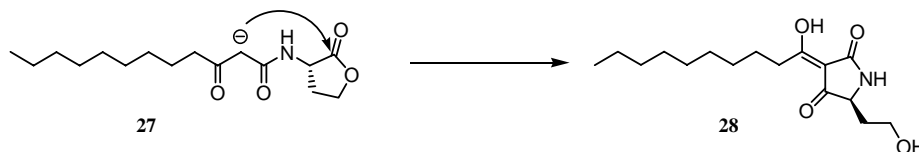
*Scheme 2: Reaction of 3-oxo-AHL **27** to generate tetramic acid **28**.*

The formed tetramic acid **28** is postulated as being used as an interference strategy against encroachment by competing bacteria, behaving therefore as quorum sensors. This is an intriguing hypothesis as many biologically active tetramic acids are selectively toxic against Gram-positive bacteria.[72;73]

2.2.3 Synthetic Routes to Tetramic Acids

Solution-Phase Synthesis of Tetramic Acids

Due to mounting interest in tetramic acids, various synthetic routes towards their synthesis have been established. The Lacey-Dieckmann cyclization[74] is the most widely adopted synthetic strategy for the generation of the 2,4-pyrrolidinedione core (**A**, *Scheme 3*).[75-78] It is a base-induced cyclization of *N*-(β-ketoacetyl)-α-amino esters (**30**), that are easily obtained from α-amino acids. This is an extremely flexible synthesis and is used to synthesize tetramic acids with various C3 substituents, provided the *N*-acetoacetyl-α-amino ester can be prepared. However, complete or partial racemization at C5 of the 2,4-pyrrolidinedione core has been frequently observed.[79] Recently, Schobert and coworkers reported an expedient synthesis from α-amino esters and in which the cyclization involved a domino addition-Wittig alkenation reaction with immobilized (triphenylphosphoranylidene)ketene (**33**) under neutral non-racemizing conditions (**B**, *Scheme 3*).[80] Acylation to 3-acyltetramic acids was then performed with the appropriate acyl chloride and boron trifluoride-diethyl etherate under microwave irradiation.

_____

_____
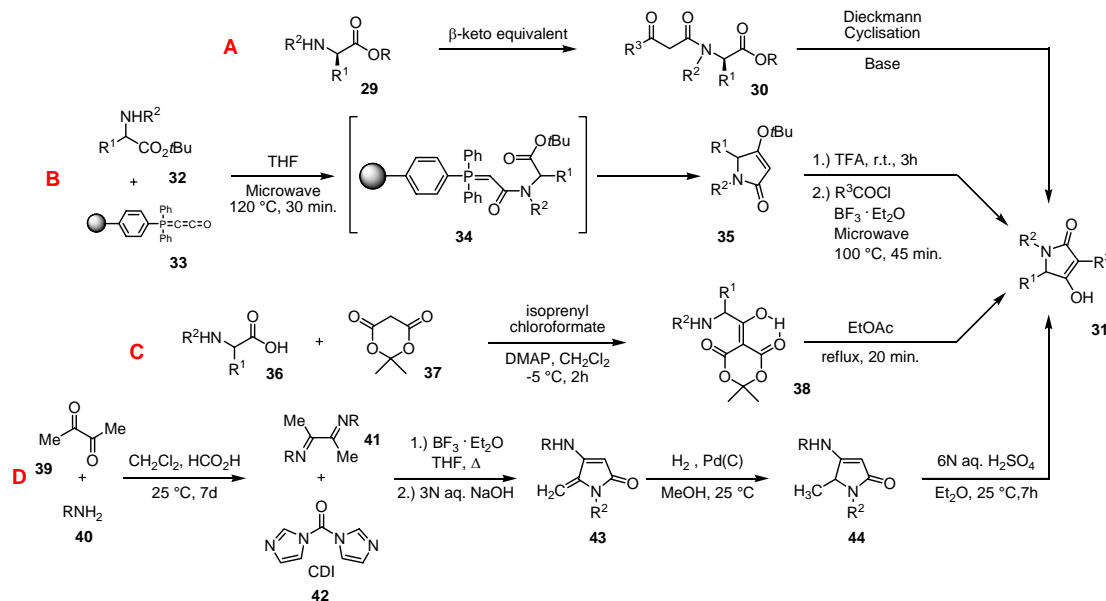
Scheme 3: Summary of recent solution-phase synthesis of tetramic acids.

Another method was used by Jouin for the generation of the tetramic acid core via the condensation of *N*-protected amino acids with Meldrum's acid **37** in the presence of isoprenyl chloroformate and DMAP (**C**, *Scheme 3*).[81] The cyclization of **38**, by heating in an organic solvent, provided *N*-protected tetramic acids. Fustero and coworkers proposed an alternative asymmetric synthesis of tetramic acids in which the key step is a carbonyl transfer from carbonyldiimidazole (**42**, CDI) to α-diimines **41** to form **43** (**D**, *Scheme 3*).[82] These compounds can then be transformed in tetramic acid derivatives in two additional steps. Unfortunately, the sequence is limited to the generation of "symmetric" tetramic acids due to the double condensation with initial dione **39**.

Solid-Phase Synthesis of Tetramic Acids

The majority of reported solid-phase tetramic acid syntheses begin with solid-phase bound amino acids **45** as building blocks and involve a Dieckmann cyclization in the cleavage step (*Scheme 4*, **A**). These methods differentiate themselves from each other by the use of different conditions and reagents to initiate the cyclative cleavage from the resin. Matthews and Rivero[83] report the synthesis of mostly 3-unsubstituted tetramic acids, employing NaOEt and heating to 85 °C to cyclize from the solid support. Ganesan and co-workers[84] report the preparation of tetramic acids without

_____

_____

substitution at the 3-position using tetrabutylammonium hydroxide as the cyclization agent. The product needs however to be treated with strongly acidic Amberlyst A-15 ion exchanger resin in order to remove this reagent. Weber et al.[85] demonstrate the synthesis of 3-acyl tetramic acids using Meldrum's acid to acylate at the 3-position, but by using DIPEA and heat for the cyclization the products underwent racemization. Finally, Romoff[86] reported a method where the cleavage is effected in the ultimate step by a Dieckmann cyclization in the presence of KOH/MeOH at room temperature, without apparent loss of chirality.
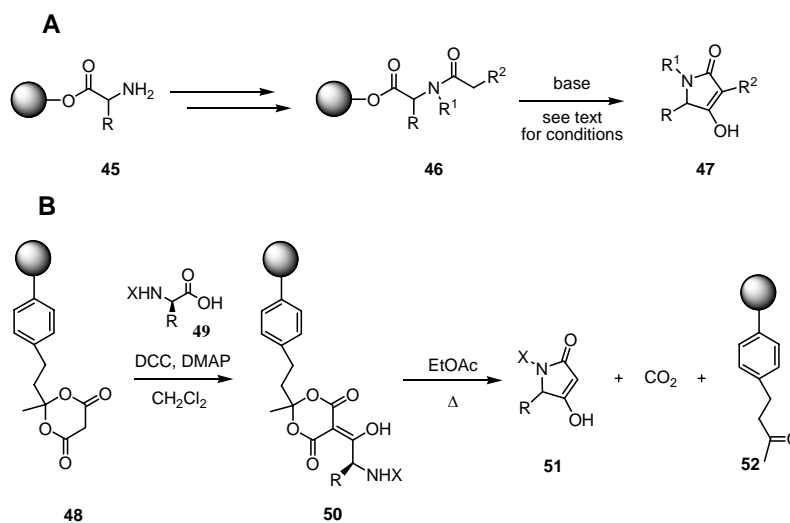
Scheme 4: Solid-phase synthesis of tetramic acids using Lacey-Dieckmann cyclization (A) and according to Huang (B).

Huang and co-workers (*Scheme 4,* **B**) devised an alternative synthesis based on the condensation of resin-bound Meldrum's acid **48** with *N*-acylated amino acids **49**.[87] Cyclative cleavage was effected by heating in ethyl acetate. This method is restricted to the synthesis of tetramic acids without an acyl substituent at the 3-position.

All of the above-mentioned syntheses demonstrate the synthetic feasibility of the route using aromatic or aliphatic amino acids such as phenylalanine or valine but do not thoroughly probe the scope of their synthesis.

_____

_____

3 Aim of the Dissertation

The use of small molecules as probes to investigate complex biological systems is termed chemical genetics. This is a powerful method to study such phenomena like signal transduction or for the search for novel antibiotics. Key to this approach is the design of an effective compound library. Inspiration for such a library can be taken from natural products, which are themselves pre-validated structures.[59] An example of such a privileged scaffold is the tetramic acid (2,4-pyrrolidinedione) ring system. It is present in numerous natural products that display diverse biological activities[2] making it a particularly suitable template for a natural-product-based library for a chemical genetics approach to study cellular signaling.

The first aim of this thesis was to develop a strategy for the synthesis of tetramic acids in a minimal number of steps, in an efficient manner and by maximizing diversity. Ideally, this approach should allow the introduction of different functional groups at all three modifiable positions of the tetramic acid scaffold (*Figure 15*).
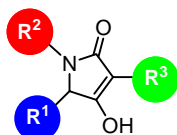
Figure 15: Positions open for diversification on the tetramic acid scaffold.

To demonstrate the feasibility of this strategy, the synthesis of a small library of tetramic acids should be undertaken. A successful route to the tetramic acid scaffold should open up synthetic pathways for a number of analogs of the natural product Laccarin. In an interesting extension of the synthesis, the tetramic acid scaffold should be substituted with indole moieties. Therefore, the development of a synthesis of tryptophan analogs should be carried out.

In light of the documented biological activities of tetramic acid natural products,[2] the final objective of this thesis should be the testing of the synthesized tetramic acid library against biological targets. First, the compound collection should be assayed to uncover modulators of the Ras/MAPK signaling cascade in cell-based tests.

_____ 23

_____

Furthermore, their inhibitory activity for phosphatases should also be investigated. Ultimately, the effect of tetramic acids on bacterial cell growth should be examined.

4 Results and Discussion

4.1 Synthesis of tetramic acid libraries

4.1.1 Synthetic plan

The synthetic route chosen is based on a solid phase approach and provides access to diverse tetramic acids. The building blocks stem from the chiral pool: amino acids are used as the starting material for the synthesis.
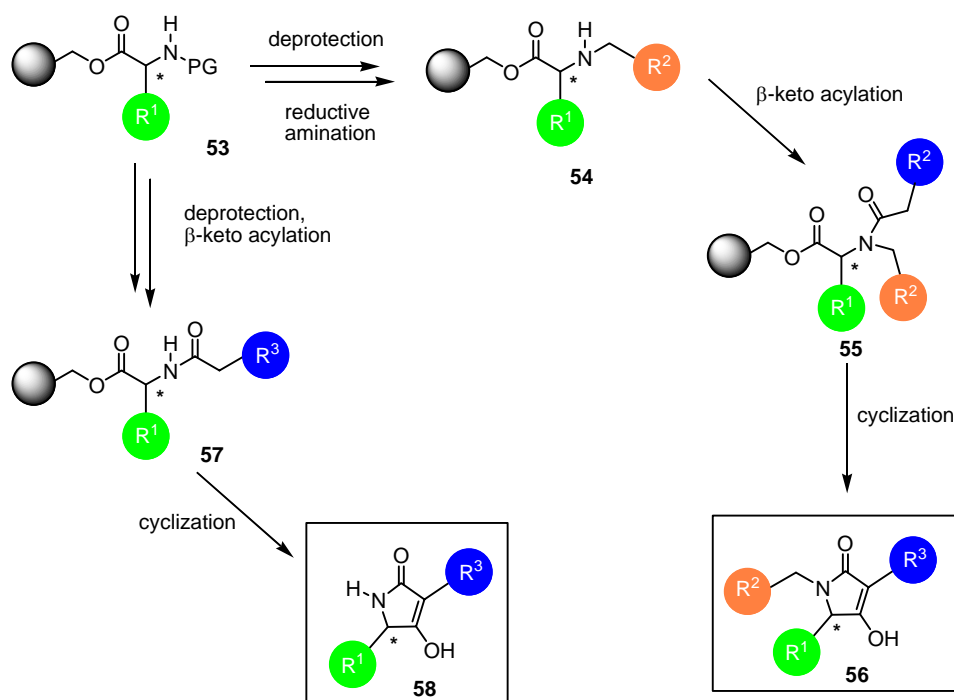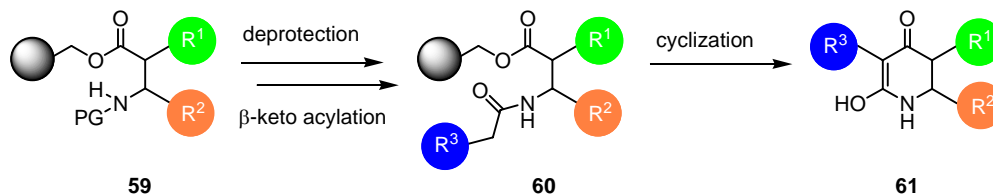

Scheme 5: Synthetic strategy towards the synthesis of 3-acyl tetramic acids.

In the first step, *N*-protected α-amino acids are condensed with a hydroxyl-functionalised resin (*Scheme 5*). After deprotection of the *N*-terminus of the amino acid, the resulting amine can be converted to secondary amine **54** in a reductive amination step. Next, this amine can be acylated with β-keto equivalents to generate cyclization precursor **55**. Finally, cleavage from the resin is achieved by base catalyzed cyclization to the tetramic acid **56**. Alternatively, after condensation of the α-amino acid with the resin and deprotection of the *N*-terminus, the resulting amine

_____

can be directly acylated with a β-keto equivalent to **57**. Cleavage is achieved analogously to provide **58**.

A similar strategy can be applied for the synthesis of 6-membered tetramic acid analogs **61**. Instead of using α-amino acids as the starting material, β-amino acids like β-alanine or the more constrained anthranilic acid are to be used (*Scheme 6*).

Scheme 6: Synthetic strategy towards the synthesis of 6-membered ring tetramic acid analogs.

Examples of natural products containing quinoline-3-carboxamide **62** (*Figure 16*) are Linomide (**63**, immunomodulator as well as anti-angiogenic activities)[88;89] and the Militarinone[90] class of compounds (**64**).
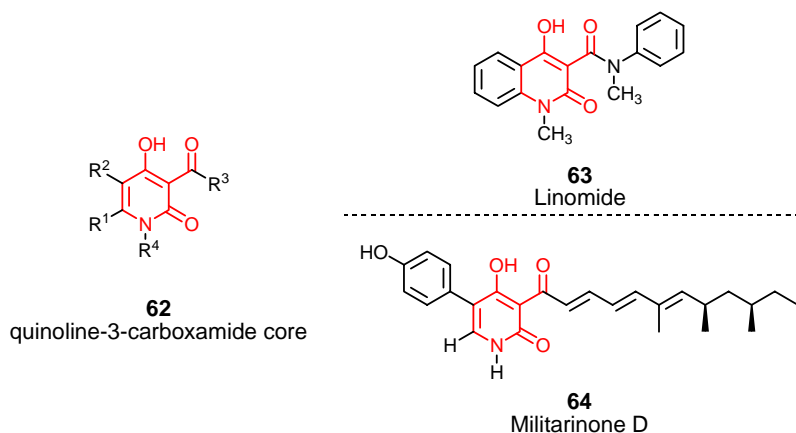
*Figure 16: Structure of quinoline-3-carboxamide core **62** and representative natural products Linomide (**63**) and Militarinone D (**64**).*

The modular assembly of tetramic acids by using a variety of commercially available or easily synthesized building blocks allows the synthesis of a diverse tetramic acid library. Furthermore, by using a solid-phase approach, not only is the carboxylic

_____

_____

functionality of the amino acid temporarily protected by being bound as an ester to the resin, time consuming workup steps and the purification of synthetic intermediates are eliminated. This is realized by washing the solid-phase with a cocktail of solvents; reactions on the solid-phase can be driven to completion by using large excesses of reagents. The cleavage method also ensures that only selected compounds are released from the solid phase: only substances with a β-keto entity will undergo concomitant cyclization and cleavage from the solid support. This synthetic strategy is amenable for larger scale solution phase synthesis of tetramic acids.

4.1.2 Implementation and Optimization of the Synthesis

Immobilization of the amino acid building blocks

The first step in the synthetic sequence is the immobilization of the amino acids to the solid phase. As delineated above, the amino acid is loaded onto the linker as an ester and the cleavage of the product from the resin is effected through a base-mediated cyclization and not an acid-mediated ester cleavage. Therefore, any hydroxyl-linker may be used, for example Merrifield or Wang resin. Wang resin (**65**, *Scheme 7*) was chosen because it allows the monitoring of intermediate compounds by cleavage with TFA, that can be undertaken using conventional glassware. Cleavage of intermediates from Merrifield resin would necessitate special apparatus because of the use of HF as the cleavage reagent.

For the synthesis of a diverse tetramic acid library, a variety of different α-amino acids were used as starting material: apolar (glycine (**66a**), valine (**66b**), leucine (**66c**)), heterocyclic (tryptophan (**66f**)) and basic (ornithine (**66d**) and arginine (**66e**)) amino acids were employed (*Scheme 7*).

All amino acids were protected on the *N*-terminus with the base-labile Fmoc group, enabling facile loading determination. Orthogonal protection of side chain functionalities was achieved with acid-labile protecting groups, such as the *tert*-butyloxycarbonyl (Boc, for lysine and ornithine), and pentamethyldihydrobenzofuran (Pbf, for arginine) protecting groups. A protecting group was not necessary for the indole nitrogen of tryptophan.

_____
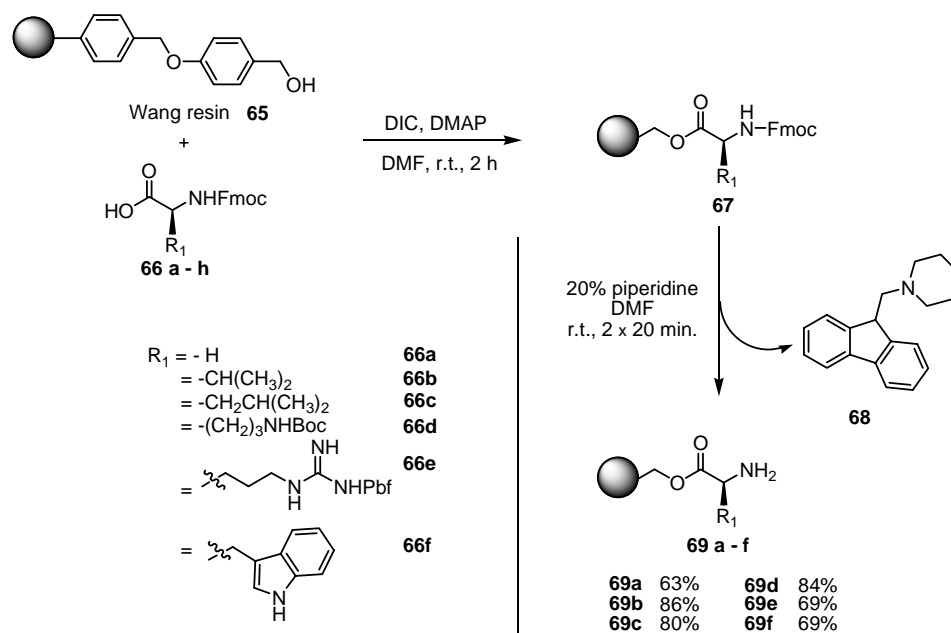
Scheme 7: Loading of Fmoc-protected amino acids onto Wang resin.

Secondary amino acids such as proline were also used and generated bicyclic tetramic acid **74** (*Scheme 8*). Such a bicyclic moiety was recently disclosed as part of the core structure of UCS1025A (**75**), an inhibitor of the telomerase enzyme.[91-93]
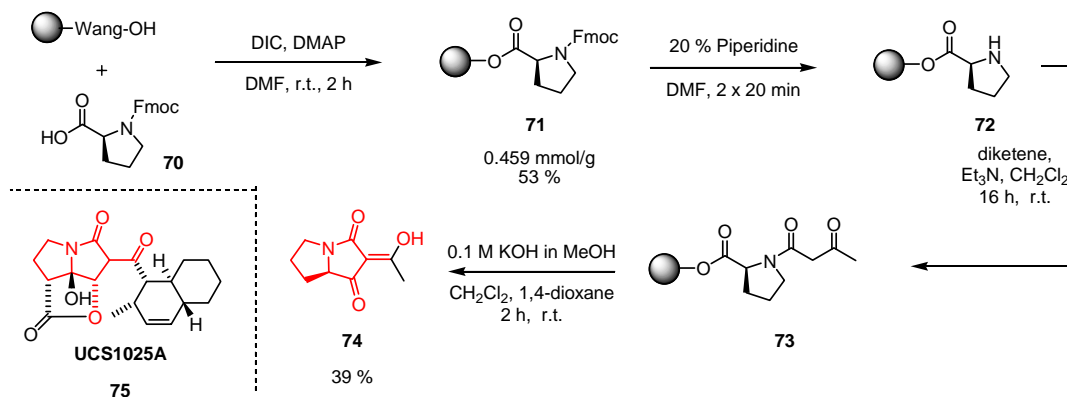

*Scheme 8: Proline-based tetramic acid bicycle **74** and structure of telomerase inhibitor UCS1025A (**75**).*

All *N*-Fmoc-protected α-amino acids were condensed with Wang-functionalized resin (1% DVB crosslinking, 100-200 mesh, 1.2 mmol/g), via a Steglich esterification (DIC, 5 mol% DMAP, DMF, 2 hours, r.t.).[94]

Loading of the resin was determined by the Fmoc-method[95] with spectrometric monitoring the absorbance of dibenzylfulvene-piperidine adduct **68** formed in the cleavage of Fmoc with piperidine in DMF (*Scheme 7*). The resin loadings ranged between 0.40 mmol/g and 0.75 mmol/g (63-86%), in reasonable agreement with published values.

For the synthesis of six-membered-ring tetramic acid analogs, β-amino acids were used as the starting materials. The simple β-amino acid β-alanine was loaded onto the resin using the Steglich esterification method described previously to provide Wang-β-alanine-Fmoc resin (**64**) in 68% yield (*Scheme 11*). Loading of conformationally restrained anthranilic acid (**76**) onto the resin to provide **78** proved to be more challenging (*Scheme 9*). After protecting anthranilic acid **76** with Fmoc-Cl and Na$_2$CO$_3$ in 1,4-dioxane from 0 °C to room temperature overnight in 86% yield, it was not possible to load it onto the resin via the Steglich esterification method, even after double coupling. This is probably due to the steric bulk of the system.
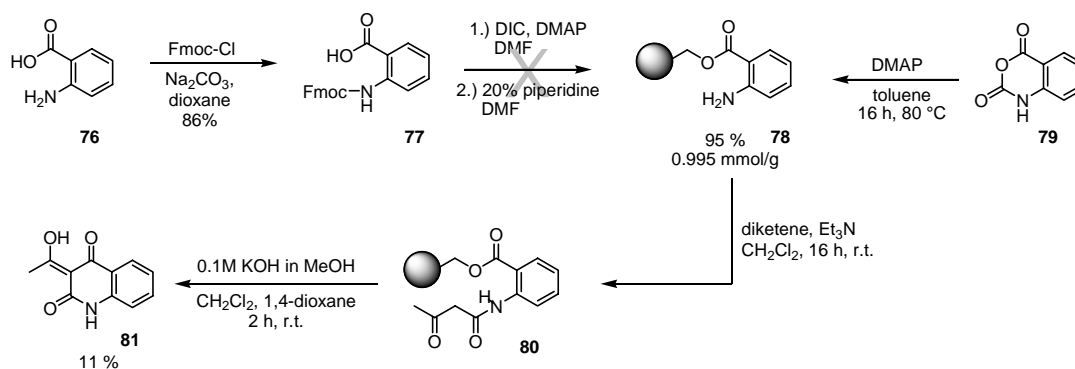
*Scheme 9: Loading of anthranilic acid onto Wang resin and synthesis of quinolinine-3-carboxamide **81***.

Because difficulties in loading the resin due to the steric bulk of Fmoc-anthranilic acid, a commercially available synthon, isatoic anhydride (**79**, *scheme 9*), was

_____

successfully condensed to the resin with DMAP at 60 °C for 16 h leading to resin-loaded anthranilic acid **78**. An advantage of this method is that no protecting group is needed. As the resin-bound anthranilic acid does not have a leaving group that can be spectroscopically monitored, the loading was determined by cleavage of a small aliquot of the resin with 90% TFA in dichloromethane. The determined loading demonstrated that the condensation reaction occurred in excellent yields (0.995 mmol/g, 95%).

Before any new functionalities were introduced, the Fmoc group was deprotected. This was achieved using standard conditions: 20% piperidine in DMF for 20 minutes at room temperature.

Functionalization by reductive amination

Additional diversity was introduced in a reductive amination step. After Fmoc-deprotection of an α-amino acid linked to Wang resin, the resulting primary amine **82** was treated with an aldehyde and NaBH(OAc)$_3$ in dichloromethane at room temperature for 16 h (*Scheme 10*). The aldehydes used were commercially available, and displayed a range of chemical properties: aliphatic, aromatic (electron-poor and – rich) and heteroaromatic aldehydes were successfully employed.
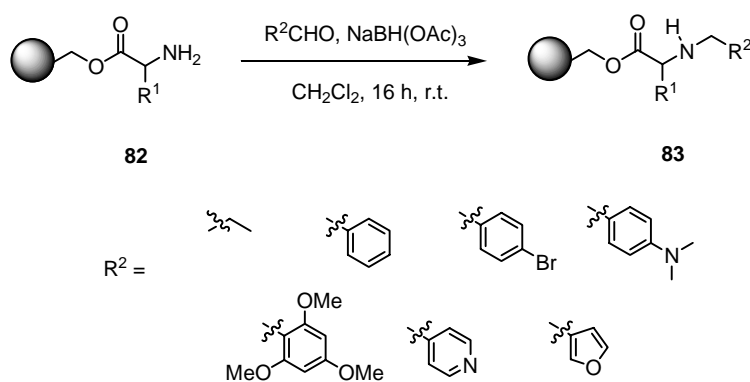
Scheme 10: Aldehydes employed to functionalize amine **82**.

Generally a 15-fold excess of aldehyde was used in the reaction. The yields ranged from 16-73%. Overalkylation to the tertiary amine accounted for the low yields, although no trends due to the nature of the aldehyde could be observed.

_____
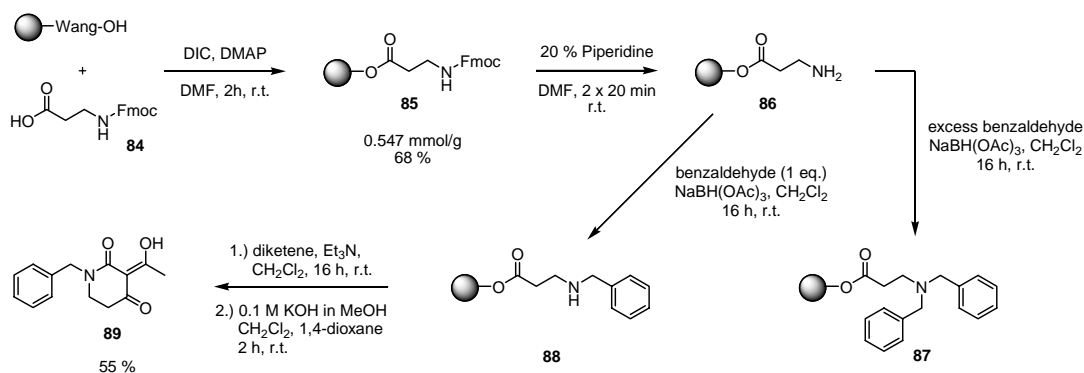
*Scheme 11: Reductive amination of β-alanine and synthesis of piperidine-2,4- dione **89**.*

Reductive amination of the β-amino acid β-alanine proved more problematic (*Scheme 11*): instead of obtaining the expected mono-alkylated product **88**, β-alanine readily underwent double alkylation to yield **87**, that was then unable to further undergo reaction with a β-keto equivalent, thus preventing the synthesis of the corresponding piperidine-2,4-dione **89**. The double alkylation may be the result of the higher pK_a, and thus higher nucleophilicity, of β-alanine's amine compared to that of an α-amino acid, as well as because of the lack of steric bulk at the α-position. This problem was overcome by reacting the β-alanine-loaded resin with only one equivalent of aldehyde to provide the desired secondary amine **88** in 83% yield as determined by cleavage from the resin with 90% TFA.

Functionalization by acylation

In a last functionalization step before cleavage, the resin-bound amino acid is acylated with a β-keto equivalent to generate the β-keto amide required for cleavage, as well as the 3-acyl moiety of 3-acyl tetramic acids. Different β-keto side chains, for example differing in length and electronic properties, were introduced in order to undertake SAR studies of the generated compounds.

To generate simple β-ketoamide **91**, commercially available diketene was reacted with triethylamine in dichloromethane for 16 h at room temperature (**A**, *Scheme 12*).[96] This method is not useful for generating more complex β-keto amides due to the lack of availability of diketene analogues.
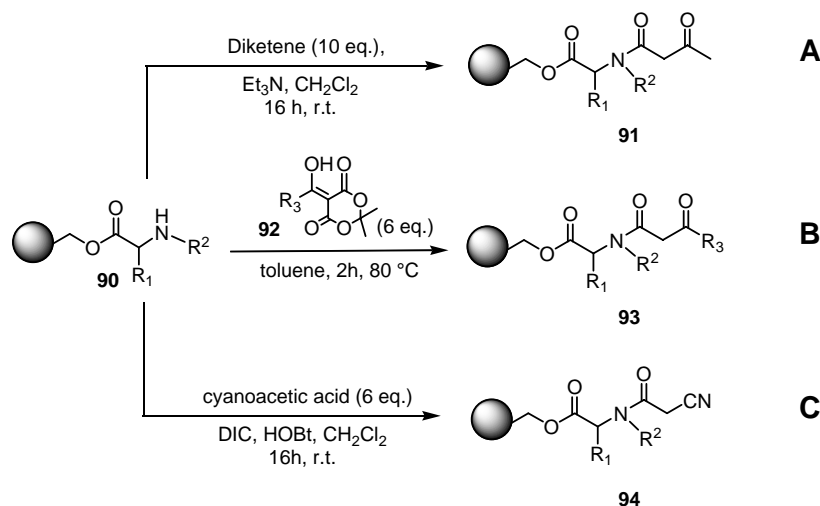
Scheme 12: Generation of various β-ketoamides with different acylating agents.

Alternatively, β-ketoamides were generated by the thermal rearrangement at 80 °C of 5-acyl Meldrum's acid **92** in toluene for 2 h.[97] This method was used to produce β-ketoamides with lipid side-chains of varying length **93** (**B**, *Scheme 12*).

As 5-acyl Meldrum's acids are not commercially available, they were prepared freshly by the reaction of a carboxylic acid **95** and Meldrum's acid (**96**) with an activating agent such as *N*, *N*-dicyclohexylcarbodiimide (DCC) together with a base (*Scheme 13*).[98] After completion of the reaction and filtration of the urea salt by-product, the generated DMAP salt of the acyl Meldrum's acid was transformed to the free 5-acyl Meldrum's acid by acidic extraction. The purity of the crude compound after acidic workup is >98% (HPLC) so that it was used directly for the next reaction without chromatographic purification. A variety of aliphatic acids including valeric (**97**, C_5), caproic (**98**, C_{10}) and palmitic acid (**99**, C_{16}) were transformed to the corresponding 5-acyl Meldrum's and used directly after workup.
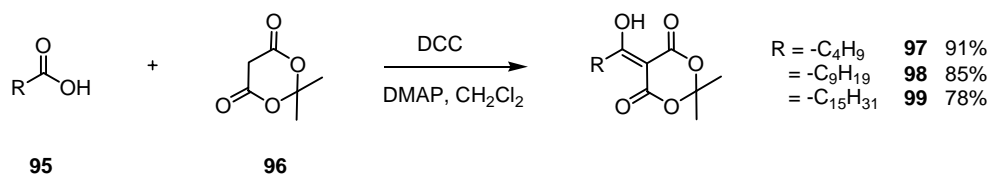
Scheme 13: Preparation of 5-acyl Medrum's acid.

_____

Resin-bound amino acids were acylated with cyanoacetic acid using *N,N*-diisopropyl carbodiimide and HOBt, as the coupling reagents, in dichloromethane for 16 h at room temperature (**C**, *Scheme 12*). These acyl-cyano amides **94** are the cyclization precursors to 3-cyano tetramic acids. Although there are no known examples of natural products with such a cyano-substitution pattern, numerous patents have been secured for their synthesis and biological activity, that ranges from activity against amgiotensin II antagonist[99] and as antihypertensive agents.[100]

Cyclization to tetramic acids

Cyclization of β-keto amides with a base is accompanied by the simultaneous cleavage of the 3-acyltetramic acid from the resin (*Scheme 14*). Side-products, such as primary amines that did not undergo β-ketoacylation, remain on the solid support as the cleavage conditions don't usually promote ester cleavage.
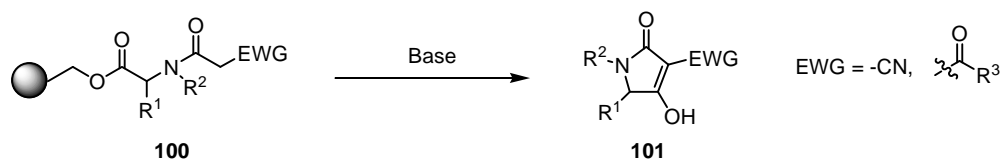
Scheme 14: Cleavage of β-keto amide 100 from the resin to generate tetramic acid 101.

Recently, there have been reports in the literature of different cyclization conditions.[84-86] The purity of the reaction products depends on the used base as well as the reaction temperature and time. Tetrabutylammonium hydroxide has been employed,[84] though it was necessary to further treat the product with Amberlyst A-15 ion exchange to remove the cleavage reagent. Cleavage with sodium ethoxide at 85 °C for 24 h or 30% DIPEA in dichloromethane[85] were also used to cleave the tetramic acids from the solid support, although the cleaved compounds underwent racemization. Cleavage with KOH in methanol[86] or with tetrabutylammonium fluoride (TBAF) in THF offer milder conditions compared to the above mentioned ones. Purity rather than yields determined the choice of the method used for cleavage in order to avoid time consuming purification steps of the compound library.

_____

_____

Especially the presence of hydroxyl nucleophiles lead to the generation of the corresponding carboxylic acids **104** and **105**, that cannot be transformed to the tetramic acid **103**, decreasing the cyclization/cleavage reaction yield (*Scheme 15*).
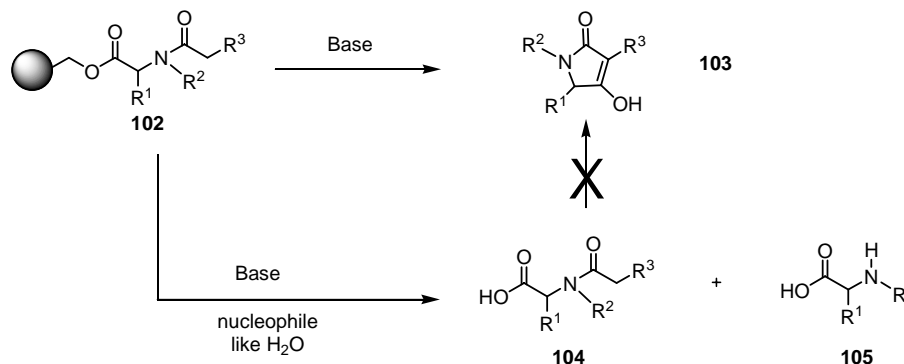
Scheme 15: Cyclization product and nucleophilically-cleaved products.

TBAF-mediated cleavage was effected by incubating a 1M solution of TBAF (in THF) with resin suspended in THF for 9h at room temperature. Although this method produces little side-products (HPLC), separation from the ubiquitous tetrabutyl ammonium salt required preparative HPLC purification, making this method not useful for the synthesis of a compound library. Cleavage with potassium hydroxide (0.1M in MeOH, 1 eq.) in dichloromethane/ methanol (1:1 mixture) for 1-2 h at room temperature provided the clean formation of the potassium salt of the tetramic acid. The formation of the carboxylic acid side-product was observed when wet solvents were used to prepare the cleavage cocktail. Due to the insolubility of tetramic acids in apolar solvents like dichloromethane, a polar solvent needed to be used in the cleavage cocktail. Initially, methanol/dichloromethane (1:1) was used; methanol though, shrinks the resin, diminishing the swelling properties of the resin and cleavage properties. 1,4-Dioxane was found to be a better alternative, enabling the resin to swell properly and also dissolving the product. The generated potassium salt of the tetramic acid was easily transformed to the tetramic acid by acidic extraction. A summary of the synthesized compounds is presented in *Table 2*.

A representative ^{1}H NMR of the cleavage product **102** directly after workup is shown in *Figure 17*.

_____
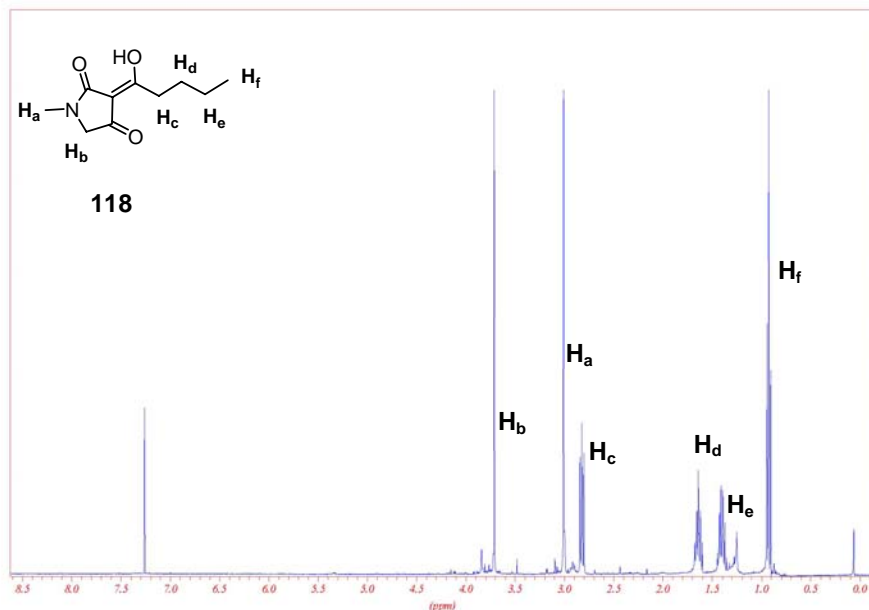
*Figure 17: ^{1}H NMR directly after cleavage from the resin of **120**.*

Un-*N*-alkylated cyanoacetic acid compounds **107** and **108** did not undergo a clean cyclative cleavage from the resin. Instead, cleavage by transesterification to the methyl ester derivative **109** occurred (*Scheme 16*).
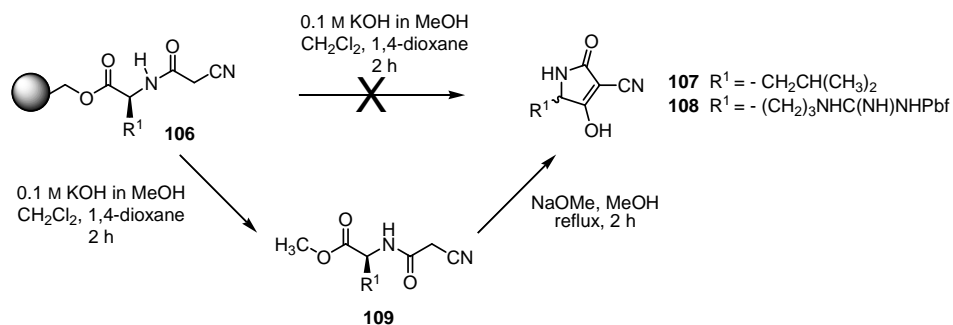
Scheme 16: Cleavage of the cyanoacetic acid derivatives

One possible explanation is that although the ester cleavage step is the same for all cleavages, the cyclization here is slower due to the stabilizing effect of the cyano group. The crude mixture was smoothly transformed to the cyclization product by refluxing for 2 h with NaOMe in methanol. Unfortunately, these conditions also promoted complete racemization at the C-5 2,4-pyrrolidinedione core, a problem that has been frequently observed in the literature.[79]

Table 2: Tetramic acids synthesized on solid support.

Entry	Nr.	Resin	Aldehyde	β-keto equivalent	Product	Yield
1	**19**		/			11 %
2	**74**		/			40 %
3	**81**		/			11 %
4	**89**					55 %
5	**107**		/			3 %
6	**108**		/			39 %
7	**110**		/			59 %
8	**111**		/			85 %
9	**112**					6 %
10	**113**		/			40 %
11	**114**		/			34 %

Entry	Nr	Resin	Aldehyde	β-keto equivalent	Product	Yield
12	**115**					38 %
13	**116**					15 %
14	**117**					18 %
15	**118**		/			43 %
16	**119**		/			42 %
17	**120**					47 %
18	**121**					8 %
19	**122**					2 %
20	**123**					16 %

Entry	Nr	Resin	Aldehyde	β-keto equivalent	Product	Yield
21	**124**					4 %
22	**125**					40 %
23	**126**					13 %
24	**127**					7 %
25	**128**					18 %
26	**129**		/	/		85 %
27	**130**		/	/		94 %

_____

4.2   Laccarin Analog Synthesis

4.2.1   Introduction

A variety of tetramic acids were synthesized according to the previously described method. To demonstrate the effectiveness of this method, the synthesis of an analog of a tetramic-acid-based natural product, Laccarin (**131**), was undertaken (*Figure 18*).

131
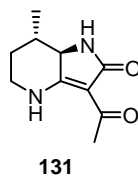
*Figure 18: Chemical structure of Laccarin (**131**).*

Laccarin (**131**) is a bicyclic tetramic acid isolated from the Japanese mushroom *Laccaria Vinaceoavellanea.*[101] It was shown to decrease the activity of cyclic-AMP phosphodiesterase by 30% at 0.64 mg/ml.[101]

4.2.2   Synthetic Plan

To date, there are no known total syntheses of this natural product. It can be retrosynthetically disconnected to tetramic acid **132** (*Scheme 20*), that can then be traced back to 1-methyl ornithine (**133**).

131   **132**   **133**
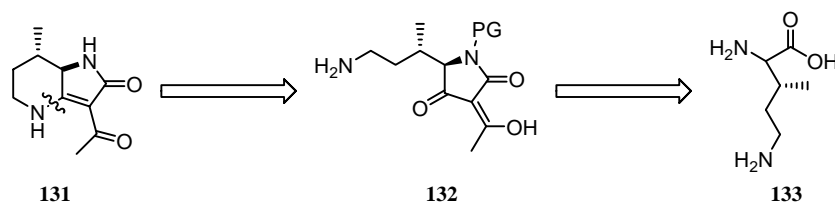
Scheme 17: Retrosynthesis of Laccarin.

Before embarking on the total synthesis of Laccarin, the synthetic sequence was tested on a model system **134** (*Scheme 18*). Enamine **134** can be disconnected to tetramic acid **135**, that should be readily synthesized from ornithine (**136**).

_____ 39

_____

134 ⟹ **135** ⟹ **136**
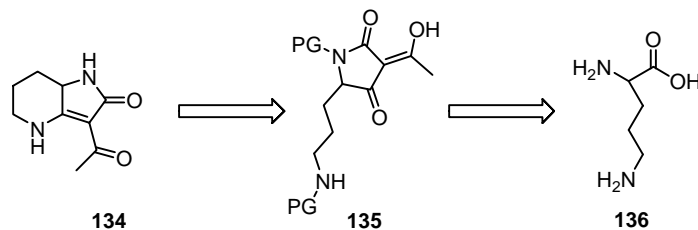
*Scheme 18: Retrosynthesis of Laccarin analog **134**.*

4.2.3 Towards the Synthesis of a Laccarin Analog

A solid-phase approach was chosen over solution-phase synthesis in order to facilitate the generation of analogs. The solid-phase synthesis began with the loading of commercially available Fmoc-L-ornithine-(*N*-Boc)-OH (**137**) on Wang resin via Steglich esterification providing **69d** in 84% yield (*Scheme 19*).[102]
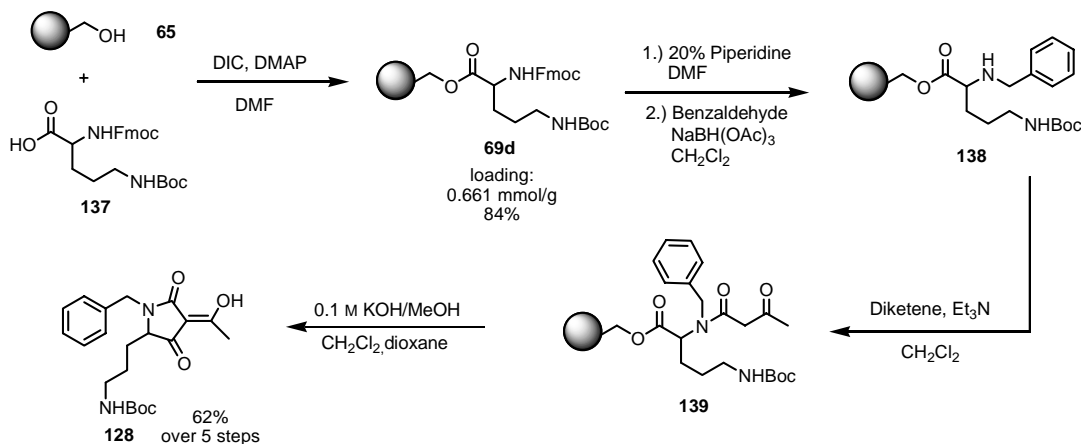
*Scheme 19: Solid phase synthesis of **128**.*

Following Fmoc deprotection with 20% piperidine in DMF, the amine was reductively alkylated with benzaldehyde and NaBH(OAc)$_3$ in dichloromethane for 18 h at room temperature to **138**. Reaction with diketene and triethylamine in dichloromethane, from 0 °C to room temperature, for 16 hours produced **139**. Cyclization and concomitant cleavage 0.1M KOH in 1:1 dichloromethane/1,4-dioxane at room temperature for 1 hour provided **128** in 62 % yield over 5 steps.

_____ 40
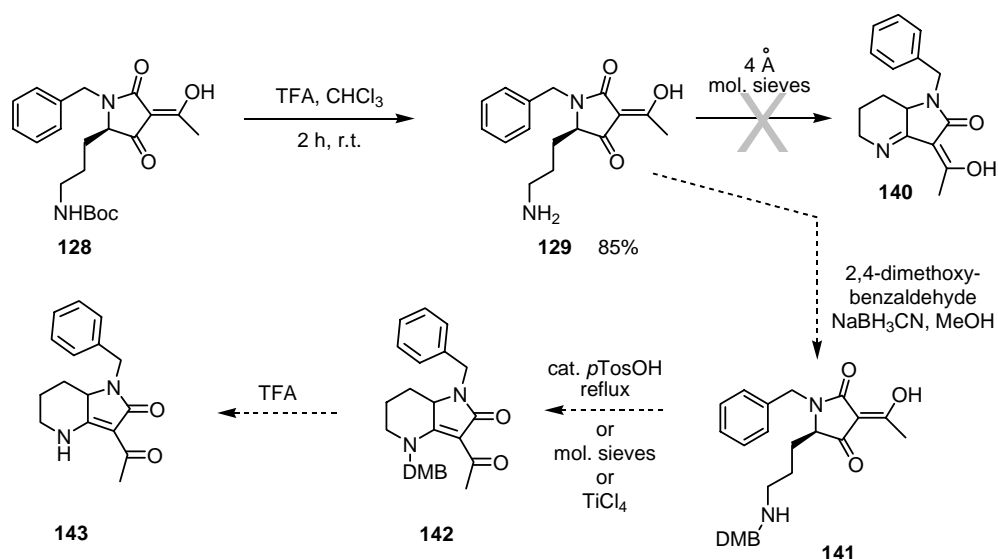
*Scheme 20: Proposed synthesis of model system **143**.*

Deprotection of the Boc group on the *N*-terminal amine of **128** was achieved with 95% TFA in chloroform for 2 hours at room temperature to give **129** in 85% yield. An attempt was made to generate imine **140** by heating to 80 °C in the presence of molecular sieves was not fruitful as only starting material was recovered. To promote the generation of enamine **143** instead of imine **140**, the terminal amine of **129** should be temporarily protected as a secondary amine. The dimethoxybenzyl (DMB) protecting group is suited to this purpose as it is readily incorporated via reductive amination with 2,4-dimethoxybenzaldehyde and can be removed under acidic conditions with TFA. Therefore, after reductive amination of **129** with 2,4-dimethoxybenzaldehyde with NaBH$_3$CN to generate **141**, enamine formation should be possible either by undertaking azeotropic distillation or by refluxing **141** in the presence of dehydrating agents such as molecular sieves or TiCl$_4$ to generate **142**. TFA-mediated cleavage of **142** should provide model compound **143**.

_____

4.3   Synthesis of Building Blocks for Indole-Based Tetramic Acids

4.3.1 Introduction

The indole moiety is one of the most widely distributed heterocyclic scaffolds in nature. Recently, a novel class of indole-containing natural product analogs, the indolyldihydroxyquinones **150** (*Figure 19*) have been reported to inhibit Cdc25A, a cell cycle control protein, in the low micromolar range.[103]
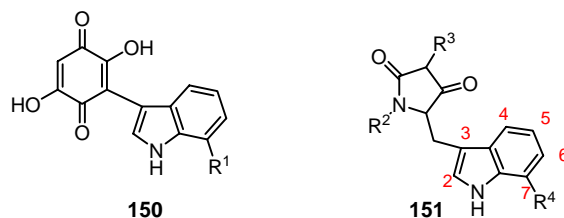
*Figure 19: Structure of indolyldihydroxyquinone **150** and indole-based tetramic acids **151**.*

The substitution pattern of the indole was varied in the reported study. Modifications at the 2- and 4-position decrease inhibitory potency. Variations at the 5-position appeared to have little effect. Substitution at the 7-position with groups larger than propyl significantly increased potency. The authors argue that the C-terminal tail of Cdc25A, that is important for binding protein substrates, is also important for binding inhibitors with hydrophobic substituents at the 7-position. Furthermore, it is assumed that the anionic quinone moiety binds to the positively charged Arg 482 in the active site of Cdc25A.[104] Intrigued by these finding and also by the fact that the tetramic acid core also behaves as a negatively charged head group,[105] a synthetic route was established to provide chimeric molecules of the basic structure **151**, with a tetramic acid core and a 7-substituted indole side-chain.

4.3.2 Synthetic Strategy

To access such compounds, a modular strategy was chosen involving a biomimetic synthesis of tryptophan analogs **152** starting from an indole **153** and serine (**154**, *Scheme 21*).

_____

_____
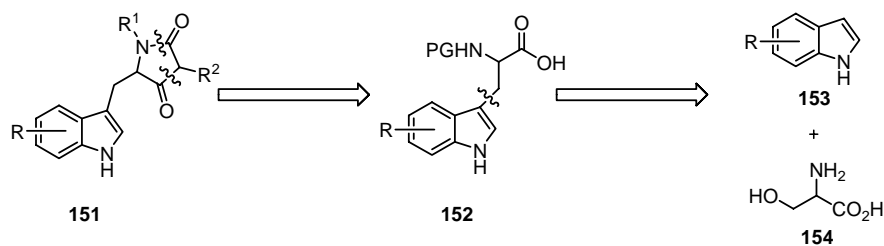
*Scheme 21: Retrosynthesis of indole-based tetramic acids **151**.*

This is a concise and modular synthesis. The indole building blocks can be produced with various functionalities and substitution patterns from the many developed indole syntheses.

4.3.3 Indole Synthesis

As the indole core is a reoccurring scaffold in both natural and synthetic products, many methods are available for their synthesis including the classical Fischer indole synthesis,[106] the Madelung synthesis[107] as well as numerous Pd-catalyzed cyclizations.[108] However, few methods have been developed to specifically synthesize 7-substituted indoles. Currently, the Bartoli indole synthesis is the quickest and simplest method to access 7-substituted indoles **157** from readily available nitroarenes **155** and 3 equivalents of vinyl Grignard reagents (**156**, *Scheme 22*).[109]
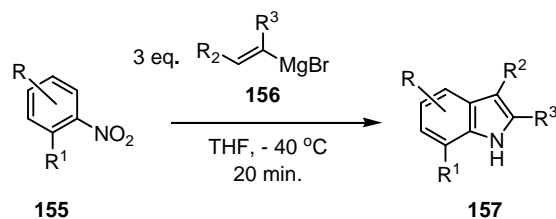
Scheme 22: Bartoli indole synthesis.

The mechanism involves the generation of nitrosoarene complex **158** that undergoes single electron transfer (SET) then a [3,3]-sigmatropic rearrangement followed by a cyclization to afford indole **157** (*Scheme 26*).[110]

_____

_____
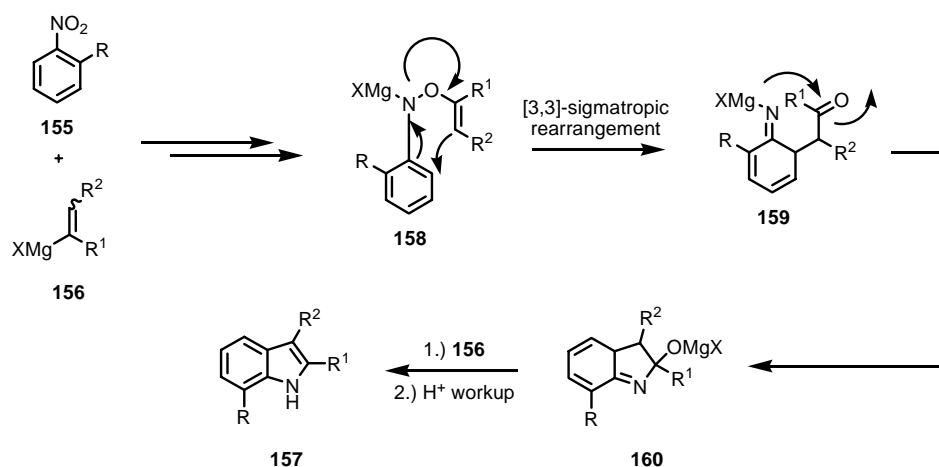
Scheme 23: Proposed mechanism for the Bartoli indole synthesis.

Ortho-substituents are necessary for this reaction to take place. It is assumed that the *o*-substituent is needed in order to push the nitro-group out of the aromatic plane.[110]

All nitroarenes used were commercially available except compounds **163** and **164**, that were synthesized from 4-bromophenol in three steps. First, 4-bromo-phenol **161** was nitrated using silica gel impregnated with nitric acid,[111] then the phenol moiety was protected as either a benzyl- or TBDPS-ether (*Scheme 24*).[112]
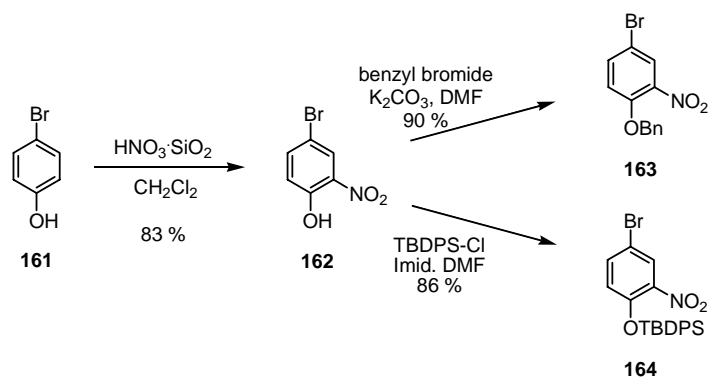
*Scheme 24: Synthesis of substituted nitroarenes **163** and **164**.*
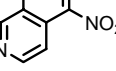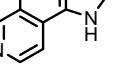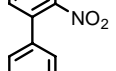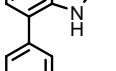
_____

_____
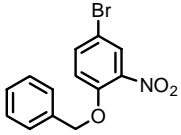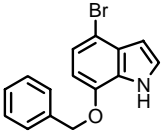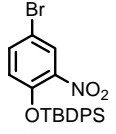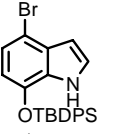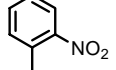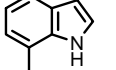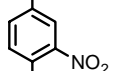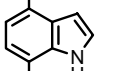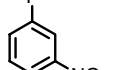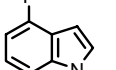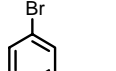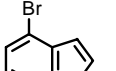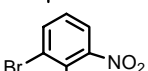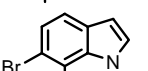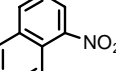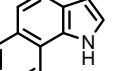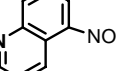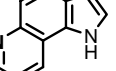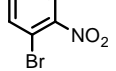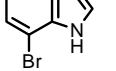
Nitroarenes **163-174** were used in the synthesis (*Table 3*). Halogenated and non-halogenated nitroarenes with methyl substituents at the ortho position were successfully employed.

The isolated yields ranged from 6 to 61%, and are lower than literature reported yields.[109;113;114] A major byproduct isolated was the corresponding aniline from the nitroarene starting material. Attempts were made to optimize yields. Reduction of the reaction temperature below -40 °C did not provide better yields, most likely due to the decreased solubility of the Grignard reagent at those temperatures. Addition of solubilizing agents like dimethoxyethane was not helpful. The order of reagent addition was also reversed: instead of adding the Grignard to the nitroarene, the nitroarene was added to the cooled Grignard solution in order to maintain an excess of Grignard at all times. Unfortunately, these attempts were not fruitful either.

Some nitroarenes that could not be converted to 7-substituted indoles (entries 2, 11, 12 in *Table 3*). In the case of **176**, it is plausible that the bulk of the TBDPS group shields the nitro group, sterically restricting the formation of the required nitroso-Grignard intermediate. A similar reasoning could account for the lack of product formation for **186**.

With the 7-substituted indole building blocks in hand, it was now possible to undertake the synthesis of 7-substituted tryptophan analogs.

Table 3: Indoles synthesized via Bartoli indole synthesis.

| Entry	Subst. Nr.	Nitroarene	Prod. Nr.	Product	Yield
1	**163**		**175**		43 %
2	**164**		**176**		0 %
3	**165**		**177**		6 %
4	**166**		**178**		38 %
5	**167**		**179**		31 %
6	**168**		**181**		41 %
7	**169**		**181**		61 %
8	**170**		**182**		8 %
9	**171**		**183**		15 %
10	**172**		**184**		51 %
11	**173**		**185**		0 %
12	**174**		**186**		0 %

_____

4.3.4 Tryptophan Synthesis

Snyder first described a biomimetic synthesis of tryptophan based on the heating of an indole **187** with *N*-acetyldehydroalanine (**188**, *Scheme 25*, **A**).[115] Yokoyama investigated this reaction and modified it to increase the yields and to use readily available, cheap starting materials: instead of beginning the synthesis with acetyl dehydroalanine, a reactive intermediate is generated in situ by heating *dl*-serine (**154**) with acetic acid and acetic anhydride to 80 °C (*Scheme 25*, path **B**).[116]
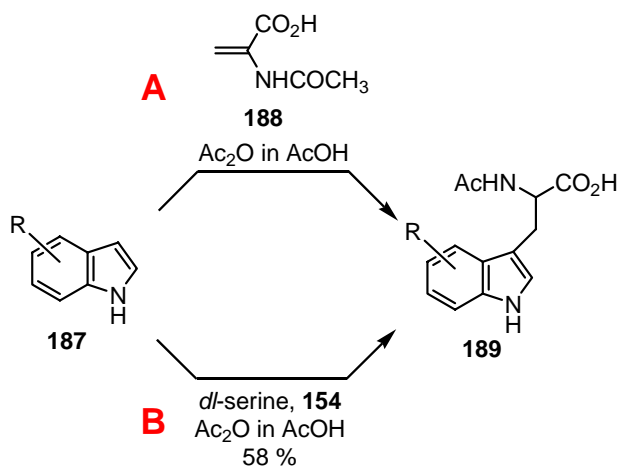
*Scheme 25: Synthesis of tryptophan analogs according to Synder (**A**) and Yokoyama (**B**).*

This biomimetic route to tryptophan analogs has the advantage that it requires only two steps and does not involve expensive reagents. Deprotection of the generated acyl group can be achieved either chemically or enantioselectively with an acylase such as *Aspergillus* Acylase I.[117] A plausible mechanism for this reaction is delineated in *Scheme 26*.[118] Since product **194** is completely racemized, nucleophilic substitution at the hydroxyl carbon of (L)-serine (**195**) can be excluded. Two equivalents of acetic anhydride are required for the reaction when starting with serine. It is assumed that the first equivalent of Ac_2O acetylates the amine, while the second equivalent reacts with the carboxylic acid causing spontaneous formation of oxazolone **191**. After dehydration, Michael addition of the indole to the reactive double bond of the conjugated oxazolone **192** provides tryptophan analog **194**.

_____

_____
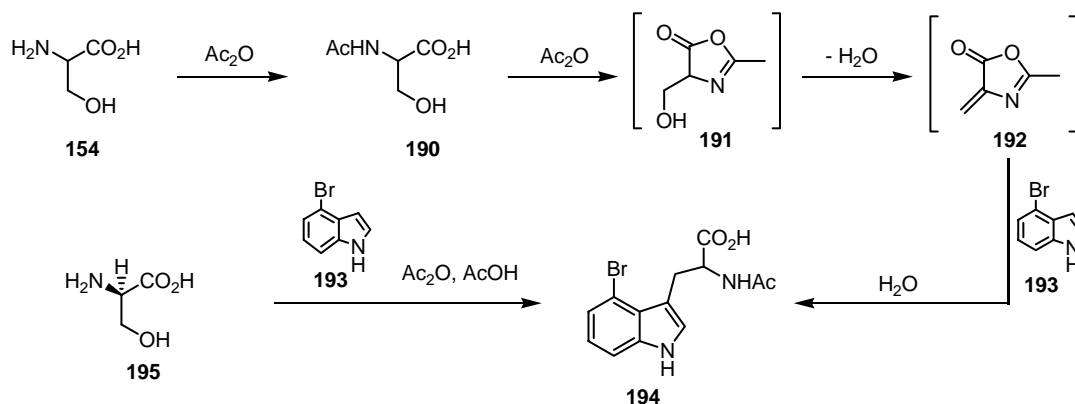
*Scheme 26: Proposed mechanism for the biomimetic synthesis of 4-bromotryptophan (**194**).*

Selected indoles were used as substrates in this reaction (*Table 4*). Halogenated indoles were particularly interesting as they can be modified in later synthetic steps using palladium-catalyzed chemistry to generate different substituents. The yields vary from 6 to 42%. Many byproducts are formed under these reaction conditions. The major side-product isolated was dehydroalanine. Other products evolved from the decomposition of the indole under rather harsh acidic conditions. The formation of 4-fluorotryptophan (*Table 4*, entry 4) was not successful: the electron-withdrawing properties of fluorine might account for the lack of reactivity.

_____

_____

Table 4: Tryptophan analogs synthesized.
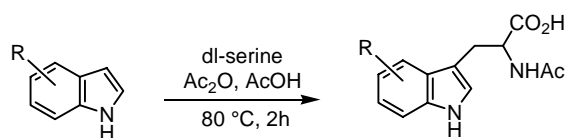
Entry	Indole Nr.	Indole	Prod. Nr	Product	Yield
1	**175**		**196**		42 %
2	**177**		**197**		16 %
3	**178**		**198**		14 %
4	**179**		**199**		0 %
5	**180**		**200**		6 %
6	**181**		**201**		19 %
7	**193**		**194**		31 %

_____

_____

4.4 Investigation of the Biological Properties of the Tetramic Acid Library

The following sections deal with the testing of the synthesized tetramic acid library to find modulators of the Ras signaling cascade, of phosphatase activity and of bacterial growth.

4.4.1 Targeting the Ras Signaling Pathway

Small molecules that modulate the function of macromolecular targets in the cell are invaluable tools to dissect cellular processes. One such process is epithelial-mesenchymal transition (EMT), that involves the transformation of a cell from a round, epithelial to an elongated, fibroblastoid phenotype. This occurs as a key developmental step in embryonic morphogenesis and has now been implicated in the progression of primary tumors towards metastasis.[22] Multiple signaling pathways, including a hyperactive Ras pathway, are involved in inducing EMT (see *Figure 7*, p. 8).

Various epithelial cell-lines, like the murine NIH3T3[119] or canine Madine-Darby canine kidney cells (MDCK),[120] have been observed to undergo EMT-like transformation from a round to an elongated cell shape when transformed with oncogenic Ras. There have also been reports of small molecules that reversed the phenotype of such transformed cells: Sulindac[121] and Sulindac analogs[122] have been shown to induce such a phenotypical reversal in Ras-transformed MDCK cells. The tetramic acid natural products Melophlin A and B (*Figure 12*, p. 17), isolated from marine sponges, have also been reported to reverse the phenotype of NIH3T3 Ras-transformed cells.[64]

Based on this interesting observation, a screening strategy was established to identify compounds from the tetramic acid library that affect the EMT-like phenotype in H-Ras transformed cells and to begin to elucidate their mechanism of action (*Figure 20*). To this purpose, the synthesized collection of compounds was first tested for cytotoxicity as compounds that are more toxic towards the transformed cell lines may be interesting lead structures. The compounds were also subjected to a phenotype-based assay. A compound was considered a hit when it reversed the morphology of H-

_____

_____

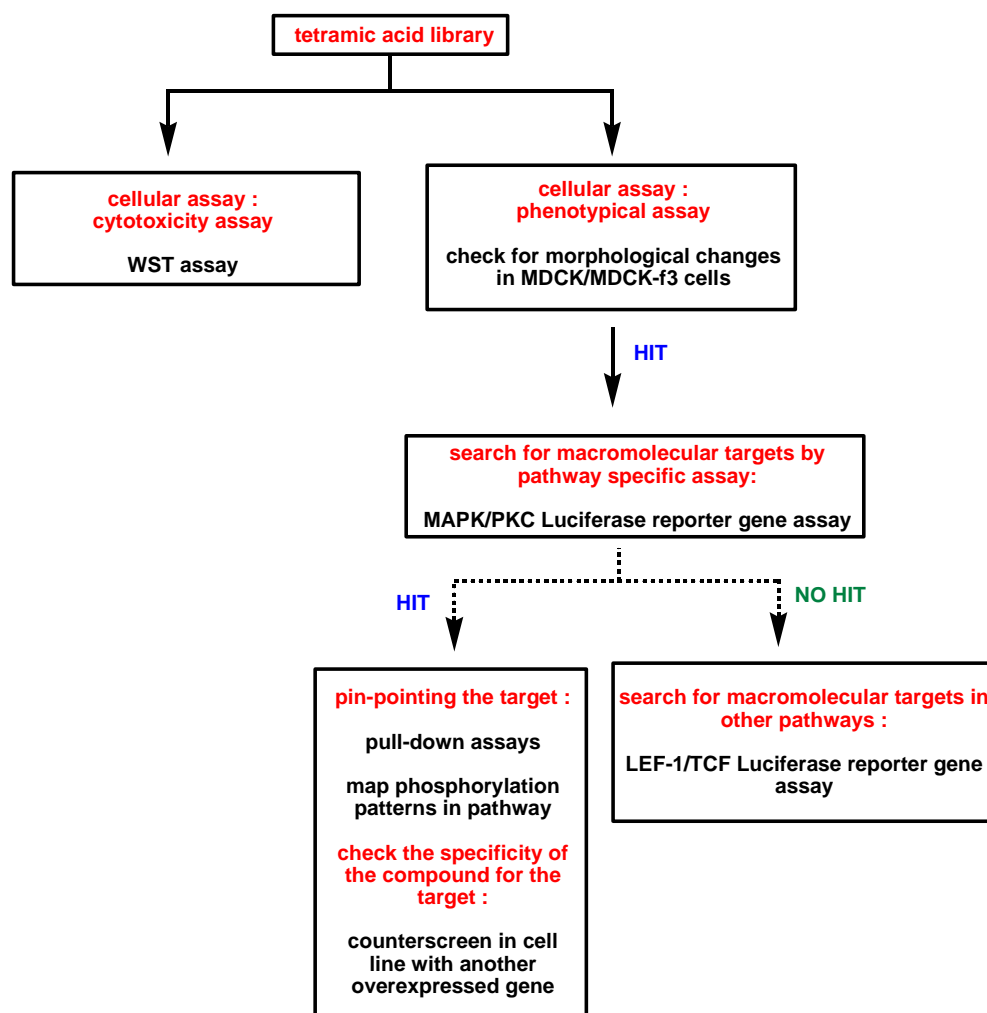Ras transformed cells. Next, the hit compounds were tested in pathway-specific cellular assays.

Figure 20: Screening strategy for the tetramic acid library.

In the following sections, the outcome of the application of this strategy will be presented: the results of the cytotoxicity assay and phenotypical assay on H-Ras transformed MDCK cells will first be presented. The attempts to elucidate the pathway modulated by hit compounds by using a pathway-selective assay will then be described.

Cytotoxicity assay

When treating cells with compounds, it is necessary to evaluate the effect of the stimuli on the proliferative activity and survival/viability of the cell. These parameters

_____

_____

can be effectively monitored by taking advantage of the reducing potential of the cell mitochondrion: mitochondrial dehydrogenases reduce tetrazolium compounds inducing colorimetric changes. A commonly used indicator is 3-(4,5-dimethylthiazol-2-yl)-2,5-diphenyl tetrazolium bromide (MTT).[123] Living cells convert the yellow-colored MTT to a dark blue, water insoluble formazan. For colorimetric determination, the MTT-formazan needs to be dissolved in isopropyl alcohol. To overcome this solubilization step, an alternative tetrazole was used: 4-[3-(4-Iodophenyl)-2-(4-nitrophenyl)-2H-5-tetrazolio]-1,3-benzene disulfonate (WST-1, *Scheme 27*).[124] The slightly red WST-1 (**210**) is converted upon reduction to the dark red formazan **211**, that is measured at 540 nm.
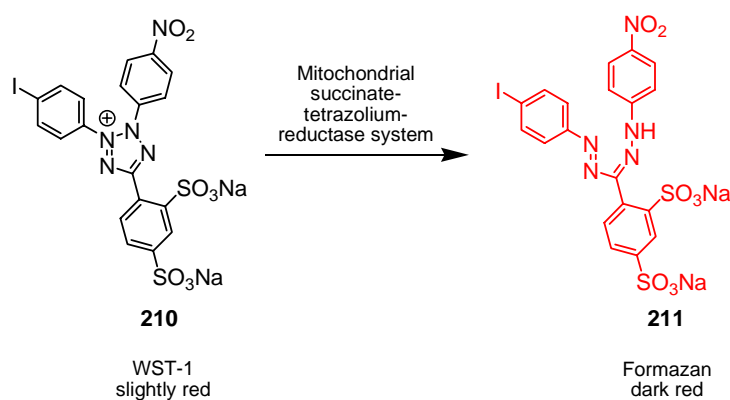
*Scheme 27: Conversion of WST-1 (**210**) to a formazan **211** by the mitochondrial succinate tetrazolium reductase system.*

The intensity of the signal correlates to the cell count and metabolic activity of the cell. As apoptosis is an active mode of cell death requiring metabolic activity, colorimetric assays might underestimate cellular damage from the tested compounds and detect cell death only at later stages of apoptosis when the metabolic activity is already reduced. Comparison of the percentage of living MDCK and MDCK-f3 cells also provides information on the sensitivity of the cell towards the compounds. It would be desirable to have compounds that are selectively cytotoxic towards oncogenic MDCK-f3 cells.
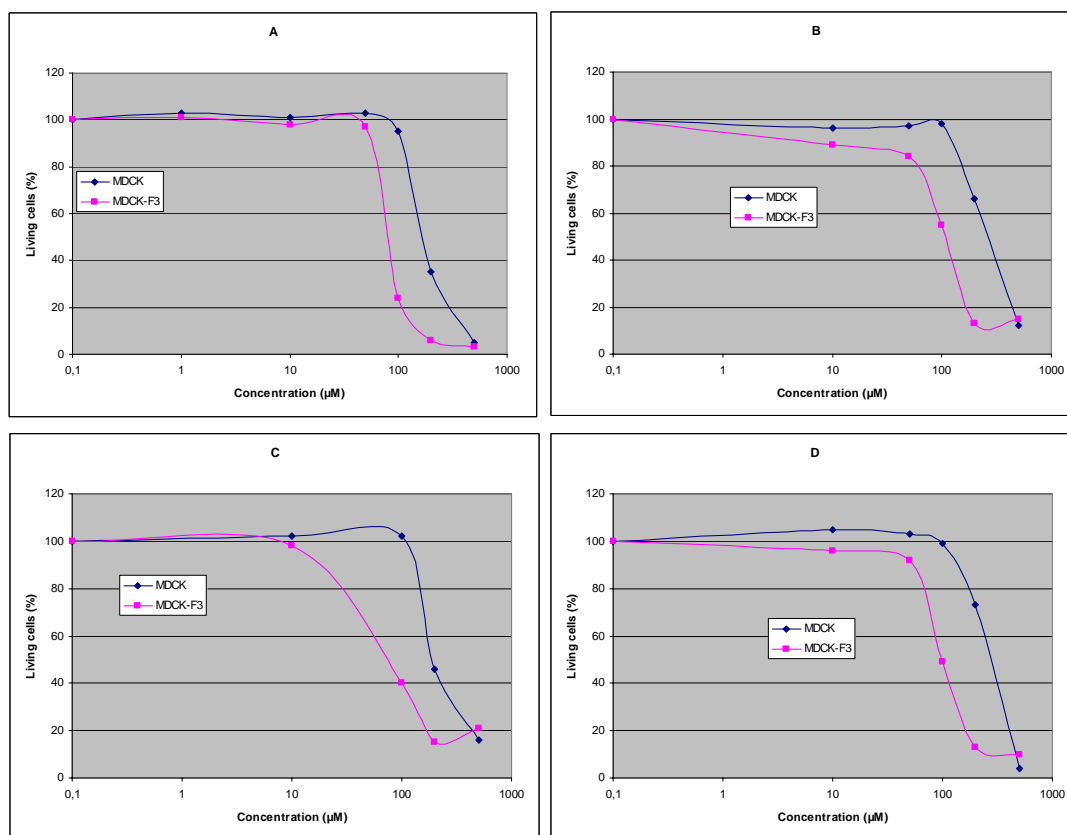
_____

_____

*Diagram 1: Cell cytotoxicity assay results for compounds **19** (**A**), **118** (**B**), **119** (**C**), and **120** (**D**). Curves depict the dependence of the percentage of living cells on the concentration of compounds.*

Four compounds were identified to have an effect on the cell viability of MDCK and MDCK-f3 cells: **19**, **118**, **119**, **120** (*Figure 21*).
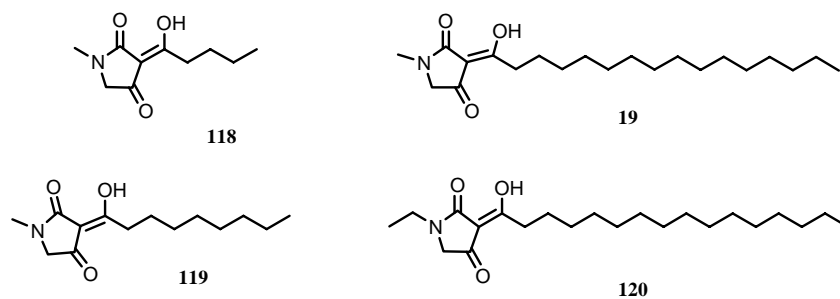

*Figure 21: Structure of cytotoxic compounds **19, 118, 119, 120**.*

The IC$_{50}$s range from 150-280 µM for MDCK cells and 60-100 µM for MDCK-f3 cells. Interestingly, these compounds are structurally similar to Melophlin A: all

_____

_____

glycine-based tetramic acids with a lipophilic tail (C_4-C_{14}) and are *N*-alkyl substituted (*N*-methyl or *N*-ethyl). Generally, the Ras-transformed MDCK-f3 cells appear to be at least two-fold more sensitive towards the tested compounds than the untransformed MDCK cells. All other compounds tested were found not to be cytotoxic towards either MDCK or MDCK-f3 cells.

Phenotypical Assay

Transformation of cells with the Ras oncogene leads chronic activation of the MAPK pathway and in certain cell lines to significant morphological changes. When Madine-Darby canine kidney cells (MDCK), an immortalized epithelial cell line, are stably transfected with the Ras oncogene, the resulting MDCK-f3 cells are long and spindle-shaped, grow in multiple layers without regular cell-cell contacts (*Figure 22*).
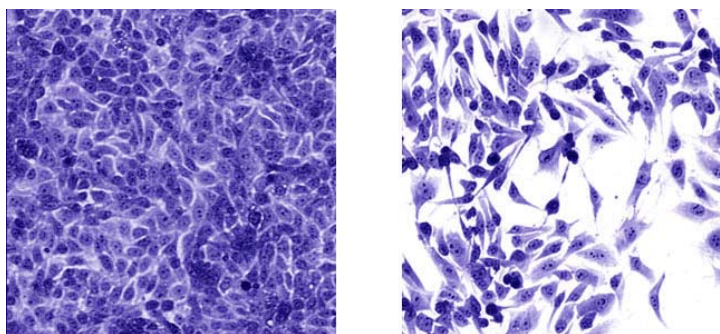

Figure 22:   Morphology of normal MDCK (left) and H-Ras transformed MDCK-f3 cells (right).

Since transformation with H-Ras induces such a significant morphological change, alterations in cellular morphology can be used as a parameter for measuring the effects of a compound on an activated H-Ras pathway.

Before assaying the tetramic acid library, the validity of this MDCK-Ras phenotypical assay was tested using a known mitogen activating protein kinase kinase (MEK-1) inhibitor, PD98059.[125] MEK proteins are dual-specificity kinases that occur as two homologues that are ubiquitously expressed in mammals. They play a central role in the mitogen activating protein kinase (MAPK) pathway and in transducing proliferative stimuli in a broad spectrum of human cancer cells. They have also been

_____

_____

implied in the development of a range of human tumors,[126] that make them interesting targets to study the progression of cancer and to develop potential therapeutics. PD98059 (**4**, *Figure 23*), was one of the first documented MEK inhibitors[125] and has become an invaluable tool for exploring the role of MEK in a number of physiological processes.

4
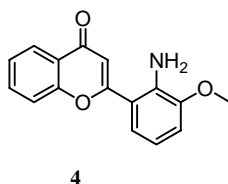
*Figure 23: Chemical structure of PD98059 (**4**).*

It acts as a non-competitive ATP inhibitor with an IC_{50} of 5 μM. By binding to the inactive form of MEK, PD98059 prevents the activation of MEK by upstream kinases.[127]

PD98059 was used as a positive control to validate the Ras-transformed MDCK phenotypical assay. A reversal of the phenotype of transformed MDCK-f3 cells is expected upon incubation with PD98059. This is indeed what is observed: islands of epithelioid cells were detected among transdifferentiated, fibroblast-like MDCK-f3 cells (*Figure 24*). The morphology of the cells changed in a concentration-dependent manner forming a tight cobblestone-like monolayer at confluence. The phenotypical change is visible beginning at a concentration of 10 μM whereas below this concentration, the cells retain their fibroblast-like structure. Dudley et al. report a similar morphological change in Ras-transformed NRK rat kidney cells, but only measured at a single concentration, 50 μM.[125]

These results with PD98059 validate the use of this phenotypical assay to screen for compounds that may affect the Ras/MAPK signaling pathway.
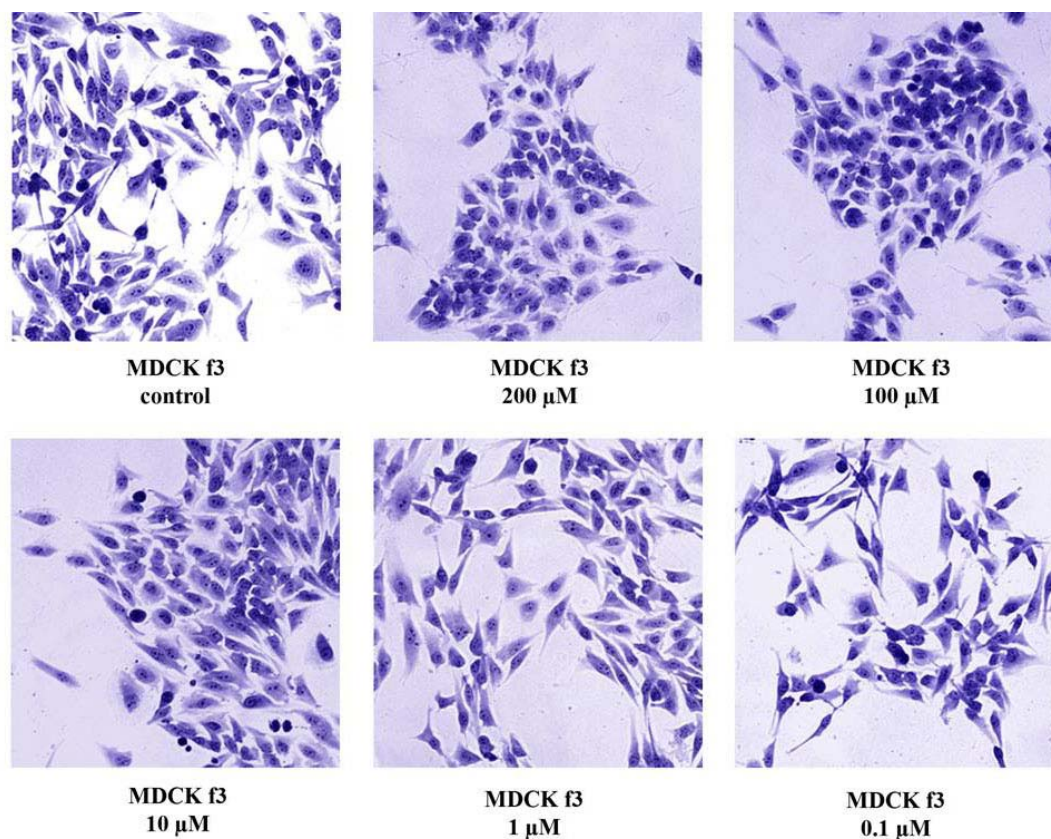
_____

Figure 24: Morphological reversion of MDCK-f3 cells following addition of PD98059 at various concentrations.

The compounds from the tetramic acid library were tested in this phenotypical assay (see Appendix B). Two compounds **110** and Melophlin A (**19**, *Figure 25*) induced a concentration-dependant morphological change of the MDCK-f3 cells from the elongated to the more cell-cell adhesive phenotype beginning at a concentration of 50 µM. Below this concentration, the cells retained their native spindle shape.
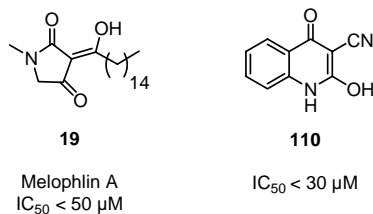
*Figure 25: Structures of active, screened compounds **19** and **110**.*

_____

As mentioned before, Melophlin A has been shown to transform the cell morphology in Ras-transformed mouse fibroblast cells NIH3T3 at a concentration of 13 μM.[64] The three-fold higher concentration observed here for MDCK-f3 cells (*Figure 26*) is in reasonable agreement with literature values given that several assay parameters differ. Deviations may be due to the low solubility of **19** in aqueous solution. Another possibility is that a different cell line was used than described in the literature: Melophlin A was originally tested in a murine cell line instead of the canine cell line used in these experiments. Furthermore, serum conditions may differ from the literature reported experiments.

MDCK f3   **MDCK f3**   **MDCK f3**
control   **50 μM**   **10 μM**
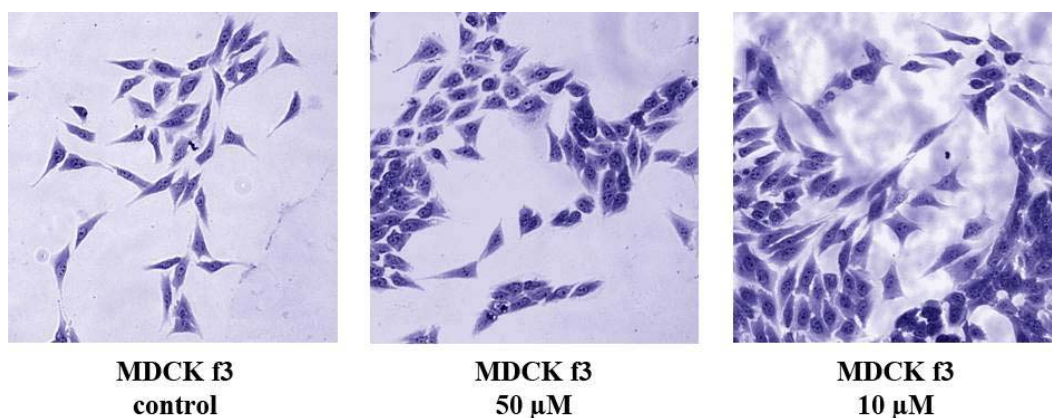
*Figure 26: Morphological reversion of MDCK-f3 cells following addition of Melophlin A (**19**) at various concentrations. Concentrations of Melophlin A higher than 100 μM are cytotoxic for the cells.*

Three other analogs, differing from Melophlin A in the length of the side chain (**118** and **119**, *Figure 27*) and in the *N*-alkylation pattern (**120**), were tested in the phenotypical assay. The analogs with C$_4$ or C$_8$ lipid side-chains were not able to reverse the phenotype of MDCK-f3 cells, indicating that there appears to be a minimum length for the lipid side-chain in order to observe activity. Furthermore, *N*-ethyl-derivative **120** was not able to reverse the morphology of the cells, pointing out that longer or bulkier *N*-alkyl groups probably hinder modulation of the target protein(s).
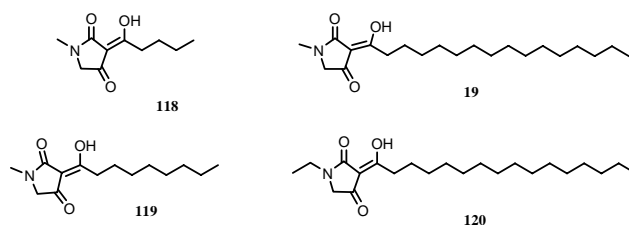
_____

_____

Figure 27: Chemical structure of Melophlin A analogs tested in the MDCK/MDCK-f3 phenotypical assay.

Interestingly, hydroxyquinolinone **110** was also able to induce morphological changes in MDCK-f3 cells beginning at a concentration of 50 µM (*Figure 28*). No cytotoxic effects were observed towards either MDCK or MDCK-f3 cells. In contrast, hydroxyquinolinone **81** did not demonstrate an effect. There is no known precedence for the ability of cyanohydroxyquinolinones to reverse the morphology of H-Ras transformed cells, making this an interesting lead structure.
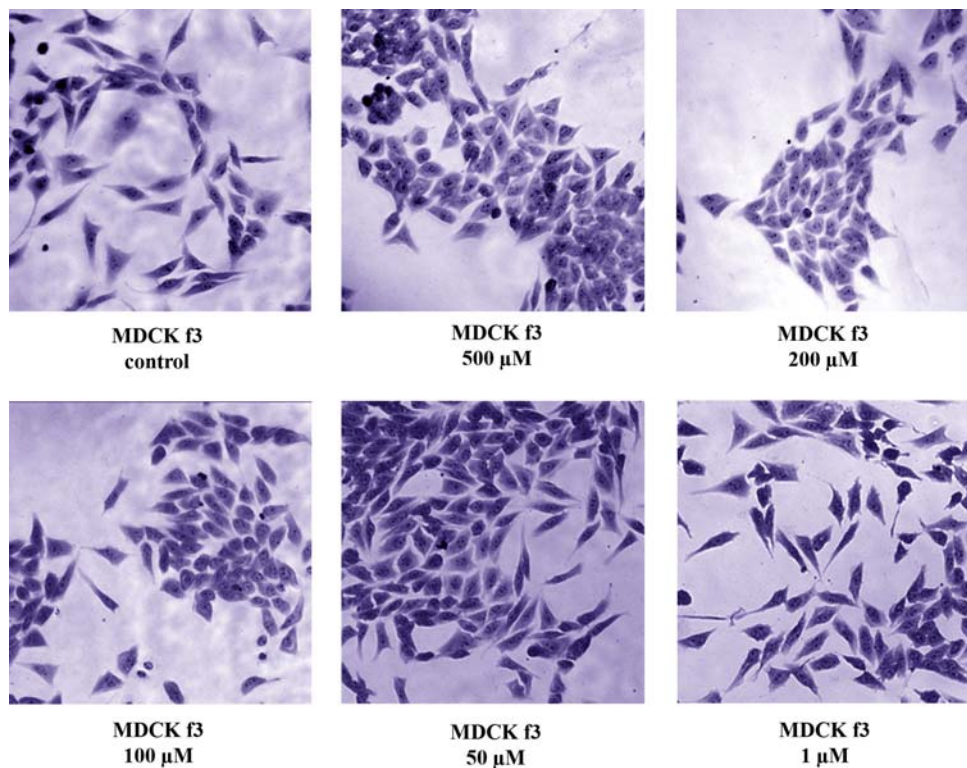
*Figure 28: Morphological reversion of MDCK-f3 cells following addition of **110** at various concentrations.*

_____

_____

Summarizing, two molecules from the small library were identified with the ability to induce phenotypical changes in Ras-transformed MDCK cells. A more precise localization of the target protein(s) cannot be deduced from the results of this assay as several pathways are involved in the change of phenotype. To identify the target(s), not only is it necessary to evaluate the compound in a cellular assay specific to the Ras signaling cascade, but also run biochemical analyses on individual pathway proteins, once the targets pathway is uncovered. In the case of the Ras-Raf-Erk signaling pathway, this would mean determining the phosphorylation patterns of significant pathway kinases.

Reporter Gene Assay

To begin to elucidate the target(s) of the hits of the above-described phenotypical assay, a cellular assay with a readout specific for the Ras/MAPK signaling pathway was needed. One method that fulfills this requirement was a Ras/MAPK reporter gene assay.
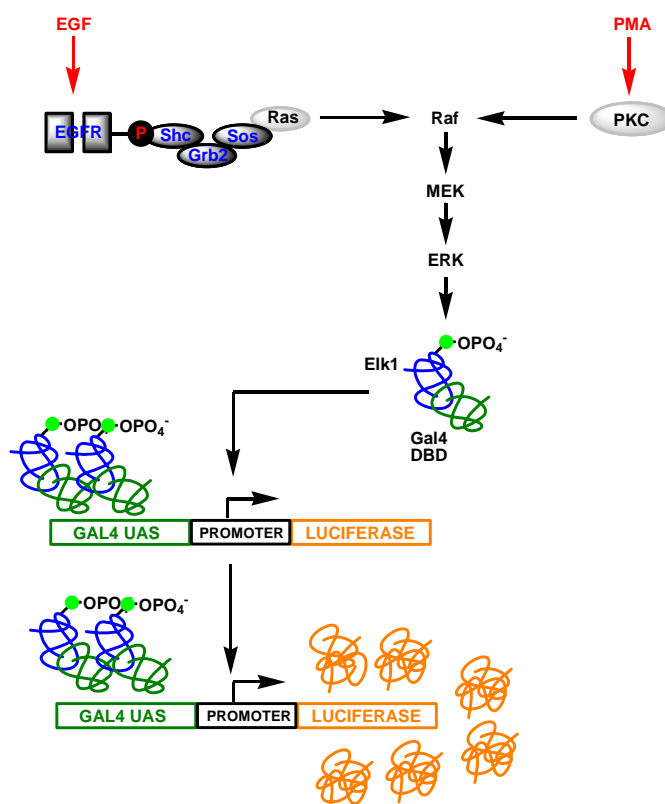

Figure 29: Schematic diagram of the transactivating production of luciferase.

_____

_____

This assay makes use of a genetically modified cell that has been tailored to express a reporter gene product when the Ras/MAPK signaling pathway, upstream to the transcriptional activator of the reporter gene, is not disrupted (*Figure 29*). These experiments were done in collaboration with Dipl. Biol. Sascha Menninger from the Dept. of Chemical Biology of the Max-Planck-Institute for Molecular Physiology.

More specifically, PathDetect **H**eLa **L**uciferase **R**eporter (HLR) cells were used to monitor the expression of Luciferase, a protein which catalyzes the transformation of Luciferin (**212**) to Oxoluciferin (**213**) and light (*Scheme 28*). The HLR cell line contains an integrated synthetic promoter consisting of five consecutive repeats of the yeast GAL4 binding site that controls the expression of the luciferase reporter gene from *Photynus pyralis*, the American firefly.
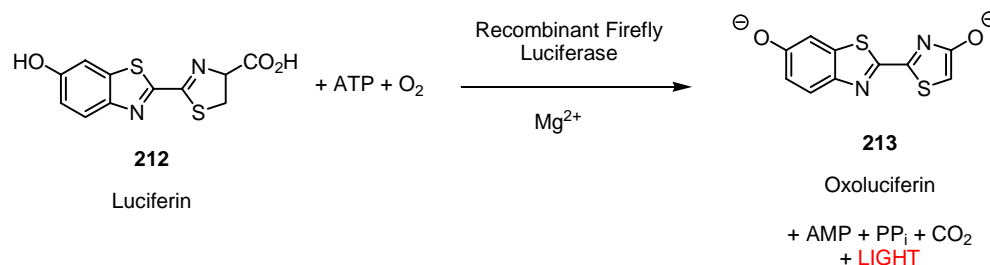
*Scheme 28: Transformation of Luciferin (**212**) to Oxoluciferin (**213**) and light by expressed Firefly luciferase.*

Activation of the promoter occurs when transactivator Elk1 (fused to a Gal4 DNA binding domain) is phosphorylated by MAPK and can thereby bind to the GAL4 UAS binding site, promoting the transcription of the luciferase enzyme. This is monitored by observing the amount of light produced when Luciferin is added to lysed HLR cells which express luciferase.[128;129] Transcriptional activation of Luciferase thus reflects the in vivo activation of the coupled Erk-MAPK signaling pathway.

External stimuli are needed to enhance the signaling. Two different external stimuli, phorbol 12-myristate 13-acetate (PMA) and the epidermal growth factor EGF, were used to activate the transcription by alternative pathways. PMA, member of the phorbol ester family of tumor promoters, activates several of the protein kinase C

_____

_____

(PKC) isoforms in a way similar to their activation by their natural secondary messenger diacylglycerol, DAG. After activation by PMA, the PKCs activate transcription by the Ras/Raf/MAPK signaling pathway.[130] Unfortunately, the PKC family of proteins is not the only receptor for PMA. Mammalian cells express at least five types of different PMA/DAG receptor classes: the chimaerins, PKD1, RasGRP, Munc13 and DAG kinase γ.[131] In fact, it is increasingly believed that not PKC but RasGRP is responsible for PMA-induced effects in the Ras/Raf/MAPK signaling pathways.[131]

The other activator used in this luciferase assay, EGF, binds to EGF receptor (EGFR) at the cellular membrane promoting the dimerisation of this receptor tyrosine kinase, which then via the Ras/Raf/MAPK signaling pathway starts transcription.

To test the validity of the luciferase reporter gene assay, PD98059 was used again as a positive control (*Diagram 2*).
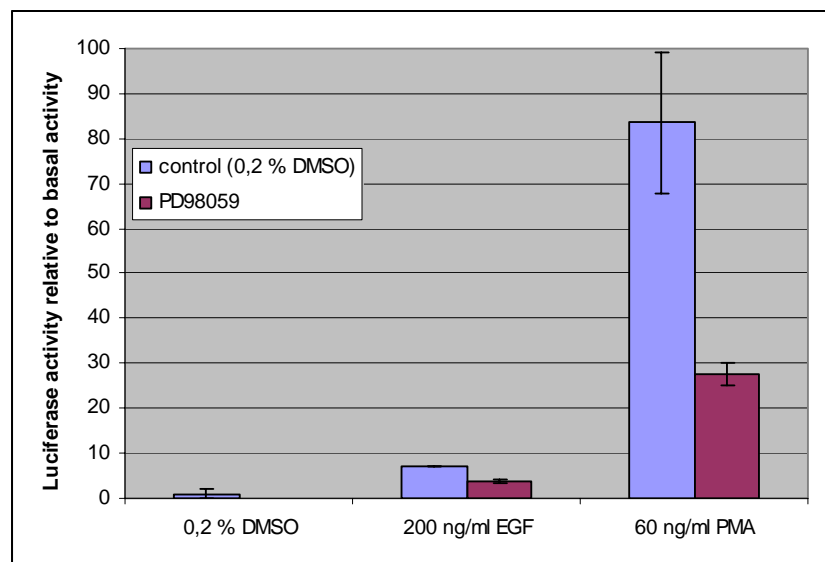
Diagram 2: Luciferase activity upon treatment with PD98059.

Upon activation of the cells with 200 ng/ml EGF, incubation with PD98059 is expected to decrease the amount of luciferase expressed because it stops the transfer of signaling in the MAPK pathway at the MEK level. The experimental result

_____

_____

confirms this hypothesis: at a concentration of 20 μM, a decrease of 46% relative to the control (0.2% DMSO) luciferase activity is observed. In the case of activation of the cells with PMA, a 66% decrease in luciferase activity relative to the control is observed. The high residual luciferase activity upon activation with both EGF and PMA indicates that at a concentration of 20 μM of PD98059, MEK activity is not entirely inhibited. This result is consistent with the observations of Alessi and coworkers, although they used a higher concentration of inhibitor (50 μM).[127]

Melophlin A was tested in the reporter gene assay. Upon stimulation with EGF, luciferase activity decreased by 54% relative to the control experiment, which contained no Melophlin A. More dramatically, upon activation of the cells with PMA, the luciferase activity in the presence of Melophlin A drops to 97% of the control value. Although the inhibition of luciferase activity in both activation cases provides a hint that Melophlin A probably modulates protein activity downstream of Ras and Raf, it is not possible, from these experimental results, to rule out the interaction of Melophlin A with targets in different signaling pathways. This may be achieved by performing a counter-screen on another signaling pathway such as the Wnt pathway, which plays a vital role in multiple developmental processes.[132]
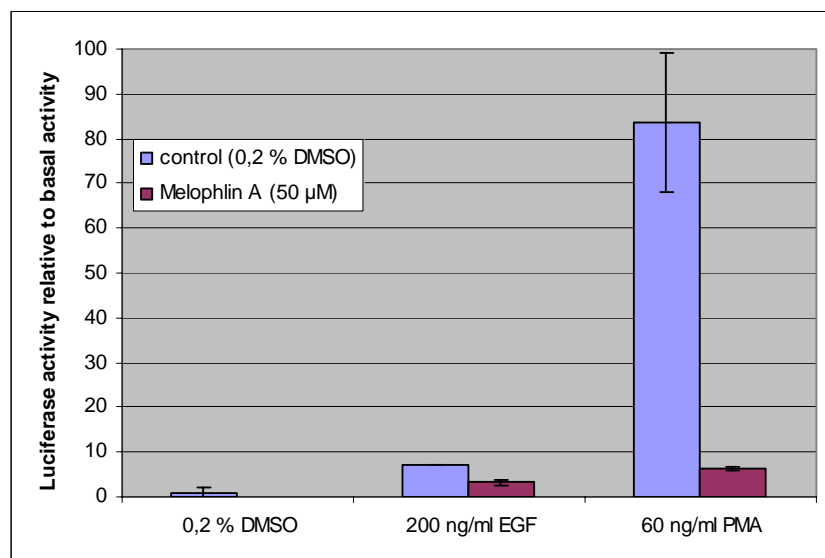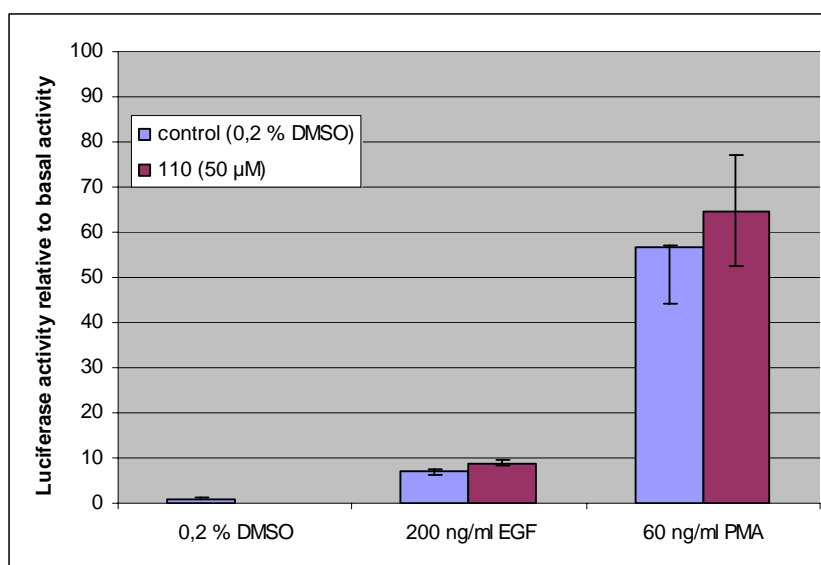

Diagram 3: Luciferase activity upon treatment with 50 μM Melophlin A.

_____ 62

_____

The effect of hydroxyquinolinone **110**, which induced a reversal in phenotype in Ras-transformed MDCK-f3 cells (see p. 66), on the expression of luciferase was also investigated. Instead of observing a decrease in luciferase activity upon treatment with **110**, a slight stimulation was observed in both cases of activation (*Diagram 4*). The minor increase is negligible as it is within the error range and may be due to inhomogeneous cell growth of cells in the experimental setup. From the results obtained from this experiment, it is reasonable to assume that hydroxyquinolinone **110** does not inhibit the expression of luciferase. Furthermore, it is highly likely that **110** does not inhibit a protein in the Ras-Raf-Erk signaling pathway. It is also unlikely that **110** interacts with a protein from the PKC signaling pathway which leads to the expression of luciferase.

*Diagram 4: Luciferase activity upon treatment with 50 µM **110**.*

The mechanism of action of **110** may involve other signaling pathways. For example, Ras functions through numerous other downstream effectors (see *Figure 5,* p. 6). One of these, PI3K functions through the AKT/protein kinase B (PKB) pathway and has been implicated in EMT.[133] Many other signaling pathways contribute to EMT (see *Figure 7,* p. 8), such as the IKK/NF-κB, Hedgehog, Notch or Wnt signaling pathways.[134] From the phenotypic and reporter-gene experiments it is not possible to

_____

_____

deduce the possible target. Therefore **110** needs to be further tested in assays specific for the above mentioned signaling pathways.

4.4.2 Targeting Phosphatases

The central role of protein phosphatases in cellular signaling make them attractive targets to study with small molecules such as tetramic acids. In the following section, the results of the inhibition assay of various phosphatases by compounds from the tetramic acid library will be presented and discussed. The phosphatase activity of the tetramic acids was investigated by PD Dr. H. Prinz and H. Rimpel from Dept. of Chemical Biology of the Max-Planck-Institute for Molecular Physiology. Among the different phosphatases assayed were PP1, Mptp1B, PTP1B, SHP2, Cdc25A and VHR.

Phosphatase inhibition was measured by monitoring the turnover of p-nitrophenyl phosphate (pNPP, **214**, *Scheme 29*) to yellow colored nitrophenol **215** in the presence of a phosphatase and an inhibitor.
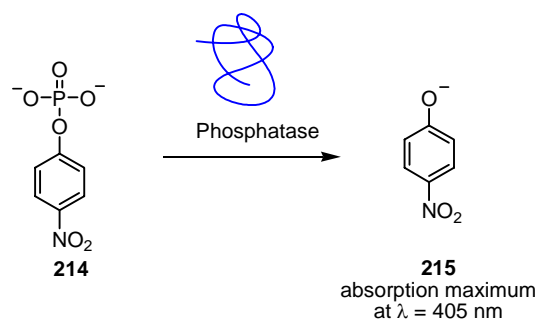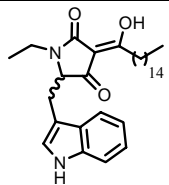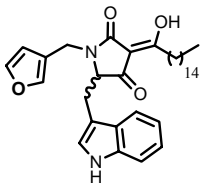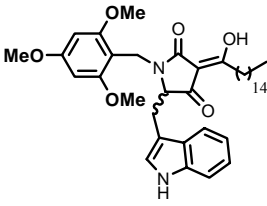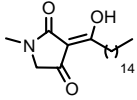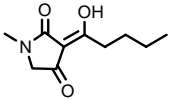

Scheme 29: Enzymatic hydrolysis of unnatural substrate p-nitrophenyl phosphate.

The dephosphorylation of pNPP (**214**) is monitored by its change in absorption at $\lambda = 405$ nm. As it is a direct measure of the amount of p-nitrophenol **215** produced, it is an indicator of enzyme activity. The results should be taken cautiously as pNPP is an unnatural substrate for all of the enzymes tested, and may not emulate the activities with natural peptidic substrates. Nonetheless, the use of small molecule substrates enables the comparison of experimental and modeling data with previously reported inhibitors. Moreover, the selectivity of the inhibitor against different phosphatases can be examined using the same substrate.

_____

_____

The tetramic acids which inhibited phosphatase activity are presented in *Table 5*. None of the compounds inhibited the metal-containing serine/threonine protein phosphatase PP1. The compounds are only moderately active, with IC_{50}s ranging from 30-100μM. It appears that only tetramic acids with alkyl side-chains display inhibitory activity. Tryptophan-based tetramic acids show a slight selectivity towards PTPs (PTP1B and MptpB) and apart from **127**, do not appear to inhibit any DSPs. In the case of **127**, some selectivity (3-fold lower IC_{50}) towards PTP1B was registered. In contrast, the Melophlin analogs are either specific (**118**) for DSPs or unselective (**19**). None of the compounds inhibited SHP2 or VHR.

Table 5: IC_{50} values for the inhibition of different phosphatases by compounds from the tetramic acid library; n.i. = no inhibition, IC_{50} >100 μM.

Entry	Cpd. Nr.	Structure	MptpB	PTP1B	SHP2	Cdc25A	VHR	PP1
1	**125**		93 μM ± 6.14	n.i.	n.i.	n.i.	n.i.	n.i.
2	**127**		68 μM ± 8.31	10 μM ±1.6	n.i.	95 μM ± 8.85	n.i.	n.i.
3	**122**		70 μM ± 9.13	n.i.	n.i.	n.i.	n.i.	n.i.
4	**19**		83 μM ± 6.3	37 μM ± 5.78	n.i.	60 μM ± 4.9	n.i.	n.i.
5	**118**		n.i.	n.i.	n.i.	92 μM ± 9.05	n.i.	n.i.

Summarizing, the C3 alkyl side-chain is important for phosphatase activity. Additionally, an aromatic substituent like an indole at the C5 position is beneficial for activity. This reasonably correlates with results observed for tetronic acids, where the

_____

_____

length of the C3 alkyl side-chain was found to be important in order to enable binding to the hydrophobic groove of the catalytic domain,[44] although the results for the tetronic acids were for Cdc25. Furthermore, the tetramic acids did not inhibit the other class of phosphatases, the serine/threonine phosphatase PP1, also in accordance with tetronic acid results.[135]

To better understand the structure-activity relationships of **127** and **19**, preliminary molecular modeling studies were performed by docking the active molecules into a PTP1B crystal structure.[136] The docking experiments were performed by Dipl. Chem. Stefan Wetzel.

Docking experiments on **127** indicate that the catalytic site is too small to accommodate the tetramic acid core along with the bulky N-acyl furan side chain (*Figure 30*), especially when the flexible WPD loop is closed upon the active site. Instead, **127** seems to bind to the vicinal phosphate site, via hydrogen-bonding of the indole NH with Asp 29, the exocyclic β-keto carbonyl with Arg 24 and the furan oxygen with Gly 259. The large anionic electrostatic potential on the carbonyl group may form favorable interactions with the positively charged guanidinium side chain of Arg 24. Furthermore, the hydrophobic side-chain at the C3 position extends along the hydrophobic groove into the catalytic site, blocking substrate entry. This may be a rational for the inhibition of PTP1B by **127**. The presence of the furan group seems to be essential for activity.
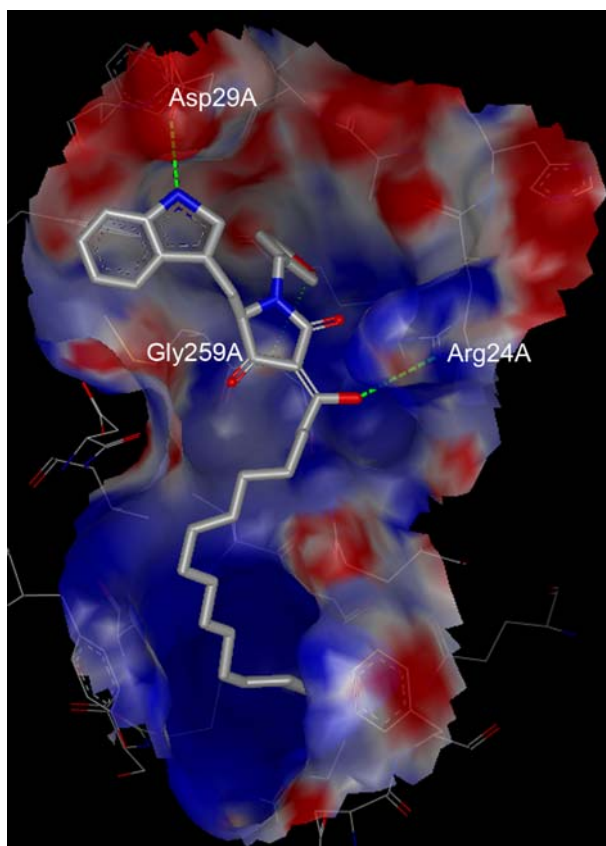
_____

_____

*Figure 30: Model of **127** anion bound to PTP1B active site.*

In contrast to compound **127**, Melophlin A (**19**) can be docked into the phosphatase active site (*Figure 31*). The results show that the tetramic acid ketone at C4 undergoes backbone bonding to the amide proton of Ala 217. The methyl group on the N1 of Melophlin A is accommodated into the active site but larger substituents, such as an ethyl moiety, most likely would not fit in, which is in agreement with experimental results. A free amine at N1 could potentially increase affinity by creating additional positive interactions with other residues in the active site. Furthermore, the lipid side-chain extends into the hydrophobic cleft. The length of the hydrophobic side-chain is determinant as shorter side-chains do not display activity. Affinity might also be increased by introducing an aromatic moiety on C4 or C5 of the lipid side chain to create π-stacking interactions between Phe 182 and Tyr 46, amino acids that are positioned at the entry of the catalytic site.

_____ 67

_____
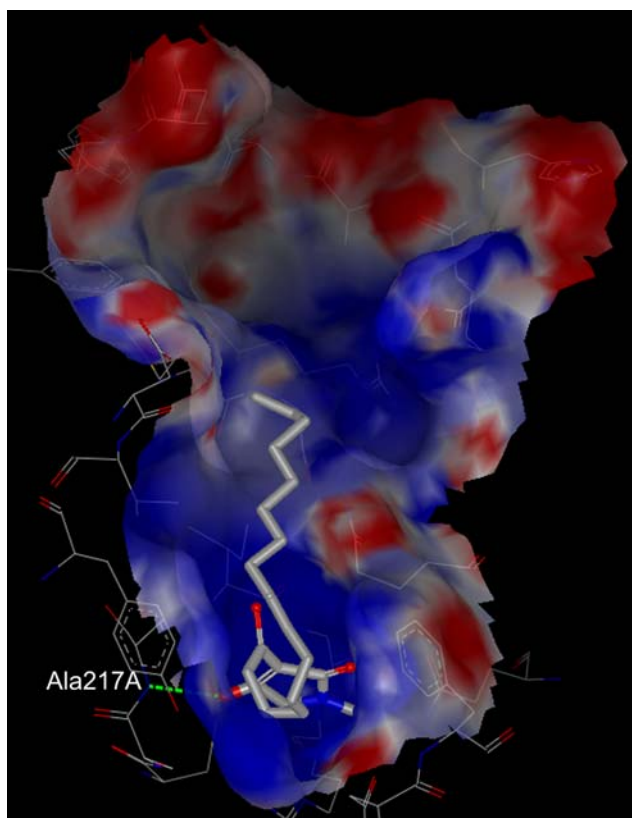
*Figure 31: Model of Melophlin A, **19**, anion bound to PTP1B active site.*

The combination of a phosphate isostere with a hydrophobic side-chain is a reoccurring motif in the structure of several natural product-based phosphatase inhibitors (*Figure 33*).
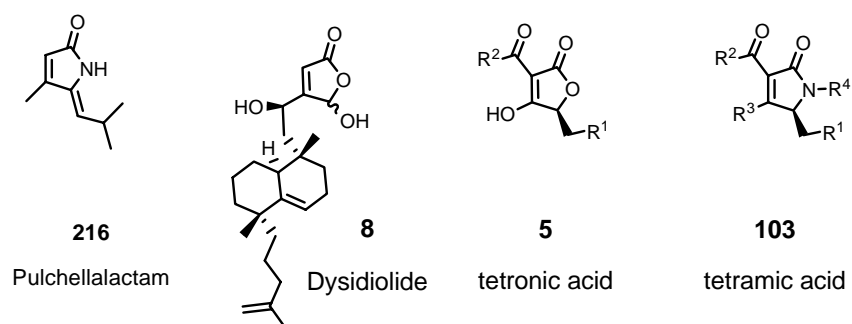

216

Pulchellalactam

8

Dysidiolide

5

tetronic acid

103

tetramic acid

*Figure 32: Chemical structure of Pulchellalactam (**216**), Dysidiolide (**8**), the tetronic (**5**) and tetramic acid cores (**103**).*

_____

_____

This motif is found in Dysidiolide (**8**), where it was suggested that the hydroxybutenolide moiety is a phosphate surrogate and that the long chain occupies the hydrophobic pocket of Cdc25A.[137-139] Although not yet experimentally documented, the lactam moiety of Pulchellalactam (**216**) might also be a phosphate mimic.[140] The results of the preliminary modeling studies performed for Melophlin A (**19**) and **127** in PTP1B provide evidence that the charged tetramic acid core may be a phosphate mimic. This is especially apparent in the case of **127** as the delocalized anionic carbonyl moiety appears to interact with Arg 24, a residue essential for binding phosphate residues in the second aryl phosphate-binding site of PTP1B.[45]
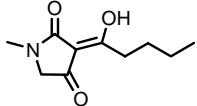
4.4.3 Targeting Bacteria
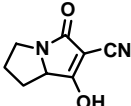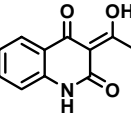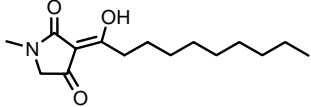
The antibacterial activity of the tetramic acids was determined by Dipl. Biochem. B. Ellinger for one strain of Gram-positive bacteria, *Bacilus subtilisis*, and one strain of Gram-negative bacteria, *Escherichia coli*.

None of the compounds were toxic to *E. coli* cultures. Instead, four compounds (**81**, **111**, **118**, **119**) were identified as having a significant effect on the growth of *B. subtilisis*. The MIC values are presented in *Table 6*. Although the MIC values of active tetramic acids are moderate in comparison to more potent bactericidal agents such as ampicilin (MIC 0.13 mg/l), vancomycin (0.5 mg/l) and tetracyclin (1 mg/l), they constitute an interesting lead structure to be further optimized to study their mechanism of action and identify their biological target.

Interestingly, only Gram-positive bacteria were sensitive to tetramic acids. This is in agreement with the results observed for several natural products containing tetramic acids (*Figure 33,* p.71). Reutericyclin (**217**) selectively inhibits Gram-positive bacterial cell growth.[141] Tetramic acid 3-(1-hydroxydecylidene)-5-(2-hydroxyethyl)pyrrolidine-2,4-dione (**28**), derived from *N*-(3-oxododecanoyl)-L-homoserine lactone (**27**, *Scheme 2*, p. 23) is also selective against a series of Gram-positive bacteria.[71] Vancoresmycin **221**, isolated from the microorganism *Amycolatopsis*, exhibits antibiotic activity more potent than Vancomycin against a series of strains of *S. aureus* and *Enterococcus faecalis*.[73] No inhibitory effect was

_____

observed in Gram-negative bacteria. Three members of the Melophlin family of tetramic acids, Melophlin C (**218**), G (**219**), and I (**220**), also exhibit selectivity towards *B. subtilisis* and *S. aureus*,[72] although no mention is made about their activity in Gram-negative bacteria.

Table 6: Minimal inhibitory concentration (MIC) of selected active tetramic acids. (n.d. = not determined)

| Entry | Cpd. Nr. | Structure | Gram-Negative | Gram-Positive | |
			E. coli	*B. Subtilisis*	*S. aureus*
1	**111**		not active	> 250 mg/l	>250 mg/l
2	**81**		not active	n.d.	not active
3	**119**		not active	70 mg/l	not active
4	**118**		not active	>250 mg/l	not active

Gänzle has studied the mechanism of action of Reutericyclin (**217**), produced by lactic acid bacteria *Lactobaccilus reuteri*.[105;141] The investigation was based on the hypothesis that the bacterial membrane is the cellular target, as **217** is an amphiphilic molecule consisting of a negatively charged head group with hydrophobic side-chains.[105] It was demonstrated that **217** acts as a proton ionophore, thereby dissipating the transmembrane proton potential, leading to cell lysis. Based on the structural similarities between **121** and Reutericyclin (C$_{10}$ lipid side-chain, tetramic acid core), it may be speculated that the bactericidal effects of **119** occur via a similar mode of action. It has a shorter lipid side-chain, which may decrease its membrane-binding affinity and explain the higher effective minimal inhibitory concentration. To confirm this hypothesis, the dissipation of transmembrane potential by the aforementioned compounds needs to be determined.
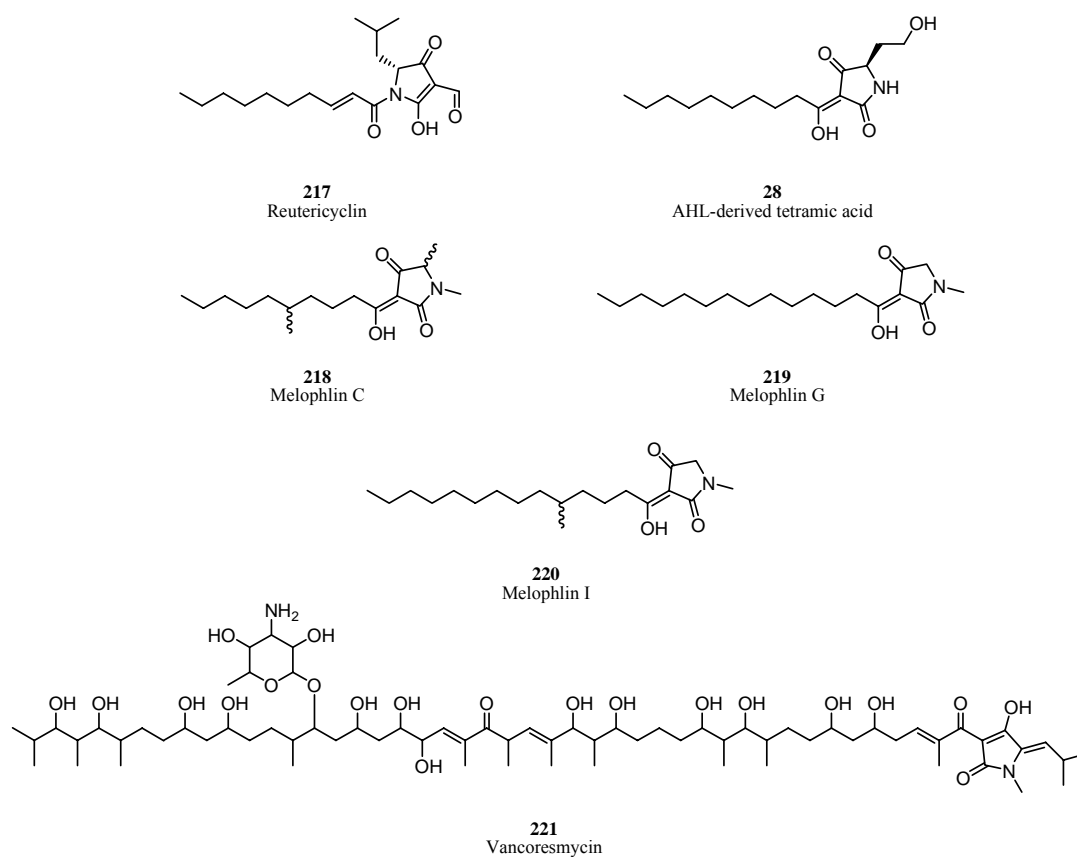
Figure 33: Chemical structures of tetramic acids with known selective antibiotic activity against Gram- positive bacteria.

None of the active compounds from the synthesized tetramic acid library are known natural products, but all posses a common 2,4-pyrrolidinedione scaffold. Based on the mounting evidence that tetramic acid natural products selectively inhibit the growth of Gram-positive bacteria, and based the results obtained here, it appears that the tetramic acid core may constitute a privileged structure for Gram-positive bactericidal activity.

_____

5   Conclusion

As many tetramic acid-containing natural products have been shown to display diverse and interesting biological activities,[2] the tetramic acid moiety was chosen as the structural basis for the design of a natural product-based library for a chemical genetics approach to the study of cellular signaling and bactericidal activity

A library of 30 tetramic acids was synthesized in a four-step solid-phase sequence beginning from Fmoc-protected amino acids and Wang resin (*Figure 34*). Diversity was introduced in each synthetic step: various aldehydes were used to functionalize the amines of resin-bound amino acids in a reductive amination step. The secondary amine was then functionalized by acylation with either diketene, 3-acyl Meldrum's acids or cyanoacetic acid. Finally, a KOH- or NaOMe-promoted cyclization of the acyclic tertiary amide precursor and concomitant cleavage provided the desired tetramic acid compounds.
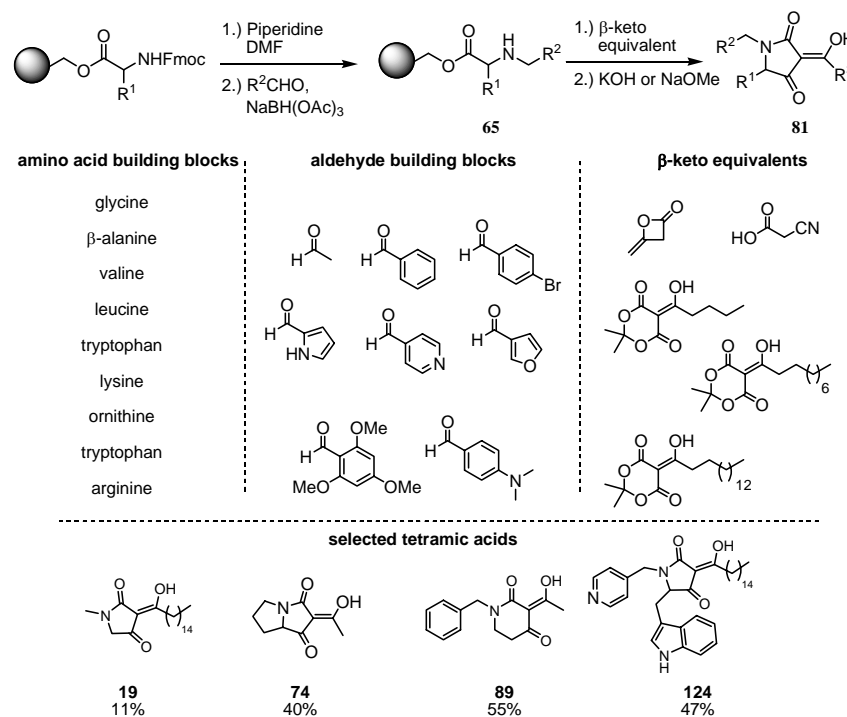
Figure 34: Summary of solid-phase synthesis of tetramic acids.

β-Amino acids were also used as starting materials to provide piperidine-2,4-diones. The synthesis with β-alanine as a building block proceeded analogously to synthesis
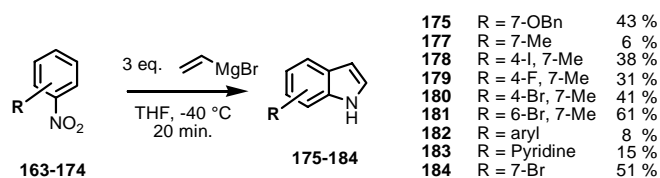
_____

_____

with α-amino acids. Resin-bound anthranilic acid could be converted to quinoline-3-carboxamides using this methodology. Overall, the yields ranged from 3 to 57%. Common side-products isolated were dialkylation products and uncyclizable carboxylic acid generated by base-promoted cleavage of the ester.

To further demonstrate the effectiveness of this method, the synthesis of an analog of Laccarin **142** was undertaken (*Scheme 30*). Wang resin loaded with Fmoc-Ornithine(*N*-Boc)-OH (**137**) was Fmoc deprotected then aminated with benzaldehyde and NaBH(OAc)$_3$. Acylation with diketene provided cyclization precursor **139** that was then cyclatively cleaved with 0.1M KOH in methanol. Deprotection of the Boc group with TFA yielded precursor **129**, with an overall yield of 52% over 5 steps. Imine formation was attempted with the help of molecular sieves but only starting material was recovered. Conversion of the free amine to a DMB protected secondary amine may facilitate the formation of the desired enamine product **142** upon azeotropic distillation or upon use of drying agents.
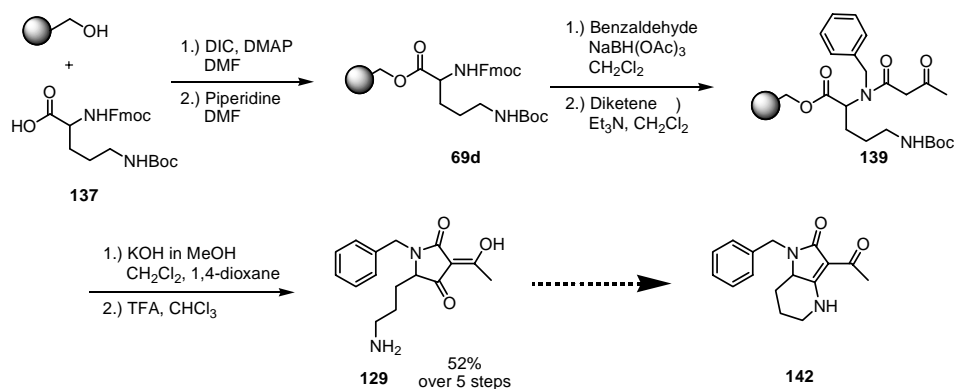
*Scheme 30: Summary of the synthetic steps towards Laccarin analog **142**.*

Due to interest in generating a library of 7-substituted indole-based tetramic acids, a synthetic route was established to generate the tryptophan building blocks needed starting from indoles. Indole synthesis was effected via the Bartoli method beginning from an *o*-nitroarene and 3 equivalents vinyl Grignard to produce 7-substituted indoles. In total, a set of 8 indoles was synthesized with yields ranging from 6 to 61% (*Scheme 31*).

_____

_____

175	R = 7-OBn	43 %
177	R = 7-Me	6 %
178	R = 4-I, 7-Me	38 %
179	R = 4-F, 7-Me	31 %
180	R = 4-Br, 7-Me	41 %
181	R = 6-Br, 7-Me	61 %
182	R = aryl	8 %
183	R = Pyridine	15 %
184	R = 7-Br	51 %

*Scheme 31:Summary of the synthesis of indoles **175**-**184** via the Bartoli methodology.*

Tryptophan analogs were generated in a biomimetical fashion by treating an indole with serine and acetic anhydride in acetic acid (*Scheme 32*). Six tryptophan analogs were generated via this method with yields ranging from 6 to 42%. In a last step, deacylation with *Asp.* Acylase I should provide enantiomeric pure tryptophan analogs that can be used for the synthesis of indole-substituted tetramic acids.

194	R = 4-Br	31 %
196	R = 7-Me	15 %
197	R = 7-OBn	42 %
198	R = 4-I, 7-Me	14 %
200	R = 4-Br, 7-Me	6 %
201	R = 6-Br, 7-Me	19 %
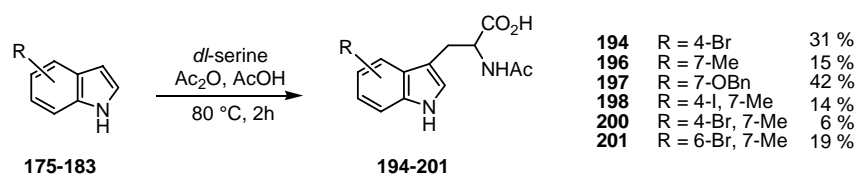
*Scheme 32: Summary of the synthesis of tryptophan analogs **194**-**201**.*

The collection of tetramic acids synthesized was used to study various biological systems and a selection of the results are presented in *Table 7*. In the first study, the tetramic acids were tested for cytotoxicity and their ability to reverse the morphology of Ras transformed MDCK cells, in an EMT model system. Two compounds, Melophlin A (**19**) and **110** reversed the phenotype of the transformed cells. Although **19** was recently documented to induce such an effect,[64] none of the other Melophlin A analogs (**118**, **119**, **120**, *Figure 27*, p. 64) induced a change in morphology. Furthermore, these analogs were cytotoxic beginning at a concentration of 50 µM. In an attempt to better understand the compound-induced morphological effects, the compounds were subjected to a MAPK/PKC pathway specific luciferase reporter gene assay. Melophlin A (**19**) decreased luciferase activity by 75% and 54% upon PMA and EGF activation, respectively, indicating that its protein target must lie downstream to the Ras and Raf proteins in the MAPK signalling pathway. A change in luciferase activity wasn't recorded upon assaying **110**, demonstrating that **110** probably doesn't target a protein in the MAPK pathway. Its ability to induce morphological changes in Ras-transformed cells is probably due to modulation of
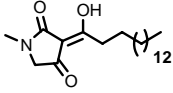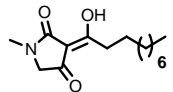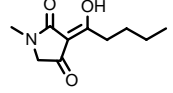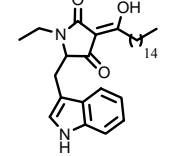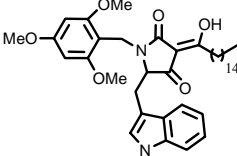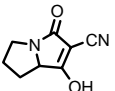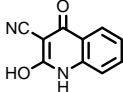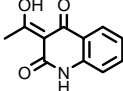
_____

_____
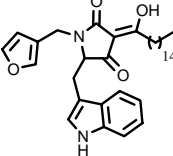
other signalling pathway involved in EMT, such as the IKK/NF-κB, Hedgehog, Notch or Wnt signaling pathways. With the help of pull-down assays using biotinylated analogs and phosphorylation mapping of signaling pathways, it may be possible to isolate the target(s) of these molecules and study their mechanism of action.[142]

The tetramic acid library was screened for inhibitory activity against a panel of five different phosphatases: PP1, Mptp1B, PTP1B, Cdc25A and SHP2. Six compounds (**19**, **118**, **122**, **125** and **127,** *Table 7*) demonstrated moderate IC_{50} values for Mptp1B, PTP1B and Cdc25A. The presence of an alkyl side-chain was important for the activity of all compounds. Tryptophan-based tetramic acids demonstrated a slight selectivity towards PTPs. Preliminary molecular modelling experiments provided some insight into structure-activity relationships. In the case of **127**, activity may be explained by the binding of the tetramic acid core to the second aryl-phosphate site, with the lipid tail extending along the hydrophobic grove into the catalytic site, thereby blocking the entry of the substrate. Melophlin A (**19**) binds unspecifically to the catalytic site, with the delocalized anionically-charged tetramic acid core acting as a phosphate mimic

The members of the tetramic acid library were also tested for bactericidal activity in a growth assay against Gram-positive (*B. subtilisis*) and Gram-negative bacteria (*E. coli*). None of the tetramic acids tested were bactericidal on Gram-negative bacteria, supporting the hypothesis of Janda et al. that tetramic acids act on a target found specifically in Gram-positive bacteria.[71] Moderate bactericidal activity was observed for four compounds, **81**, **111**, **120**, **121** (*Table 7*). These compounds can be used as a starting point to uncover the target and investigate the mechanism of action of the active compounds. In addition to pull-down assays, the compounds ought to be tested against classical antibacterial targets such as DNA-gyrases (inhibition of DNA replication), RNA polymerase (inhibition of protein biosynthesis) and proton pumps (cell-wall stability).

_____

Table 7: Summary of the biological properties of active tetramic acids.

Structure	Cpd Nr	Phenotypical Assay	WST-1 Assay	Phosphatase Assay	Antibiotics Assay
(structure)	19	reversal	cytotoxic	Cdc25A: 60 µM PTP1B: 37 µM MptpB: 83 µM	no effect
(structure)	119	no effect	cytotoxic	n.d.	B.Subtilisis (70 mg/l)
(structure)	118	no effect	cytotoxic	Cdc25A: 92 µM	B.Subtilisis (>250 mg/l)
(structure)	125	no effect	not toxic	MptpB: 93 µM	no effect
(structure)	127	no effect	not toxic	Cdc25A: 95 µM PTP1B: 10 µM MptpB: 68 µM	no effect
(structure)	122	no effect	not toxic	MptpB: 70 µM	no effect
(structure)	111	no effect	not toxic	MptpB: >100 µM	B.subtilisis (>250 mg/l)
(structure)	110	reversal	not toxic	MptpB: >100 µM	no effect
(structure)	81	no effect	not toxic	Cdc25A:>100 µM	B.Subtilisis (MIC n.d.)

_____

6   Materials and Methods

6.1   *Synthetic Materials and Methods*

6.1.1   General

Nuclear Magnetic Resonance Spectroscopy

^{1}H and ^{13}C NMR spectra were recorded on one of the following instruments

Varian Mercury 400	400 MHz, ^{1}H NMR; 100.6 MHz, ^{13}C NMR
Bruker DRX 400	400 MHz, ^{1}H NMR; 100.6 MHz, ^{13}C NMR
Bruker DRX 500	500 MHz, ^{1}H NMR; 125.8 MHz, ^{13}C NMR

with tetramethylsilane as the internal reference. The chemical shifts are provided in ppm and the coupling constants in Hz. The following abbreviations for multiplicities are used: s, singlet; d, doublet; dd, double doublet; t, triplet; q, quadruplet; m, multiplet; br, broad; ar, aromatic.

Mass Spectrometry

The high and low resolution EI- and FAB- mass spectra were recorded on a Finnigan MAT MS 70 spectrometer. The MALDI-TOF spectra were recorded on a Voyager-DE Pro MALDI-TOF and with 2,5-dihydroxybenzoic acid (DHB) as the matrix (20 mg DHB, 900 µl H_2O, 90 µl ethanol, 10 µl TFA).

Gas-Chromatography Mass-Spectrometry

GC-MS spectra were recorded with a Hewlett-Packard gas-chromatograph (6890) coupled to a mass-detector (5973), fitted with a HP-5TA capillary column (0.33 mm x 0.2 mm ID). The temperature gradient began at 80 °C (3 min) then was raised to 240 °C over 17 min.

Reversed-Phase High-Pressure Liquid Chromatography

Analytical HPLC was recorded on an Agilent HPLC (1100 series machine). The standard gradient began at 10% acetonitrile and was raised to 90% over 15 min. After 3 min at 90% acetonitrile, the column was washed for 5 min with 100% acetonitrile. The column was then equilibrated for 3 min with 10% acetonitrile. TFA (0.1% v/v) was added to the HPLC solvents. Analytical HPLC-MS measurements were recorded

_____ 77

_____

on an Agilent HPLC (1100 series) coupled to a Finnigan LCQ ESI spectrometer. The column used is indicated in parenthesis. Preparative HPLC was run on an Agilent HPLC (1100 series) using a 125/21 NUCLEODUR C_{18} Gravity, 5 μ (Macherey-Nagel) column.

Thin-Layer Chromatography (TLC)

Thin-layer chromatography (TLC) plates were obtained from Merck (Silica gel 60, F254). The TLCs were visualized by UV light (λ = 254 nm, 366 nm) or by staining with one of the following stains:

      Stain A: 0.3 g Ninhydrin, 3 ml acetic acid, 97 ml ethanol.

      Stain B: 1.6 g $KMnO_4$, 10 g K_2CO_3, 2.5 ml 5% NaOH, 200 ml H_2O.

The solvent system and R_f values are noted for the synthesized compounds.

Flash Chromatography

Flash column chromatography[143] was performed using flash silica gel (Merck, Darmstadt, 40-64 μM) with pressure ranging from 0.5 - 1.0 bar. A 70 - 100-fold excess of silica gel to the crude product was used.

Ultraviolet Spectroscopy

UV/VIS spectra were measured with a Cary 100 Spectrometer (Varian Inc.).

Optical Rotation

Optical rotations were measured with a Schmidt + Haensch Polartronic HH8 polarimeter at 589 nm. Concentrations are given in g/100 ml.

Chemicals

Chemicals were obtained from the following suppliers and used without further purification: Acros, Aldrich, Avocado, Biosolve, Fluka, Lancaster, Novabiochem, Senn Chemicals. The solid support was purchased from Novabiochem.

With the exception of DMF and NMP, all solvents were distilled prior to use following standard protocols.[144] Dry DMF was purchased from Fluka. Unless otherwise noted, all reactions were stirred or shaken under inert atmosphere (argon).

_____

6.1.2   Compounds from Chapter 4.1

General Procedure 1 (GP1): Resin loading with an amino acid

To an ice-cooled solution of Fmoc-amino acid (2.75 eq.) in freshly distilled dichloromethane (0.6 M) was added *N*, *N*-diisopropylcarbodiimide (5.5 eq.). After stirring for 30 min at 0 °C, the solution was evaporated under reduced pressure. The residue was dissolved in as little dry DMF as possible and added to a round-bottom flask containing preswelled Wang-resin (1 eq.). After addition of DMAP (10 mol %), the mixture was shaken for 2h at room temperature. Following filtration, the resin was washed seven times with DMF (20 ml), then seven times with dichloromethane (10 ml) and dried under reduced pressure.

General Procedure 2 (GP2): Resin loading with isatoic anhydride

A suspension of isatoic anhydride (10 eq.), DMAP (10 eq.) and Wang-resin (1 eq.) in dry toluene in a round-bottom flask was heated at 60 °C for 16 h. After cooling to room temperature, the resin was filtered and washed (7 x toluene, 7 x CH_2Cl_2, 5 x MeOH, 7 x CH_2Cl_2) and dried under reduced pressure.

General Procedure 3 (GP3): Fmoc Deprotection

To the Fmoc-Wang resin was added 20% piperidine/DMF and the suspension was mixed at room temperature for 20 minutes. This procedure was repeated twice before filtering, washing (7 x DMF, 7 x CH_2Cl_2) and drying the resin in vacuo.

Loading determination

Resin (2-3 mg) was weighed into a 10 ml volumetric flask and filled with 20% piperidine in DMF. After 20 minutes of gentile agitation, 3 ml was transferred to a quartz UV cuvette and the absorbance was measured against reference at $\lambda = 301$ nm. The loading c_L is determined according to Beer's Law, A = εcd, where $\varepsilon = 7800$ at 301 nm.

$$c_V = \frac{A}{\varepsilon \times d} = \frac{A \times 10^3}{7800}$$

$$c_L = \frac{c_V \times V}{m} = \frac{A \times 10^4}{7800 \times m}$$

_____

where c_V is the volume concentration, A is the absorbance, d is the path length of the UV cuvette, V is the total volume, m is the mass of the resin.

Determination of Theoretical Loading

The theoretical loading of the resin was determined according to the following formula:

$$\text{Loading}_{new} \text{ (mol/g)} \quad = \quad \frac{\text{loading}_{old} \text{ (mol/g)}}{1 + \Delta \text{ x loading}_{old} \text{ (mol/g)}}$$

Where loading$_{old}$ is the previous loading and Δ is the mass difference of the added compound to the resin.

General Procedure 4 (GP4): Reductive Amination

To the appropriate resin (1 eq.) swelled in freshly distilled dichloromethane was added the appropriate aldehyde (1 eq.), and the reaction was vigorously mixed at room temperature for 1 h. After addition of NaBH(OAc)$_3$ (1 eq.), the resin was vigorously mixed at room temperature for 18 h. The reaction was quenched with MeOH (10 ml). The resin was filtered and washed with 7 x DMF, 7 x DMF:H$_2$O (1:1 v/v), 7 x MeOH, 7 x CH$_2$Cl$_2$. The resin was then dried in vacuo.

General Procedure 5 (GP5): Diketene ß-keto amide formation [96]

To a cooled suspension of the appropriate resin (1 eq.) in CH$_2$Cl$_2$ in a round bottom flask was added Et$_3$N (10 eq.) and then diketene (10 eq.) in a dropwise fashion. The suspension was shaken for 12 h at room temperature under argon. The mixture was transferred to a syringe reactor and washed with 7 x CH$_2$Cl$_2$, 7 x DMF, 7 x MeOH, 7 x CH$_2$Cl$_2$. The orange coloured resin was then dried in vacuo.

General Procedure for the Synthesis of Acylated Medrum's Acid [98]

The appropriate acid (1 eq.) was dissolved in freshly distilled CH$_2$Cl$_2$, then DMAP (1.05 eq.) and DCC (1.1 eq.) were added. Meldrum's acid was then added and the mixture stirred for 18 h at room temperature. The isoluble urea was then filtered over celite, and the filtrate evaporated under reduced pressure. The crude product was

_____ 80

_____

redissolved in ethyl acetate and washed with 1M HCl. The organic phase was dried over Na_2SO_4, filtered and evaporated. The product was used without further purification.
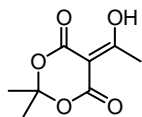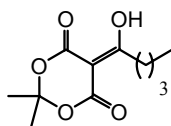

230

5-(1-hydroxyethylidene)-2,2-dimethyl-1,3-dioxane-4,6-dione

Using acetic acid (144 µl, 2.5 mmol) and according to the above-described procedure, **230** was obtained as a colorless oil in 74% yield (306 mg).

^{1}H NMR (400 MHz, $CDCl_3$): δ = 2.67 (s, 3H, -CH_3), 1.73 (s, 6H, -$(CH_3)_2$).

^{13}C NMR (100.6 MHz, $CDCl_3$): δ = 194.6, 170.1, 111.5, 106.4, 26.8, 23.5.

97

5-(1-hydroxypentylidene)-2,2-dimethyl-1,3-dioxane-4,6-dione

Using valeric acid (0.2 g, 1.96 mmol) and according to the above-described method, **97** was obtained as a yellow amorphous solid in 91% yield (0.408 g).

^{1}H NMR (400 MHz, $CDCl_3$): δ = 3.00 (t, J = 8 Hz, 2 H, -CH_2-), 1.66 (s, 6H, -$(CH_3)_2$), 1.64-1.60 (m, 2H, -CH_2-), 1.40-1.34 (m, 2H, -CH_2), 0.88 (t, J = 8 Hz, 3H, -CH_3).

^{13}C NMR (100.6 MHz, $CDCl_3$): δ = 195.4, 169.8, 111.5, 106.4, 29.4, 26.8, 23.5, 14.3.

General Procedure 6 (GP6): ß-keto amide formation with Meldrum's acid [98]

After preswelling the appropriate resin (1 eq.) in freshly distilled CH_2Cl_2 in a round bottom flask, it was then washed with dry toluene. A solution of the appropriate acyl Meldrum's Acid (6 eq.) in dry toluene was then added to the resin. The suspension was shaken at 100 °C for 3 hours, then cooled to room temperature. The resin was transferred to a syringe reactor for washing (3 x toluene, 3 x CH_2Cl_2) and dried in vacuo.

General Procedure 7 (GP7): Acylation with cyanoacetic acid

_____ 81

_____

After preswelling the appropriate resin (1 eq.) in freshly distilled CH_2Cl_2 in a round-bottom flask, HOBt (15 eq.) and cyanoacetic acid (15 eq.) was added. After cooling to 0 °C, DIC (20 eq.) was added. The reaction was shaken for 18 h at room temperature then transferred to a syringe reactor for washing (5 x DMF, 5 x MeOH, 5 x DMF) and dried in vacuo.

General Procedure 8 (GP8): Cyclative Cleavage with TBAF

To a suspension of the resin (1 eq.) in THF was added TBAF in THF (1M, 10 eq.). After 9 hours the resin was filtered and washed with 3 x CH_2Cl_2, 2 x MeOH then 2 x CH_2Cl_2. The combined washings were evaporated, and the crude residue was dissolved in a mixture of 1M HCl and ethyl acetate. The phases were separated and the aqueous phase extracted twice more with ethyl acetate. The combined organic phases were dried over Na_2SO_4 and evaporated under reduced pressure. The tetramic acid was then purified by column chromatography.

General Procedure 9 (GP9): Cyclative Cleavage with KOH in Methanol

To the pre-swelled resin (1 eq.) in freshly distilled CH_2Cl_2 in a round bottom flask was added an equal volume of dry 1,4-dioxane and 0.1 M KOH solution (1 eq.). The suspension was shaken vigorously at room temperature for 1 h, then filtered. The resin was washed with 50 ml CH_2Cl_2/MeOH (1:1 v/v) and evaporated under reduced pressure to yield the potassium salt of the acyl tetramic acid. The potassium salt was converted to the free acid by dissolving in ethyl acetate and washing with 1M HCl. The combined organic phases were dried over Na_2SO_4 and evaporated under reduced pressure. The crude product was then purified either by flash chromatography or by preparative HLPC.

Tetramic Acids Synthesized
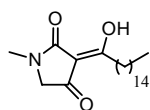
19

(Z)-3-(1-hydroxyhexadecylidene)-1-methylpyrrolidine-2,4-dione

The Fmoc group was cleaved from Fmoc-sarcosine-Wang resin according to *GP3*. The resulting amine was then acylated with palmitoyl Meldrum's acid according

_____

to *GP6*. Cyclative cleavage according to *GP9*, followed by chromatography in 1:2 EA/CH afforded the title compound as a white amorphous solid (9 mg, 11 %).

R*f* = 0.07 (EA = 100%).

^{1}H NMR (400 MHz, CDCl$_3$): δ = 3.70 (s, 2H, α-CH$_2$), 3.00 (s, 3H, -CH$_3$), 2.80 (t, J = 7 Hz, 2H, pal -CH$_2$), 1.66-1.60 (m, 4H, pal -CH$_2$), 1.26-1.24 (s, br, 22H, pal -CH$_2$), 0.88 (t, J = 7 Hz, 3H, pal -CH$_3$).
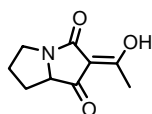
^{13}C NMR (100.6 MHz, CDCl$_3$): δ = 191.2, 187.5, 173.53, 101.5, 57.6, 32.6, 31.8-29.1, 28.3, 25.9, 22.6, 14.0.

LC-MS: (C$_4$) 352.66 [M + H]$^+$; rt = 9.91 min.

HPLC: (C$_4$) rt = 7.75 min.

HRMS (FAB) *m/z* calc'd for [C$_{21}$H$_{38}$NO$_3$ + H]$^+$: 352.2773, found 352.2829.

The spectroscopic data is in agreement with the assigned structure and those reported by Aoki et al.[64]

74

(E)-tetrahydro-2-(1-hydroxyethylidene)-2H-pyrrolizine-1,3-dione

The Fmoc group was cleaved from Fmoc-proline-Wang resin according to *GP3*. The resulting amine was then acylated with diketene according to *GP5*. Cyclative cleavage according to *GP9* afforded the title compound as a yellow oil (7.5 mg, 40%, rac. mixture).

^{1}H NMR (400 MHz, CDCl$_3$): δ = 3.99-3.94 (m, 1H, α-CH), 3.76-3.69 (m, 1H, γ-CH$_2$), 3.27-3.21 (m, 1H, γ-CH$_2$), 2.43 (s, 3H, -CH$_3$), 2.18-2.10 (m, 4H, β-CH$_2$, δ-CH$_2$).

^{13}C NMR (100.6 MHz, CDCl$_3$): δ = 191.3, 187.5, 171.7, 102.5, 61.4, 49.3, 27.7, 23.1.

LC-MS: (C$_{18}$) 182.01 [M + H]$^+$; rt = 5.49 min.

HRMS (FAB) *m/z* calc'd for [C$_9$H$_{12}$NO$_3$ + H]$^+$: 182.0739, found 182.0812.
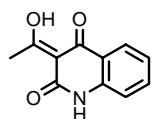
81

(E)-3-(1-hydroxyethylidene)quinoline-2,4(1H,3H)-dione

Wang-resin was loaded with anthranilic acid according to *GP2* and acylated with diketene according to *GP5*. Cyclative cleavage according to *GP9* afforded the title
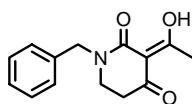
_____

compound as a yellow oil (7.5 mg, 11%).

¹H NMR (400 MHz, d_6-DMSO): δ = 7.98 (d, J = 8 Hz, 1H, arom. CH), 7.68 (t, J = 7 Hz, 1H, arom. CH), 7.29 (d, J = 8Hz, 1H, arom. CH), 7.23 (t, J = 7 Hz, 1H, arom. CH), 2.71 (s, 3H, -CH₃).

¹³C NMR (100.6 MHz, d_6-DMSO): δ = 192.4, 188.6, 175.3, 130.5, 128.4, 128.3, 124.6, 103.7, 15.4.

MALDI-TOF *m/z* calc'd for $[C_{11}H_{12}NO_3 + H]^+$: 204.19; found 204.40.

HRMS (FAB) *m/z* calc'd for $[C_{11}H_{12}NO_3 + H]^+$: 204.0582, found 204.0641.

89

(Z)-1-benzyl-3-(1-hydroxyethylidene)piperidine-2,4-dione

The Fmoc group was cleaved from Fmoc-β-alanine-Wang resin according to *GP3*. The resulting amine was then reductively alkylated with benzaldehyde according to *GP4*, then acylated with diketene according to *GP5*. Cyclative cleavage according to *GP9* and preparative HPLC (C_{18}) afforded the title compound as a beige amorphous solid (13 mg, 55%).

¹H NMR (400 MHz, CD₃OD): δ = 7.33 (m, 5H, arom. CH), 4.69 (s, 2H, benz. CH₂), 3.41 (t, J = 7 Hz, 2H, CH₂), 2.57 (t, J = 7 Hz, 2H, CH₂), 2.52 (s, 3H, CH₃).

MALDI-TOF *m/z* calc'd for $[C_{14}H_{16}NO_3+H]^+$: 246.10, found 246.40.

HRMS (FAB) *m/z* calc'd for $[C_{14}H_{16}NO_3 + H]^+$: 246.1052, found 246.1145.
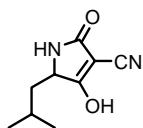
107

2,5-dihydro-4-hydroxy-5-isobutyl-2-oxo-1H-pyrrole-3-carbonitrile

The Fmoc group was cleaved from Fmoc-leucine-Wang resin according to *GP3* and then acylated with cyano-acetic acid according to *GP7*. Cleavage according to *GP9* afforded the uncyclized methyl ester which was converted to the title compound by heating for 2 h with NaOMe (1 eq.) in MeOH (2.2 mg, 3%, yellow oil, rac. mixture).

¹H NMR (400 MHz, CD₃OD): δ = 4.18 (dd, J = 4 Hz, 13 Hz, 1H, α-CH), 1.84-1.75 (m, 1H, δ-CH), 1.65 (dt, J = 4 Hz, 14 Hz, 1H, β-CH₂), 1.46-1.39 (m, 1H, β-CH₂), 0.96 (d, J = 7 Hz, 6H, γ-CH₂).

_____

_____

^{13}C NMR (100.6 MHz, CD$_3$OD): δ = 187.5, 171.9, 116.9, 112.0, 57.2, 41.1, 24.9, 22.7, 20.7.

**HRMS (EI)** *m/z* calc'd for [C$_9$H$_{12}$N$_2$O$_2$]$^+$: 180.0899, found 180.0903.
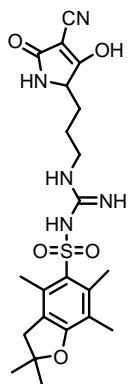
108

(3-(4-cyano-2,5-dihydro-3-hydroxy-5-oxo-1H-pyrrol-2-yl)propyl)guanidine-1(2,3-dihydro-2,2,4,6,7-pentamethylbenzofuran)-sulfonamide

The Fmoc group was cleaved from Fmoc-arginine(Pbf)-Wang resin according to *GP3*. The resulting amine was acylated with cyanoacetic acid according to *GP7*. Cyclative cleavage according to *GP9* afforded the title compound as a yellow oil (8.3 mg, 39%, rac. mixture).

^{1}H NMR (400 MHz, *d$_6$*-acetone): δ = 4.27-4.24(m, 1H, α-CH), 3.40-3.25(m, 2H, β-CH$_2$), 3.01(s, 2H, -CH$_2$), 2.57(s, 3H, arom. -CH$_3$), 2.50(s, 3H, arom. -CH$_3$), 1.95-1.9 (m, 1H, -CH$_2$), 1.75-1.5 (m, 3H, -CH$_2$), 1.45 (s, 6H, -(CH$_3$)$_2$).

HRMS (FAB) *m/z* calc'd for [C$_{22}$H$_{29}$N$_5$O$_5$S + H]$^+$: 476.1889, found 476.1974.
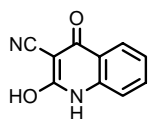
110

1,4-dihydro-2-hydroxy-4-oxoquinoline-3-carbonitrile

Wang-resin was loaded with anthranilic acid according to *GP2* and acylated with cyanoacetic acid according to *GP7*. Cyclative cleavage according to *GP9* afforded the title compound as a yellow oil (10.6 mg, 59%).

^{1}H NMR (400 MHz, *d$_6$*-DMSO): δ = 11.64 (s, 1H, NH), 7.98 (dd, J = 1 Hz, 8 Hz, 1H, arom. CH), 7.61 (dt, J = 1 Hz, 9 Hz, 1H, arom. CH), 7.28 (d, J = 8 Hz, 1H, arom. CH), 7.21 (dt, J = 2 Hz, 10 Hz, 1H, arom. CH).

MALDI-TOF *m/z* calc'd for [C$_{10}$H$_6$N$_2$O$_2$ + H]$^+$: 187.16, found 187.40.

HRMS (FAB) *m/z* calc'd for [C$_{10}$H$_6$N$_2$O$_2$ + H]$^+$: 187.0429, found 187.0630.
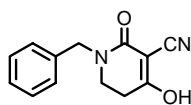
_____
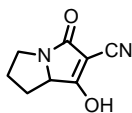
5,6,7,7a-tetrahydro-1-hydroxy-3-oxo-3H-pyrrolizine-2-carbonitrile

111

The Fmoc group was cleaved from Fmoc-proline-Wang resin according to *GP3*. The resulting amine was acylated with cyanoacetic acid according to *GP7*. Cyclative cleavage according to *GP9* afforded the title compound as a yellow oil (8.3 mg, 85%).

^{1}H NMR (400 MHz, CD$_3$OD): δ = 4.31 (q, J = 6 Hz, 1H, α-CH), 3.47 (dt, J = 8 Hz, 8 Hz, 1H, γ-CH), 3.20-3.14 (m, 1H, γ -CH$_2$), 2.25-2.14 (m, 3H, β-CH$_2$, δ-CH$_2$), 1.54-1.46 (m, 1H, δ -CH$_2$).

^{13}C NMR (100.6 MHz, CD$_3$OD): δ = 188.0, 174.7, 118.6, 66.4, 47.3, 44.5, 28.8, 27.6.

HRMS (FAB) *m/z* calc'd for [C$_8$H$_8$N$_2$O$_2$ + H]$^+$: 164.0586, found 164.0646.

1-benzyl-1,2,5,6-tetrahydro-4-hydroxy-2-oxopyridine-3-carbonitrile

112

The Fmoc group was cleaved from Fmoc-β-alanine-Wang resin according to *GP3*. The resulting amine was then reductively alkylated with benzaldehyde according to *GP4*, then acylated with cyanoacetic acid according to *GP7*. Cyclative cleavage according to *GP9* afforded the title compound as a yellow oil (2.2 mg, 6%).

^{1}H NMR (400 MHz, CD$_3$OD): δ = 7.36-7.23 (m, 5 H, arom. CH), 4.55 (s, 2H, benz. CH$_2$), 3.94 (s, 2H, -NCH$_2$CH$_2$-), 3.67 (s, 2H, -NCH$_2$CH$_2$-).

HRMS (EI) *m/z* calc'd for [C$_{13}$H$_{12}$N$_2$O$_2$ + H]$^+$: 229.0899, found 229.1001.

(Z)-3-(1-hydroxyethylidene)pyrrolidine-2,4-dione

113
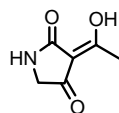
The Fmoc group was cleaved from Fmoc-glycine-Wang resin according to *GP3*. The resulting amine was then acylated with diketene according to *GP5*. Cyclative cleavage followed according to *GP9* and afforded the title compound as a yellow oil (7.5 mg, 40%).
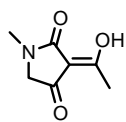
Rf = 0.17 (MeOH/CHCl$_3$ = 3/5).

^{1}H NMR (400 MHz, CD$_3$OD): δ = 9.92 (s, br, 1H, NH), 3.99 (s, br, 2H, α-CH$_2$),

_____

2.52 (s, 3H, -CH$_3$).

MALDI-TOF/MS *m/z* calc'd for [C$_6$H$_7$NO$_3$ + H]$^+$: 142.12468, found 142.2990.

HRMS (FAB) *m/z* calc'd for [C$_6$H$_7$NO$_3$ + H]$^+$: 142.0426, found 142.0479.

114

(Z)-3-(1-hydroxyethylidene)-1-methylpyrrolidine-2,4-dione

The Fmoc group was cleaved from Fmoc-sarcosine-Wang resin according to *GP3*. The resulting amine was then acylated with diketene according to *GP5*. Cyclative cleavage followed according to *GP9*. The crude product was purified by preparative HPLC (C$_{18}$) to afford the title compound as a yellow amorphous solid (14 mg, 34%).

¹H NMR (400 MHz, CDCl$_3$): δ = 3.72 (s, 2H, α-CH$_2$), 3.01 (s, 3H, -CH$_3$), 2.43 (s, 3H, -CH$_3$).

¹³C NMR (100.6 MHz, CDCl$_3$): δ = 191.5, 183.4, 173.2, 102.2, 57.6, 28.3, 19.4.

MALDI-TOF/MS *m/z* calc'd for [C$_8$H$_9$NO$_3$ + H]$^+$: 156.17, found 156.38.

HRMS (FAB) *m/z* calc'd for [C$_8$H$_9$NO$_3$ + H]$^+$: 156.0582, found 156.0615.
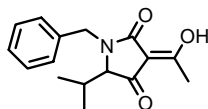
115

(Z)-1-benzyl-3-(1-hydroxyethylidene)-5-isobutylpyrrolidine-2,4-dione

The Fmoc group was cleaved from Fmoc-valine-Wang resin according to *GP3*. The resulting amine was reductively alkylated with benzaldehyde according to *GP4*, then acylated with diketene according to *GP5*. Cyclative cleavage according to *GP8* followed by flash-chromatography in 1:10 MeOH/EA afforded the title compound as a white amorphous solid (3 mg, 38%).

R*f* = 0.25 (MeOH/EA = 1/10).
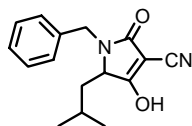
[α]^{20}$_D$ = - 7.32° (c = 0.5, MeOH).

¹H NMR (400 MHz, CD$_3$OD): δ = 7.28-7.19 (m, 5H, arom. CH), 5.15 (d, J = 15 Hz, 1H, benz. CH$_2$), 4.06 (d, J = 15 Hz, 1H, benz. CH$_2$), 2.35 (s, 3H, -CH$_3$), 2.21-2.16 (m, 1H, β-CH), 0.97 (s, 3H, CH(CH$_3$)$_2$), 0.84 (s, 3H, -CH(CH$_3$)$_2$).

¹³C NMR (100.6 MHz, CD$_3$OD): δ = 206.7, 194.4, 183.4, 135.4, 128.8, 128.0,

_____

_____

102.5, 68.1, 43.2, 29.7, 19.4, 17.7, 16.4, 14.0, 13.6.

LC-MS: (C_{18}) 274.2 [M+H]$^+$; R_t = 9.64 min.

HRMS (FAB) *m/z* calc'd for [$C_{16}H_{19}NO_3$ + H]$^+$: 274.1365, found 274.1455.

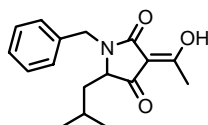**1-benzyl-2,5-dihydro-4-hydroxy-5-isobutyl-2-oxo-1H-pyrrole-3-carbonitrile**

116

The Fmoc group was cleaved from Fmoc-leucine-Wang resin according to *GP3*. The resulting amine was then reductively alkylated with benzaldehyde according to *GP4*, then acylated with cyanoacetic acid according to *GP7*. Cyclative cleavage according to *GP9* and preparative HPLC (C_{18}) afforded the title compound as a white amorphous solid (2 mg, 15%).

R*f* = 0.27 (MeOH/EA = 1/10).

[α] $_D^{20}$ = -2.60° (c = 0.7, MeOH).

^{1}H NMR (400 MHz, CD$_3$OD): δ = 7.35-7.22 (m, 5H, arom. CH), 4.95 (d, J = 15 Hz, 1H, benz. CH), 4.46-4.43 (m, 1H, α-CH$_2$), 4.18 (d, J = 15 Hz, 1H, benz. CH), 1.73-1.58 (m, 3H, γ-CH, β-CH$_2$), 0.82 (s, 3H, -CH$_3$), 0.81 (s, 3H, -CH$_3$).

HRMS (FAB) *m/z* calc'd for [$C_{16}H_{18}N_2O_2$ + H]$^+$: 271.1368, found 271.1459.

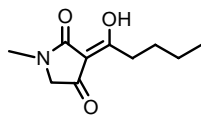**(Z)-1-benzyl-3-(1-hydroxyethylidene)-5-isobutylpyrrolidine-2,4-dione**

117

The Fmoc group was cleaved from Fmoc-leucine-Wang resin according to *GP3*. The resulting amine was reductively alkylated with benzaldehyde according to *GP4*, then acylated with diketene according to *GP5*. Cyclative cleavage according to *GP9* followed by flash-chromatography in 1:10 MeOH/EA afforded the title compound as a white amorphous solid (3 mg, 18%).

[α]^{20} $_D$ = -12.56° (c = 0.87, MeOH).

^{1}H NMR (400 MHz, CD$_3$OD): δ = 7.26-7.26 (m, 5H, arom. CH), 5.06 (d, J = 15 Hz, 1H, benz. CH), 4.20 (d, J = 15 Hz, 1H, benz. CH), 3.67-3.64 (m, 1H, α-CH), 2.44 (s, 3H, -CH$_3$), 1.79-1.73 (m, 1H, γ-CH), 1.65-1.61 (m, 2H, β-CH$_2$), 0.83 (d, J

_____

_____

= 7 Hz, 3H, -CH$_3$), 0.77 (d, J = 7 Hz, 3H, -CH$_3$).

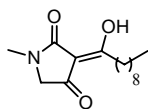**HRMS (FAB)** *m/z* calc'd for [C$_{17}$H$_{21}$NO$_3$ + H]$^+$: 288.1521, found 288.1633.

(Z)-3-(1-hydroxypentylidene)-1-methylpyrrolidine-2,4-dione

The Fmoc group was cleaved from Fmoc-sarcosine-Wang resin according to *GP3*. The resulting amine was

118

acylated with valeric Meldrum's acid according to *GP6*. Cyclative cleavage according to *GP9* afforded the title compound as a red amorphous solid (9 mg, 43 %).

^{1}H NMR (400 MHz, CDCl$_3$): δ = 3.71 (s, 2H, α-CH$_2$), 3.00 (s, 3H, -CH$_3$), 2.92 (t, J = 7 Hz, 2H, -CH$_2$), 1.67-1.59 (m, 2H, -CH$_2$), 1.44-1.37 (m, 2H, -CH$_2$), 0.92 (t, J = 7Hz, 3H, -CH$_3$).

^{13}C NMR (100.6 MHz, CDCl$_3$): δ = 191.2, 187.5, 173.5, 101.6, 57.6, 32.3, 28.0, 22.32, 13.6.

HRMS (FAB) *m/z* calc'd for [C$_{10}$H$_{16}$NO$_3$ + H]$^+$: 198.1052, found 198.1126.
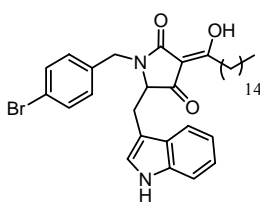
(Z)-3-(1-hydroxydecylidene)-1-methylpyrrolidine-2,4-dione

The Fmoc group was cleaved from Fmoc-sarcosine-Wang resin according to *GP3*. The resulting amine was

119

acylated with caproic Meldrum's acid according to *GP6*. Cyclative cleavage according to *GP9* followed by flash-chromatography in 1:2 EA/CH afforded the title compound as a white amorphous solid (9 mg, 42%).

^{1}H NMR (400 MHz, CDCl$_3$): δ = 3.71 (s, 2H, α-CH$_2$), 3.01 (s, 3H, -NCH$_3$), 2.81 (t, J = 7 Hz, 2H, -CH$_2$), 1.70-1.60 (m, 2H, -CH$_2$), 1.36-1.25 (m, 16H, -(CH$_2$)$_5$), 0.87 (t, J = 7 Hz, -CH$_2$CH$_3$).

^{13}C NMR (100.6 MHz, CDCl$_3$): δ = 191.2, 187.6, 173.5, 101.6, 57.6, 32.6, 31.8-29.1, 28.3, 25.9, 22.6, 14.0.

HRMS (FAB) *m/z* calc'd for [C$_{15}$H$_{25}$NO$_3$ + H]$^+$: 268.1834, found 268.1890.

_____

121

(Z)-5-((1H-indol-3-yl)methyl)-1-(4-bromobenzyl)-3-(1-hydroxyhexadecylidene)pyrrolidine-2,4-dione

The Fmoc group was cleaved from Fmoc-tryptophan-Wang resin according to *GP3*. The resulting amine was reductively alkylated with 4-bromobenzaldehyde according to *GP4*, then acylated with palmitoyl
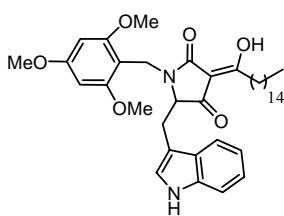
Meldrum's acid according to *GP6*. Cyclative cleavage according to *GP9* followed by flash-chromatography in 1:10 MeOH/EA afforded the title compound as a white amorphous solid (4 mg, 8%).

R_f = 0.29 (1:10 MeOH/EA).

$[\alpha]^{20}_D$ = - 13.4° (c = 0.78, MeOH).

^{1}H NMR (400 MHz, CDCl$_3$): δ = 8.19 (d, J = 8 Hz, 1H, arom. CH), 7.45 (d, J = 8 Hz, 1H, arom. CH), 7.38 (d, J = 8 Hz, 1H, arom. CH), 7.33 (d, J = 8 Hz, 1H, arom. CH), 7.10-707 (m, 1H, arom. CH), 6.99-6.95 (m, 4H, arom. CH), 5.06 (d, J = 15 Hz, 1H, benz. CH), 4.02 (d, J = 15 Hz, 1H, benz. CH), 3.66-3.50 (m, 2H, β-CH$_2$), 2.86-2.75 (m, 2H, pal CH$_2$), 1.65-1.51 (m, 2H, pal CH$_2$), 1.23 (br, 22H, pal CH$_2$), 0.87 (t, J = 7 Hz, pal CH$_3$).

HRMS (FAB) *m/z* calc'd for [C$_{36}$H$_{47}$BrN$_2$O$_3$ + H]$^+$: 635.2770, found 635.2812.

122

(Z)-5-((1H-indol-3-yl)methyl)-1-(2,4,6-trimethoxybenzyl)-3-(1-hydroxypropylidene) pyrrolidine-2,4-dione

The Fmoc group was cleaved from Fmoc-leucine-Wang resin according to *GP3*. The resulting amine was reductively alkylated with 2,4,6-trimethoxy benzaldehyde according to *GP4*, then acylated with
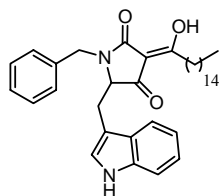
palmitoyl Meldrum's acid according to *GP6*. Cyclative cleavage according to *GP9* followed by purification by preparative tlc in 1:3 EA/CH afforded the title compound as a reddish oil (1 mg, 2%).

R*f* = 0.38 (EA/CH = 1/3).

^{1}H NMR (400 MHz, CD$_3$OD): δ = 8.08 (d, J = 7 Hz, 1H, arom. CH), 7.44 (d, J = 8 Hz, 1H, arom. CH), 7.31-7.26 (m, 2H, arom. CH), 7.18 (t, J = 7 Hz, 1H arom.

CH), 6.96 (d, J = 8Hz, 1H, arom. CH), 6.65 (s, br, 1H, arom. CH), 5.14 (d, J = 14 Hz, 1H, benz. CH_2), 3.92 (t, J = 5 Hz, 1H, α-CH), 3.85 (d, J = 14 Hz, 1H, benz. CH_2), 3.19 (d, J = 5 Hz, 2H, β-CH_2), 2.92 (s, 9H, OCH_3), 2.76-2.70 (m, 2H, pal-CH_2), 1.60-1.50 (m, 2H, pal-CH_2), 1.24 (s, br, 24H, pal-CH_2), 0.87 (t, J = 7 Hz, 3H, pal-CH_3).

123

(Z)-5-((1H-indol-3-yl)methyl)-1-benzyl-3-(1-hydroxyhexadecylidene)pyrrolidine-2,4-dione

The Fmoc group was cleaved from Fmoc-tryptophan-Wang resin according to *GP3*. The resulting amine was reductively alkylated with benzaldehyde according to *GP4*, then acylated with palmitoyl Meldrum's acid

according to *GP6*. Cyclative cleavage according to *GP9* followed by flash-chromatography in 1:2 EA/CH afforded the title compound as a white amorphous solid (8 mg, 16%).

Rf = 0.28 (EA/CH = 1/2).

$[\alpha]^{20}_D$ = -23.1° (c = 0.78, MeOH).

^{1}H NMR (400 MHz, CD_3OD): δ = 7.99 (s, br, 1H, NH), 7.54 (d, J = 8 Hz, 1H, arom. CH), 7.33 (d, J = 8 Hz, 1H, arom. CH), 7.26-7.27 (m, 1H, arom. CH), 7.17 (t, J = 7 Hz, arom. CH), 7.10-7.06 (m, 5H, arom. CH), 6.88 (s, 1H, arom. CH), 5.19 (d, J = 15 Hz, 1H, benz. CH_2), 3.96 (d, J = 15 Hz, 1H, benz. CH_2), 3.91 (t, J = 5 Hz, 1H, α-CH), 3.29 (t, J = 5 Hz, 2H, β-CH_2), 2.80-2.63 (m, 2H, pal-CH_2), 1.54-1.40 (m, 2H, pal-CH_2), 1.26 (s, br, 26H, pal-CH_2), 0.88 (t, J = 7 Hz, 3H, pal-CH_3).

LC-MS: (C_4) 557.64 $[M + H]^+$; rt = 10.49 min.

HRMS (FAB) *m/z* calc'd for $[C_{37}H_{50}N_2O_3 + H]^+$: 571.3821, found 571.4225.
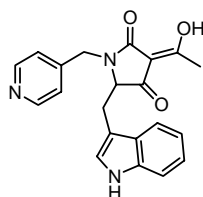
124

(Z)-5-((1H-indol-3-yl)methyl)-3-(1-hydroxypropylidene)-1-((pyridin-4-yl)methyl)pyrrolidine-2,4-dione

The Fmoc group was cleaved from Fmoc-Tryptophan-Wang resin according to *GP3*. The resulting amine was reductively alkylated with 4-pyridine benzaldehyde

_____

according to *GP4*, then acylated with diketene according

to *GP5*. Cyclative cleavage according to *GP9* followed by preparative HPLC (C_{18})

afforded the title compound as a beige amorphous solid (3 mg, 4%).

Rf = 0.35 (EA/CH = 1/3).

$[\alpha]^{20}_D$ = - 7.2° (c = 0.3, MeOH).

^{1}H NMR (400 MHz, CD$_3$OD): δ = 8.27 (d, J = 7 Hz, 1H, arom. CH), 7.36 (d, J = 7 Hz, 1H, arom. CH), 7.28 (d, J = 8 Hz, 1H, arom. CH), 7.22 (d, J = 8 Hz, 1H, arom. CH), 7.07 (t, J = 7 Hz, 1H, arom. CH), 7.00 (s, 1H, arom. CH), 6.88 (t, J = 7 Hz, 1H, arom. CH), 4.76 (d, J = 9 Hz, 2H, benz. CH$_2$), 4.40 (q, J = 4Hz, 1H, α-CH), 3.38 (dd, J = 4 Hz, 1H, β-CH$_2$), 3.13 (dd, J = 4 Hz, 1H, β-CH$_2$), 2.47 (s, 3H, -CH$_3$).

LC-MS: (C_{18}) 362.33 [M+H]$^+$; rt = 4.89 min.

HRMS (FAB) *m/z* calc'd for [$C_{21}H_{19}N_3O_3$ + H]$^+$: 362.1426, found 362.1476.
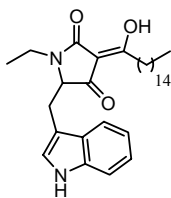
125

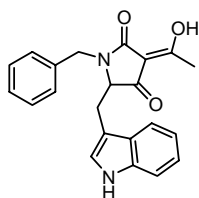**(Z)-5-((1H-indol-3-yl)methyl)-1-ethyl-3-(1-hydroxyhexadecylidene)pyrrolidine-2,4-dione**

The Fmoc group was cleaved from Fmoc-Tryptophan-Wang resin according to *GP3*. The resulting amine was reductively alkylated with acetaldehyde according to *GP4*, then acylated with palmitoyl Meldrum's acid

according to *GP6*. Cyclative cleavage according to *GP9* followed by flash-chromatography in 1:2 EA/CH afforded the title compound as a white amorphous solid (12.6 mg, 40%).

$[\alpha]^{20}_D$ = -14.72° (c = 0.66, MeOH).

^{1}H NMR (400 MHz, CD$_3$OD): δ = 8.08 (d, J = 7Hz, 1H, arom. CH), 7.44 (d, J = 8 Hz, arom. CH), 7.31-7.28 (m, 2H, arom. CH), 7.18 (t, J = 7 Hz, 1H, arom. CH), 6.97 (d, J = 8 Hz, 2H, arom. CH), 5.14 (d, J = 14 Hz, 1H, benz. CH), 3.92 (t, J =, 1H, α-CH), 3.85 (d, J = 15 Hz, 1H, benz. CH$_2$), 3.19 (d, J = 5 Hz, 2H, β-CH$_2$), 2.93 (s, 9H, OCH$_3$), 2.76-2.65 (m, 2H, pal CH$_2$), 1.65-1.5 (m, 4H, pal CH$_2$), 1.24 (s, br, 22H, pal CH$_2$), 0.87 (t, J = 7 Hz, pal CH$_3$).

HRMS (FAB) *m/z* calc'd for [$C_{31}H_{46}N_2O_3$]$^+$: 494.3508, found 494.3495.

_____

(Z)-5-((1H-indol-3-yl)methyl)-1-benzyl-3-(1-hydroxyethylidene)pyrrolidine-2,4-dione

The Fmoc group was cleaved from Fmoc-Tryptophan-Wang resin according to *GP3*. The resulting amine was reductively alkylated with benzaldehyde according to *GP4*, then acylated with diketene according to *GP5*.

Cyclative cleavage according to *GP9* followed by flash-chromatography in 1:10 MeOH/EA afforded the title compound as a white amorphous solid (4 mg, 13%).
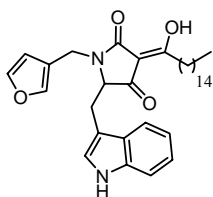
Rf = 0.20 (MeOH/EA = 1/10).

$[\alpha]^{20}_D$ = - 21.8° (c = 0.3, MeOH).

^{1}H NMR (400 MHz, CD$_3$OD): δ = 7.54 (d, J = 8 Hz, 1H, arom. CH), 7.28 (t, J = 8 Hz, 1H, arom. CH), 7.13 (s, 1H, arom. CH), 7.06-7.03 (m, 1H, arom. CH), 6.97-6.95 (m, 1H, arom. CH), 5.06 (dd, J = 16 Hz, 1H, benz. CH$_2$), 4.8-4.79 (m, 1H, α-CH), 3.83 (dd, J = 16 Hz, 1H, benz. CH$_2$), 3.70 (s, 1H, β-CH$_2$), 3.16-3.11 (m, 1H, β-CH$_2$), 2.30 (s, 3H, -CH$_3$).

MALDI-TOF *m/z* calc'd for [C$_{22}$H$_{20}$N$_2$O$_3$ + H]$^+$: 361.14, found 361.58.

HRMS (FAB) *m/z* calc'd for [C$_{22}$H$_{20}$N2O$_3$ + H]$^+$: 361.1474, found 361.1550.

(Z)-5-((1H-indol-3-yl)methyl)-1-((furan-3-yl)methyl)-3-(1-hydroxyhexadecylidene)pyrrolidine-2,4-dione

The Fmoc group was cleaved from Fmoc-Tryptophan-Wang resin according to *GP3*. The resulting amine was reductively alkylated with 3-furaldehyde according to *GP4*, then acylated with palmitoyl Meldrum's acid

according to *GP6*. Cyclative cleavage according to *GP9* followed by flash-chromatography in 1:2 EA/CH afforded the title compound as a white amorphous solid (3 mg, 7%).

Rf = 0.40 (EA = 100%).

$[\alpha]^{20}_D$ = - 17.3° (c = 0.3, MeOH).

^{1}H NMR (400 MHz, CD$_3$OD): δ = 8.03 (s, 1H, NH), 7.57 (d, J = 8 Hz, 1H, arom.

CH), 7.35-7.30 (m, 2H, arom. CH), 7.19 (t, J = 7 Hz, 1H, arom. CH), 7.11 (t, J = 7 Hz, 1H, arom. CH), 7.02 (s, 1H, arom. ,CH), 6.93 (s, 1H, arom. CH), 6.20 (s, 1H, arom. CH), 4.92 (d, J = 16 Hz, 1H, benz. CH$_2$), 3.98 (t, J = 5 Hz, 1H, α-CH$_2$), 3.82 (d, J = 16 Hz, 1H, benz. CH$_2$), 3.31-3.27 (m, 2H, β-CH$_2$), 2.80-2.66 (m, 2H, pal-CH$_2$), 1.53-1.44 (m, 2H, pal-CH$_2$), 1.26 (s, br, pal-CH$_2$), 0.88 (t, J = 7 Hz, 3H, pal-CH$_3$).

LC-MS: (C$_4$) 547.60 [M + H]$^+$; rt = 10.26 min.

HPLC: (C$_4$) rt = 8.35 min.

HRMS (FAB) *m/z* calc'd for [C$_{34}$H$_{46}$N$_2$O$_3$]$^+$: 546.3458, found 546.3459.
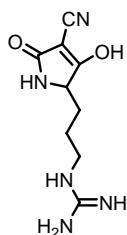

(3-(4-cyano-2,5-dihydro-3-hydroxy-5-oxo-1H-pyrrol-2-yl)propyl)guanidine

To a solution of **108** (8 mg, 0.016 mmol) in 1 ml CHCl$_3$ was added 1.9 ml TFA. The mixture was stirred for 2 h at room temperature. The solvent was then evaporated to yield 3.4 mg of **130** (94%).

130

^{1}**H NMR** (400 MHz, CD$_3$OD): δ = 3.51-3.41 (m, 1H, α-CH), 3.08-3.06 (m, 2H, δ-CH$_2$), 1.60-1.54 (m, 1H, β-CH$_2$), 1.50-1.45 (m, 2H, γ-CH$_2$), 1.37-1.33 (m, 1H, β-CH$_2$).

HRMS (FAB) *m/z* calc'd for [C$_9$H$_{13}$N$_5$O$_2$ + H]$^+$: 224.1069, found 224.1128.

6.1.3   Compounds from Chapter 4.2
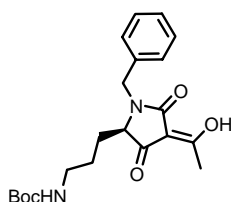
tert-butyl 3-((Z)-1-benzyl-4-(1-hydroxyethylidene)-3,5-dioxopyrrolidin-2-yl)propylcarbamate

The Fmoc group was cleaved from Fmoc-ornithine(Boc)-Wang resin according to *GP3*. The resulting amine was reductively alkylated with benzaldehyde according to *GP4*, then acylated with

128

diketene according to *GP5*. Cyclative cleavage according to *GP9* followed by flash-chromatography in 1:10 MeOH/CHCl$_3$ to provide 14 mg (18 %) product.

_____

Rf = 0.50 (MeOH/CHCl$_3$ = 3/5).

[α]$_D^{20}$ = -26.31° (c = 0.5, MeOH).

^{1}H NMR (400 MHz, CD$_3$OD): δ = 7.28 -7.17 (m, 5H, arom. CH), 5.06 (d, J = 15 Hz, 1H, benz. CH$_2$), 4.05 (d, J = 15 Hz, benz. CH$_2$), 3.48 (s, br, 1H, α-CH), 2.89 – 2.87 (m, 2H, γ-CH$_2$), 2.36 (s, 3H, -CH$_3$), 1.78 – 1.70 (m, 4H, β-CH$_2$, δ-CH$_2$), 1.42 (s, 9H, -C(CH$_3$)$_3$).

^{13}C NMR (100.6 MHz, CDCl$_3$): δ = 173.88, 173.08, 128.94, 128.22, 101.92, 101.20, 68.01, 63.65, 43.36, 40.09, 28.39, 25.37, 23.59, 20.60, 19.51.

MALDI-TOF/MS *m/z* calc'd for [C$_{21}$H$_{28}$N$_2$O$_5$ + K]$^+$: 427.45, found: 427.32.

HRMS (EI) *m/z* calc'd for [C$_{21}$H$_{28}$N$_2$O$_5$ + H]$^+$: 389.4574, found 389.2085.
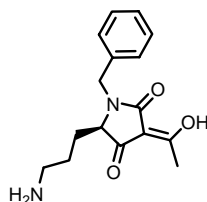
129

(Z)-5-(3-aminopropyl)-1-benzyl-3-(1-hydroxy ethylidene)pyrrolidine-2,4-dione

128 (10 mg, 0.0257 mmol) was dissolved in 2 ml CHCl$_3$ and 1.9 ml TFA was added. The mixture was stirred for 2h at room temperature. The solvent was then evaporated to yield 6 mg of **129** (85%).

Rf = 0.34 (MeOH/CHCl$_3$ = 3/5).

[α]^{20} = -10.48 ° (c = 0.96, MeOH).

^{1}H NMR (400 MHz, CD$_3$OD): δ = 7.38-7.28 (m, 5H, arom. CH), 4.99 (d, J = 15 Hz, 1H, benz. CH), 4.29 (d, J = 15Hz, 1H, benz. CH), 2.78-2.73 (m, 2H, γ-CH$_2$), 2.45 (s, 3H, -CH$_3$), 2.02-1.99 (m, 2H, δ-CH$_2$), 1.97-1.73 (m, 2H, β-CH$_2$).

MALDI-TOF/MS *m/z* calc'd for [C$_{16}$H$_{19}$N$_2$O$_5$ + H]$^+$: 288.14, found 289.48.

LC-MS: (C$_{18}$): 289.0 [M+H]$^+$; rt = 5.08 min.

HRMS (FAB) *m/z* calc'd for [C$_{16}$H$_{20}$N$_2$O$_3$ + H]$^+$: 289.1474, found 289.1846.

6.1.4 Compounds from Chapter 4.3

Preparation of silica-gel impregnated with nitric acid[111]:

Silica-gel (60 g) and nitric acid (150 ml, 63%) were shaken at room temperature for 2h. The suspension was then filtered using a glass frit (#3) and dried in vacuo.

_____ 95

_____
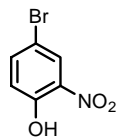
4-Bromo, 2-nitrophenol[145]

Nitric acid impregnated with HNO_3 was suspended in dichloromethane and cooled to 0 °C. The mixture was treated with 4-bromophenol (0.4 g, 2 mmol) in several portions. After 5 min the mixture was filtered, and the silica gel cake washed with dichloromethane. The concentrated filtrate yielded the desired product of sufficient purity for use in the next step (0.358 g, 83%).

R*f* = 0.70 (EA/CH = 1/2).

^{1}H NMR (400 MHz, $CDCl_3$): δ = 8.25 (s, 1H, arom. CH), 7.64 (d, J = 9 Hz, 1H, arom. CH), 7.08 (d, J = 9 Hz, 1H, arom. CH).

GCMS *m/z*: 217 [M+H]$^+$; rt = 3.20 min.

The spectroscopic data is in agreement with the assigned structure and those reported by Nugiel et al.[145]
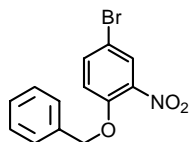
1-((4-bromo-2-nitrophenoxy)methyl)benzene

To a solution of bromo-nitrophenol **162** in DMF was added benzyl bromide (69 μl, 0.584 mmol) and K_2CO_3 (0.107 g, 0.78 mmol). The mixture was heated for 18 h at 60 °C. The resulting precipitate was filtered through a pad of celite and washed with DMF. The filtrate was concentrated under reduced pressure to an orange oil and flash-chromatographed in 1:10 EA/CH to provide 107 mg (90%) **163** as a yellow oil.

R*f* = 0.68 (EA/CH = 1/2).

^{1}H NMR (400 MHz, $CDCl_3$): δ = 7.97 (s, 1H, arom. CH), 7.58 (dd, J= 3 Hz, J^2 = 9 Hz, 1H, arom. CH), 7.44-7.33 (m, 5 H, arom. CH), 7.00 (d, J = 3 Hz, 1H, arom. CH), 5.22 (s, 2H, benz. CH_2).

^{13}C NMR (100.6 MHz, $CDCl_3$): δ = 150.8, 136.5, 134.8, 128.6, 128.2, 126.8, 116.7, 112.1, 71.4.
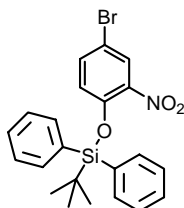
_____

_____

(4-bromo-2-nitrophenoxy)(tert-butyl)diphenylsilane

164

To a solution of **162** in dry DMF was added imidazole (63 mg, 0.917 mmol) and TBDPS-Cl (151 mg, 0.550 mmol). The mixture was stirred under argon atmosphere for 18 h. The reaction was then diluted with H_2O and extracted three times with Et_2O. The organic phase was dried over Na_2SO_4 and evaporated under reduced pressure. The resulting crude product was chromatographed in 1/10 EA:CH to provide 161 mg (86%) of **164**.

Rf = 0.72 (EA/CH = 1/2).

^{1}H NMR (400 MHz, CDCl$_3$): δ = 10.49 (s, 1H, arom. CH9, 8.25 (d, J = 3 Hz, 1H, arom. CH), 7.73-7.70 (m, 4H, arom. CH), 7.66 (dd, J = 3 Hz, J = 9 Hz, 1H, arom. CH), 7.41-7.37 (m, 5 H, arom. CH), 7.08 (d, J = 9 Hz., 1H, arom. CH), 1.07 (s, 9 H, -(-CH$_3$)$_3$).

^{13}C NMR (100.6 MHz, CDCl$_3$): δ = 153.9, 149.5, 140.1, 135.0, 134.6, 129.5, 127.6, 127.5, 127.1, 121.6, 111.6, 26.6, 19.1.

General Procedure for the Synthesis of Indoles via the Bartoli Method (GP10)

A dry 2-necked round bottom flask under argon atmosphere was charged with nitroarene (1 eq.) in freshly distilled THF and cooled to -40 °C in an acetone/dry ice bath. Vinyl Grignard (3 eq.) was then quickly added via a syringe. After 20-30 minutes, the reaction was quenched by pouring into a saturated solution of NH$_4$Cl. The aqueous phase was washed three times with Et$_2$O and the combined organic phases were dried over Na$_2$SO$_4$. The indoles were then purified by flash chromatography as indicated.

7-(benzyloxy)-4-bromo-1H-indole

175
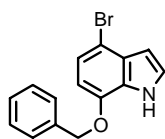
Indole **175** was synthesized according to *GP10* starting from nitroarene **163** (0.093 g, 0.303 mmol). The crude product was purified by flash chromatography in 1:10 EA/CH to provide the title compound (0.039 g, 43 %) as a yellow oil.

_____

_____

Rf = 0.87 (EA/CH = 1/2).

^{1}H NMR (400 MHz, CDCl$_3$): δ = 7.45-7.6 (m, 5H, arom. CH), 7.20 (t, J = 3 Hz, 1H, arom. CH), 7.16 (d, J = 7 Hz, 1H, arom. CH), 6.59 (d, J = 7 Hz, 1H, arom. CH), 6.56 (dd, J = 3 Hz, 6 Hz, 1H, arom. CH), 5.18 (s, 2H, benz. CH$_2$).

^{13}C NMR (100.6 MHz, CDCl$_3$): δ = 144.6, 136.4, 129.4, 128.5, 128.1, 127.6, 126.7, 125.7, 123.9, 122.3, 105.8, 104.2, 103.2, 70.5.

GCMS *m/z*: 301 [M]; rt = 6.24 min.

The spectroscopic data is in agreement with the assigned structure and those reported by Stolz et al.[113]

7-methyl-1H-indole

Indole **177** was synthesized according to *GP10* starting from 2-methylnitrobenzene (859 μl, 3.64 mmol). The crude product was purified by flash chromatography in

177

1:10 EA/CH to provide 0.056 g (6 %) of the title compound as yellow oil.

Rf = 0.13 (EA/CH = 1/10).

^{1}H NMR (400 MHz, CDCl$_3$): δ = 8.08 (s, 1H, NH), 7.52 (d, J = 8 Hz, 1H, arom. CH), 7.21 (t, J = 3 Hz, 1H, arom. CH), 7.07-7.00 (m, 1H, arom. CH), 6.57 (q, J = 2 Hz, J = 3 Hz, 1H, arom. CH), 2.51 (s, 3H, -CH$_3$).

^{13}C NMR (100.6 MHz, CDCl$_3$): δ = 135.6, 127.6, 124.0, 122.7, 120.4, 120.2, 118.6, 103.3.

GCMS *m/z*: 130 [M-H]; rt = 3.48 min.

The spectroscopic data is in agreement with the assigned structure and those reported by Bartoli et al.[109]
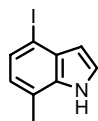
4-iodo-7-methyl-1H-indole

Indole **178** was synthesized according to *GP10* starting from 4-iodo-2-nitrotoluene (0.5 g, 1.90 mmol). The crude product was purified by flash chromatography in

178

first 1.15, then eluted with 1:8 EA/CH to provide the title compound (0.185 g, 38 %) as a yellow oil.
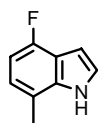
_____

_____

Rf = 0.45 (EA/CH = 1/3).

^{1}H NMR (400 MHz, CDCl$_3$): δ = 8.25 (s, br, NH), 7.43 (d, J = 8 Hz, 1H, arom. CH), 7.27-7.26 (m, 1H, arom. CH), 6.75 (d, J = 7 Hz, 1H, arom. CH), 6.49 (d, J = 7 Hz, 1H, arom. CH), 2.46 (s, 3H, -CH$_3$).

^{13}C NMR (100.6 MHz, CDCl$_3$): δ = 134.7, 131.9, 129.5, 124.3, 124.2, 124.2, 120.7, 106.8, 84.2, 16.5.

GCMS *m/z*: 257 [M+H]$^+$; rt = 7.24 min.

4-fluoro-7-methyl-1H-indole

179

Indole **179** was synthesized according to *GP10* starting from 4-fluoro-2-nitrotoluene (0.5 g, 3.22 mmol). The crude product was purified by flash chromatography in first 1:20, then 1:15 then 1:10 EA/CH to provide the title compound (0.147 g, 31 %) as a yellow oil.

Rf = 0.44 (EA/CH = 1/3).

^{1}H NMR (400 MHz, CDCl$_3$): δ = 7.19-7.18 (m, 1H, arom. CH), 6.89-6.86 (m, 1H, arom. CH), 6.72-6.64 (m, 2H, arom. CH), 2.45 (s, 3H, -CH$_3$).

GCMS *m/z*: 148 [M+H]; rt = 3.62 min.

The spectroscopic data is in agreement with the assigned structure and those reported by Blair et al.[146]
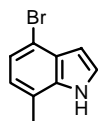
4-bromo-7-methyl-1H-indole

180

Indole **180** was synthesized according to *GP10* starting from 4-bromo-2-nitrotoluene (0.5 g, 2.31 mmol). The title compound was purified by flash chromatography in 1:5 EA/CH to yield 0.197 g (41 %).

of a yellow amorphous solid

Rf = 0.36 (EA/CH = 1/5).

^{1}H NMR (400 MHz, CDCl$_3$): δ = 8.20 (s, br, 1H, NH), 7.27 – 7.26 (m, 1H, arom. CH), 7.20 (d, J = 8 Hz, 1H, arom. CH), 6.86 (d, J = 8 Hz, 1H, arom. CH), 6.62 – 6.60 (m, 1H, arom. CH), 2.46 (s, 1H, -CH$_3$).

_____

^{13}**C NMR** (100.6 MHz, CDCl$_3$): δ = 135.6, 127.9, 124.3, 123.4, 122.7, 119.5, 111.9, 103.4, 16.3.

GCMS *m/z*: 209 [M+H]$^+$; rt = 4.64 min.

6-bromo-7-methyl-1H-indole

Indole **181** was synthesized according to *GP10* starting from 1-bromo-5-nitrotoluene (0.3 g, 1.38 mmol). The crude product was purified by flash-chromatography in 1:9 EA/CH to provide the title compound (0.177 g, 61 %) as a yellow amorphous solid.
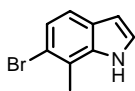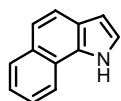
181

Rf = 0.18 (EA/CH = 1/9).

^{1}**H NMR** (400 MHz, CDCl$_3$): δ = 8.05 (br s, 1H, NH), 7.31 (d, J = 9 Hz, 1H, arom. CH), 7.22 (d, J = 9 Hz, 1H, arom. CH), 7.14 (dd, J = 3 Hz, 1H, arom. CH), 6.49 (dd, J = 3 Hz, 1H, arom. CH), 2.50 (s, 3H, -CH$_3$).

^{13}**C NMR** (100.6 MHz, CDCl$_3$): δ = 135.7, 126.3, 124.3, 124.0, 119.8, 119.2, 117.6, 103.3, 16.8.

1H-benzo[g]indole

Indole **182** was synthesized according to *GP10* starting from 4-nitronaphthalene (0.5 g, 2.88 mmol). The crude product was purified by flash chromatography in a gradient beginning with 100% CH to elution of the product in 1:20 EA/CY to provide the title compound (0.040 g, 8 %) as a yellow oil.

182

Rf = 0.21 (EA/CH = 1/10).

^{1}**H NMR** (400 MHz, CDCl$_3$): δ = 8.89 (s, 1H, NH), 8.00 (d, J = 8 Hz, 1H, arom. CH), 7.93 (d, J = 8 Hz, 1H, arom. CH), 7.73 (d, J = 9 Hz, 1H, arom. CH), 7.55-7.51 (m, 2H, arom. CH), 7.45-7.41 (m, 1H, arom. CH), 7.27 (t, J = 2 Hz, 1H, arom. CH).

The spectroscopic data is in agreement with the assigned structure and those reported Bartoli et al.[109]

_____

1H-pyrrolo[2,3-f]isoquinoline

183

Indole **183** was synthesized according to *GP10* starting from 4-nitroisoquinoline (0.5 g, 2.87 mmol). The crude product was purified by flash chromatography in 1:30 EA/CH to provide the title compound (0.072 g,

15 %) as a yellow oil.

R*f* = 0.28 (EA = 100%).

^{1}H NMR (400 MHz, CDCl$_3$): δ = 10.85 (s, 1H, NH), 9.17 (s, 1H, arom. CH), 8.39 (d, J = 4 Hz, 1H, arom. CH), 8.10 (d, J = 6 Hz, 1H, arom. CH), 7.84 (d, J = 9 Hz, 1H, arom. CH), 7.54 (d, J = 8 Hz, 1H, arom. CH), 7.46 (t, J = 3 Hz, 1H, arom. CH), 6.73 (q, J = 3 Hz, J = 2 Hz, 1H, arom. CH).

^{13}C NMR (100.6 MHz, CDCl$_3$): δ = 152.79, 140.58, 128.54, 127.78, 125.69, 125.54, 125.03, 123.02, 119.30, 114.56, 104.52.

GCMS *m/z*: 168 [M]; rt = 5.43 min.

The spectroscopic data is in agreement with the assigned structure and those reported by Vlachou et al.[114]
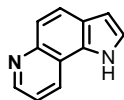
7-bromo-1H-indole

184

Indole **184** was synthesized according to *GP10* starting from 1-bromo-2-nitrobenzene (0.2 g, 1 mmol). The crude product was purified by flash chromatography in 1:30 EA/CH to provide the title compound (0.100 g,

51 %) as a yellow oil.

R*f* = 0.21 (EA/CH = 1/20).

**^{1}H NMR** (400 MHz, CDCl$_3$): δ = 8.24 (s, br, NH), 7.50 (dt, J = 1 Hz, J = 7 Hz, 1H, arom. CH), 7.27 (dd, J = 8 Hz, 1H, arom. CH),7.24 (t, J = 3 Hz, 1H, arom. CH), 7.06-7.01 (m, 1H, arom. CH), 6.64 (d, J = 7 Hz, arom. CH).

GCMS *m/z*: 195 [M+H]; rt = 3.42 min.

The spectroscopic data is in agreement with the assigned structure and those reported by Bartoli et al.[109]

_____

_____

General Procedure for the synthesis acetyl tryptophan derivatives (GP11)

DL-serine (0.673 mmol, 2 eq.) was added to a solution of indole (0.336 mmol, 1 eq.), acetic acid (785 µL, 0.427 M), and acetic anhydride (63 µL, 2 eq.). The mixture was heated to 75 °C under argon atmosphere for 2 h. After cooling to room temperature, the solution was diluted with Et_2O and the pH was adjusted to 11 with 30% NaOH. The aqueous phase was then washed three times with Et_2O, and the combined organic phases were washed with 1M NaOH. The combined aqueous phases were cooled to 0 °C before adjusting the pH to 1 with conc. HCl. The product was then extracted three times with EtOAc. The organic phases were dried over Na_2SO_4 and evaporated under reduced pressure. The product was isolated either by flash chromatography or preparative HPLC, or a combination of both.
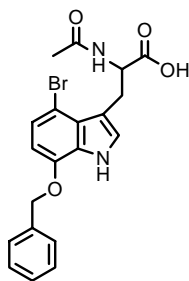
196

***dl-N*-Acetyl-7-(benzyloxy)tryptophan**

Starting from 7-(benzyloxy)-4-bromo-1H-indole (38 mg, 0.126 mmol), tryptophan **196** was synthesized according to *GP11*. The crude product was purified by flash chromatography in 1:10 MeOH/EA +1% AcOH to provide the title compound (23 mg, 42%) as a brown amorphous solid.

**R*f* = 0.25 (MeOH/EA = 1/10).

^{1}H NMR (400 MHz, CD_3OD): δ = 7.51 (d, J = 7 Hz, 1 H, arom. CH), 7.39 – 7.36 (m, 1H, arom. CH), 7.32 (d, J = 7 Hz, 1H, arom. CH), 7.09 (s, 1H, arom. CH), 7.05 (d, J = 8 Hz, 1H, arom. CH), 6.59 (d, J = 8 Hz, 1H, arom. CH), 5.20 (s, 2H, benz. CH_2), 4.84 - 4.81 (m, 1H, α-CH), 3.71 (dd, J = 15 Hz, 1H, β-CH_2), 3.21 (dd, J = 15 Hz, 1H, β-CH_2), 1.91 (s, 3H, Ac-CH_3).

LC-MS (C_{18}): 431.02 [M+H]$^+$; rt = 8.13 min.

_____
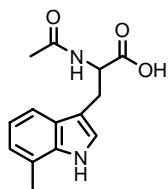
197

***dl*-*N*-Acetyl-7-methyltryptophan**

Starting from 7-methylindole (51 mg, 0.396 mmol), tryptophan **197** was synthesized according to *GP11*. The crude product was purified by preparative HPLC to provide the title compound as a yellow oil (16 mg, 16 %).
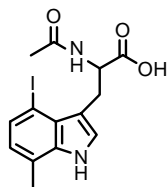
R*f* = 0.35 (MeOH/CHCl$_3$ = 3/5).

^{1}H NMR (400 MHz, *D$_6$*-acetone): δ = 7.43 (d, J = 8 Hz, 1H, arom. CH), 7.11 (s, 1H, arom. CH), 6.94-6.87 (m, 2H, arom. CH), 6.39 (s, 1H, arom. CH), 4.73-4.70 (m, 1H, α-CH), 3.29 (dd, J = 8 Hz, 20 Hz, 1H, β-CH$_2$), 2.45 (s, 3H, -CH$_3$), 1.87 (s, 3H, -CH$_3$).

^{13}C NMR (100.6 MHz, CD$_3$OD): δ = 178.2, 165.7, 123.9, 122.8, 119.9, 117.1, 116.3, 115.7, 113.9, 56.2, 28.9, 22.8, 16.9.

LC-MS: (C$_{18}$): 261.03 [M+H]$^+$; rt = 6.33 min.

HRMS (FAB) *m/z* calc'd for [C$_{14}$H$_{16}$N$_2$O$_3$ + H]$^+$: 261.1161, found 261.1210.

The spectroscopic data is in agreement with the assigned structure and those reported by Yabe et al.[147]

198

***dl*-*N*-Acetyl-4-iodo-7-methyltryptophan**

Starting from 4-iodo-7-methylindole (0.2 g, 0.778 mmol), tryptophan **198** was synthesized according to *GP11*. The crude product was purified by flash chromatography in 3:5 MeOH:CHCl$_3$ to provide the title compound (41 mg, 14%).

R*f* = 0.23 (MeOH/CHCl$_3$ = 3/5).

^{1}H NMR (400 MHz, CD$_3$OD): δ = 7.45 (d, J = 8 Hz, 1H, arom. CH), 6.6 (d, J = 8 Hz, 1H, arom. CH), 6.23 (s, 1H, arom. CH), 4.67-4.50 (m, 1H, α-CH), 3.78-3.60 (m, 2H, β-CH$_2$), 3.30 (s, 3H, -CH$_3$), 2.4 (s, 3H, -CH$_3$).

^{13}C NMR (100.6 MHz, CD$_3$OD): δ = 173.9, 170.8, 137.9, 131.8, 128.5, 126.8, 124.6, 122.4, 113.0, 112.9, 54.5, 28.7, 16.7.

LC-MS: (C$_{18}$): 387 [M+H]$^+$, rt = 7.15 min.

HRMS (FAB) *m/z* calc'd for [C$_{14}$H$_{15}$IN$_2$O$_3$]$^+$: 386.0127, found 386.0151.

_____
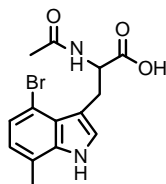
200

dl-N-Acetyl-4-bromo-7-methyltryptophan

Starting from 4-bromo-7-methylindole (0.173 g, 0.831 mmol), tryptophan **200** was synthesized according to *GP11*. The crude product was purified by preparative HPLC to provide the title compound (19 mg, 6%) as a colorless oil.

¹H NMR (400 MHz, D_6-acetone): δ = 10.30 (s, 1H, CO_2H), 7.36 (d, J = 8 Hz, 1H, NH), 7.30 (d, J = 3 Hz, 1H, arom. CH), 7.11 (d, J = 8 Hz, 1H, arom. CH), 6.81 (d, J = 8 Hz, 1H, arom. CH), 4.90-4.85 (m, 1H, α-CH), 3.72 (dd, J = 5 Hz, J = 15 Hz, 1H, β-CH_2), 3.26 (dd, J = 5 Hz, J = 15 Hz, 1H, β-CH_2), 2.43 (s, 3H, acetyl CH_3), 1.83 (s, 3H, -CH_3).

MALDI-TOF *m/z* calc'd for $[C_{14}H_{15}BrN_2O_3 + Na]^+$: 361.02, found 361.49.

HRMS (FAB) *m/z* calc'd for $[C_{14}H_{15}BrN_2O_3]^+$: 338.0266, found 338.0252.

201

dl-N-Acetyl-6-bromo-7-methyltryptophan

Starting from 6-bromo-7-methylindole (30 mg, 0.144 mmol), tryptophan **201** was synthesized according to *GP11*. The crude product was purified by flash chromatography in 1:10 MeOH/EA to provide the title compound (9 mg, 19 %) as a reddish oil.
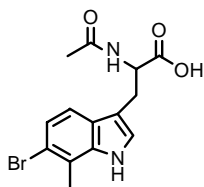
R*f* = 0.14 (MeOH/EA = 1/10).

¹H NMR (400 MHz, CD$_3$OD): δ = 7.29 (d, J = 9 Hz, 1H, arom. CH), 7.16 (d, J = 9 Hz, arom. CH), 7.09 (s, 1H, arom. CH), 4.69 (dd, J = 8 Hz, 1H, α-CH), 3.33-3.28 (m, 1H, β-CH_2), 3.11 (dd, J = 8 Hz, 1 H, β-CH_2), 2.51 (s, 3H, -CH_3), 1.90 (s, 3H, Ac-CH_3).

¹³C NMR (100.6 MHz, CD$_3$OD): δ = 172.7, 137.6, 129.7, 128.9, 127.6, 124.8, 121.2, 118.0, 111.9, 54.9, 28.5, 22.5, 16.8.

LC-MS: (C_{18}): 337 $[M+H]^+$, rt = 5.05 min.

_____

194

dl-N-Acetyl-4-bromotryptophan

Starting from 4-bromo-indole (1.12 g, 5.7 mmol), tryptophan **194** was synthesized according to *GP11*. The crude product was purified by flash chromatography in 1:20 MeOH/EA to provide the title compound (0.576 g, 31 %) as a reddish oil.
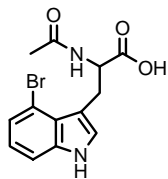
Rf = 0.51 (MeOH/EA = 1/10).

^{1}H NMR (400 MHz, CD$_3$OD): δ = 10.6 (s, br, 1H, COOH), 7.30 (d, J = 7 Hz, 1H, arom. CH), 7.17 (d, J = 1 Hz, 1H, arom. CH), 7.15 (t, J = 1 Hz, 1H, arom. CH), 6.93 (t, J = 8 Hz, 1H, arom. CH), 4.85 (dd, J = 5 Hz, 1H, α-CH), 3.73 (dd, J = 5 Hz, 1H, β-CH$_2$), 3.22 (dd, J = 5 Hz, 1H, β-CH$_2$), 1,90 (s, 3H, AcNH).

^{13}C NMR (100.6 MHz, CD$_3$OD): δ = 180.6, 173.8, 139.16, 126.7, 126.5, 126.3, 124.1, 123.2, 114.2, 112.0, 54.5, 29.1, 22.7.

HRMS (FAB) *m/z* calc'd for [C$_{13}$H$_{13}$BrN$_2$O$_3$]$^+$: 324.0110, found 324.0135.

The spectroscopic data is in agreement with the assigned structure and those reported Yokoyama et al.[116]

_____

6.2   Biochemical and Biological Materials and Methods

6.2.1   Materials

Laboratory equipment and Material

Pipettes: Sterile serological pipettes 1 ml, 10 ml, 25 ml (Becton Dickinson, U.S.A)

Cell culture flasks: Tissue culture flask, 175 cm^2, polystyrene (Becton Dickinson, U.S.A.)

96-well plates: Microtest 96 (Becton Dickinson, U.S.A.)

Microscope: Axiovert 200M (Zeiss)

Imaging software: MetaMorph v6.2r2 (Universal Imaging Corp., U.S.A.)

The UV-absorption measurements for the Phosphatase and Cell Proliferation assays were run on a Multiscan Microplate-Reader (Ascent).

Chemicals

All chemicals were purchased from the following suppliers and used without further purification:

Invitrogen(GIBCO): Dubelco's MEM; L-Glutamine; Calf Serum; Na-Pyruvate; non-essential amino acids; Trypsin/EDTA

Sigma: Penicillin-Streptomycin

Roche Bioscience: WST-1

Calbiochem: PD98059

Cell Lines

The MDCK and MDCK-f3 cell lines were kindly provided by PD Dr. O. Müller (Max-Planck-Institute for Molecular Physiology, Dortmund, Germany). The MDCK-f3 cell line is a sub-clone of the MDCK-Ras-f cell line that is a virally transformed derivative of the Ras cell line[120].

The PathDetect HLR-Elk1 cell line was purchased from Stratagene (U.S.A).

Media and Reagents

Growth Medium

> 500 ml of Dulbecco's Modified Eagle Medium (DMEM)(high glucose, without
>
> L-glutamine, without sodium pyruvate)

_____ 106

_____

5 ml of 200 mM L-glutamine

5 ml of penicillin (5000 U/ml)-streptomycin (5000 μg/ml) mixture

5 ml of 100 mM sodium pyruvate

5 ml of 100x non-essential amino acids (without glutamine)

50 ml of fetal calf serum, heat inactivated

Starving Medium

500 ml of Dulbecco's Modified Eagle Medium (DMEM)(high glucose, without L-glutamine, without sodium pyruvate)

5 ml of 200 mM L-glutamine

5 ml of penicillin (5000 U/ml)-streptomycin (5000 μg/ml) mixture

2.5 ml of fetal calf serum, heat inactivated

Phosphate-buffered Saline (PBS 1 x)

137 mM NaCl

2.6 mM KCl

10 mM Na_2HPO_4

1.8 mM KH_2PO_4

adjusted pH to 7.4 with HCl, then sterile filtered.

Trypsin-EDTA

0.53 mM EDTA

0.05 % trypsin

Formalin Fixing Reagent

10 ml 37 % formaldehyde solution

90 ml PBS

Celestine Blue Staining Reagent

100 ml 5 % $NH_4Fe(SO_4)_2 \cdot 12\ H_2O$

0.5 g Celestine Blue

Boil for 3 minutes; cool to room temperature; filter;

Dilute with 14 ml Glycerin

_____

_____

Cell Lysis Buffer (5 x)

     40 mM tricine (pH 7.8)

     50 mM NaCl

     2 mM EDTA

     1 mM $MgSO_4$

     5 mM DTT

     1 % Triton® X-100

Luciferase Assay Reagent (1 x)

     40.0 mM tricine (pH 7.8)

     0.5 mM ATP

     10 mM $MgSO_4$

     0.5 mM EDTA

     10.0 mM DTT

     0.5 mM coenzyme A

     0.5 mM luciferin

Cdc25A-Buffer A

     50 mM Tris

     50 mM NaCl

     adjust to pH 8.0, filter and degass

Cdc25A- Buffer B

     50 mM Tris

     5 mM NaCl

     1 mM EDTA

     adjust to pH 8.0, filter and degass

PP1-Buffer

     40 mM Tris

     30 mM $MgCl_2 \cdot 6H_2O$

     20 mM KCl

     adjust to pH 8.1, filter and degass

_____

_____

VHR-Buffer

      25 mM Mops

      5 mM EDTA

      adjust to pH 6.5, filter and degass

PTP1B-Buffer

      25 mM HEPES-Na salt

      50 mM NaCl

      2.5 mM EDTA

      adjust to pH 7.2, filter and degass

6.2.2 Methods

Note: all procedures from this point on were performed using sterile technique. Medium was stored at 4 °C but warmed to 37 °C directly before use.

Starting the Cells in Culture

The frozen cryovial of cells was thawed within 40-60 seconds by rapid agitation in a 37 °C water bath. The cryovial was then immersed in 70% (v/v) ethanol at room temperature. The cell suspension was transferred to a 75–cm^2 tissue culture flask containing 10 ml pre-warmed Growth Medium. The culture flask was then placed in a 37 °C incubator at 5% CO_2.

Cell Growth and Passaging of Cells

The cells were grown in a 37 °C incubator at 5% CO_2 until the cell monolayer reached 80-90% confluence (3-5 days).

The cells were passaged according to the following protocol: the medium was removed, and the cells rinsed twice with 2 ml PBS. The PBS was removed by aspiration. Trypsin-EDTA solution (4 °C, 1.5 ml) was added to the tissue culture flask and incubated with the cells for 3 minutes. The flask was tapped a few times to release any adherent cells. Medium (6 ml) was added to inactivate the trypsin. The cellular suspension is transferred to a new 75-cm^2 tissue culture flask and incubated at 37 °C at 5% CO_2.

_____

_____

Counting the Cells

A well-mixed 20-50 µl aliquot of well-dissociated cells was transferred to a Neubauer cell counting chamber. The number of cells present in a 1 mm^2 area were counted and this procedure was repeated in the three other fields. The concentration of cells per milliliter was calculated according to the following equation:

$$C = \tilde{N} \times 10^4$$

where C is the number of cells per milliliter, $\tilde{N}$ is the average of cells counted and 10^4 the volume conversion factor for 1 mm^2.

Ras Phenotype Assay

Cells (MDCK: 1×10^4 cells, MDCK-f3: 5×10^3 cells) were seeded out in 90 µl Growth Medium in each well of a 96-well tissue culture plate. After incubating for 18 h at 37 °C in 5% CO_2, the compounds to be tested (90 µl, various concentrations ranging from 0.1 µM to 500 µM) were pipetted to the cells and incubated for 24h. Following cytotoxicity assays, the cells are fixed with formalin and stained with Celestine Blue for visualization.

Cytotoxicity Assay (Wst-1 assay)

Cell proliferation reagent WST-1 (10µl) was added to each well of 96-well plate cultures with cells. After incubating for 2 h in a humidified atmosphere (37 °C, 5% CO_2), the well plate was shaken vigorously for 1 min and the absorbance of the sample was measured against a background control at 540 nm.

Formalin Fixing and Celestine Blue Staining of Cells

The Growth Medium was removed from the wells and the cells were washed twice with 90 µl PBS. The cells were then fixed by adding 90 µl of Formalin and incubated at room temperature for 30 min. The fixed cells were then washed twice with dd H_2O and incubated for 2 minutes in H_2O. After aspiration of the water, freshly prepared Celestine Blue (90 µl) was incubated for 30 seconds with the cells, then removed. The cells were then washed with 180 µl ethanol, and the left to stand for 5 minutes. After washing the cells twice with 180 µl PBS, the cells were visualized by microscopy.

Luciferase MAPK Reporter Gene Assay

_____

_____

HLR cells $(2x10^5)$ were seeded in 3 cm cell culture plates in 2 ml Growth Medium and incubated at 37 °C in 5% CO_2 overnight. The next day, the medium was changed to Starving Medium and the cells pre-incubated with the compounds to be assayed. After 24 h of incubation, the medium was changed and starving medium containing compounds to be assayed and along with activators (EGF-100 ng/ml or PMA-100 nmol) were added. The cells were incubated for 4 h, washed and lysed with the Cell Lysis Buffer. After scraping from the cell culture plates, the cells were transferred to Eppendorf tubes on ice, and centrifuged at 13000 rpm at 4 °C. To assay Luciferase activity, 10 µl of cell lysate was mixed with 100 µl Luciferase Reagent and the light emitted was measured with a luminometer.

Phosphatase Assays

The assays were run by H. Rimpel in 96 well-plate format.

General procedure for Cdc25A phosphatase assay:

The following solutions were pipetted in each of the well of the 96 well-plate:

37 µl *Cdc25A-Buffer A*

2 µl 0.1 M solution of DTE in *Cdc25A-Buffer B*

10 µl Cdc25A (~10 U / ml) in *Cdc25A-Buffer A*

In the first row, 1 µl of inhibitor solution (10 mM in DMSO) was added. In each of the following rows, the concentration of inhibitor was diluted by a factor of 0.5. The eighth row did not have an inhibitor and was used as a positive control. After incubating at 37 °C for 20 minutes, 50 µl of solution of *p*-NPP (0.1 M in Cdc25A-Buffer B) was added to each well. The UV-absorption (λ = 405 nm) at 37 °C was measured for the next 80 minutes using a microtiter plate reader.

General procedure for the PP1 Phosphatase assay:

The following solutions were pipetted into each well of a 96-well plate:

37 µl PP1-Buffer

2 µl 0.1 M DTE solution (in PP1-Buffer)

10 µl PP1

_____

_____

The assay was run analogously to the Cdc25A assay.

General procedure for VHR phosphatase assay:

The following solutions were pipetted into each well of a 96-well plate:

46 µl VHR-Buffer

2 µl 0.1 M DTE solution in VHR-Buffer

1 µl VHR

The assay was run analogously to the Cdc25A assay.

General procedure for PTP1B phosphatase assay:

The following solutions were pipetted into each well of a 96-well plate:

6 µl PTP1B-Buffer

2 µl 0.1 M DTE solution in PTP1B-Buffer

1 µl PTP1B

The assay was run analogously to the Cdc25A assay.

Molecular Modeling

For the docking experiments, the cocrystal structure of PTP1B in complex with a synthetic substrate was downloaded from the Brookhaven Protein Data Bank (PDB ID 2BGD). Preparation of the protein structure was conducted with Maestro 7.5 (Schrödinger Inc.). Missing side chains of amino acids were added as well as hydrogens. Then a short energy minimization (1000 steps, Polak–Ribiere conjugate gradient (PRCG), gradient 0.05 kcal/mol) was performed to remove clashes using Macromodel 9.1 (Schrödinger Inc.) and its built-in OPLS2003 force field together with a GB/SA solvation model for water. Ligands were prepared in their possible tautomeric states using Maestro but not energy minimized.

The docking itself was performed using Glide 4.0 in the extra precision mode. If not described otherwise, standard parameters were used. For docking to the catalytically

_____

_____

active site, the site itself was defined by the cocrystallized ligand in the protein file (2BGD) where as the size of the box was extended to 23 Å. Constraints were set on the known hydrogen bond donor/acceptors[148] in this site (Arg221, Gly220, Ile219, Gly218, Ala217, Ser216, Cys215) two of which had to be satisfied. Experiments targeting the second binding site employed 4 known hydrogen bond donors/acceptors [148] as constraints (Met258, Gly259, Arg254, Arg24). Satisfaction of 2 constraints was required for each solution accepted. The same residues were also used to define the center of the site while the edge length of the box defining the site was set to 26 Å. Evaluation of the docking results was done by Maestro and Vida2 (OpenEye Scientific Software[149]). The images shown were generated with Vida2.

7 References

[1.]   P. Ehrlich, *Lancet* **1913,** *2*, 445-451.

[2.]   B. Royles, *Chem.Rev.* **1996,** *95*, 1981-2001.

[3.]   International Human Genome Sequencing Consortium, *Nature* **2004,** *431*, 931-945.

[4.]   S. L. Schreiber, *Bioorg.Med.Chem.* **1998,** *6*, 1127-1152.

[5.]   T. U. Mayer, T. M. Kapoor, S. J. Haggarty, R. W. King, S. L. Schreiber, T. J. Mitchison, *Science* **1999,** *286*, 971-974.

[6.]   A. Blangy, H. A. Lane, P. Dherin, M. Harper, M. Kress, E. A. Nigg, *Cell* **1995,** *83*, 1159-1169.

[7.]   K. E. Sawin, K. LeGuellec, M. Philippe, T. J. Mitchison, *Nature* **1992,** *359*, 540-543.

[8.]   K. W. Wood, W. D. Cornwell, J. D. Jackson, *Curr.Opin.Pharmacol.* **2001,** *1*, 370-377.

[9.]   J. Sebolt-Leopold, D. Dudley, R. Herrera, K. Van Becelarere, A. Wiland, R. C. Gowan, H. Tecle, S. D. Barrett, A. Bridges, S. Przybranowski, W. R. Leopold, A. R. Saltiel, *Nature Medicine* **1999,** *5*, 810-816.

[10.] P. J. Alaimo, M. A. Shogren-Knaak, K. M. Shokat, *Curr.Opin.Chem.Biol.* **2001,** *5*, 360-367.

[11.] A. C. Bishop, O. Buzko, K. M. Shokat, *Trends Cell.Biol.* **2001,** *11*, 167-172.

[12.] J. R. Peterson, T. J. Mitchison, *Chem.Biol.* **2002,** *9*, 1275-1285.

[13.] T. U. Mayer, *Trends Cell.Biol.* **2003,** *13*, 270-277.

[14.] J. R. J. Yeh, C. M. Crews, *Dev.Cell* **2003,** *5*, 11-19.

[15.] A. Wittinghofer, H. Waldmann, *Angew.Chem.Int.Ed.* **2000,** *39*, 4192-4214.

[16.] J. Downward, *Nat.Rev.Cancer* **2003,** *3*, 11-22.

[17.] B. Weiss, G. Bolag, K. Shannon, *Am.J.Med.Genet.* **1999,** 14-22.

[18.] J. Mendelsohn, J. Balsega, *Oncogene* **2000,** *19*, 6550-6565.

[19.] A. Bellacosa, D. Defeo, A. K. Godwin, D. W. Bell, J. Q. Cheng, D. A. Altomare, M. H. Wan, L. Dubeau, G. Scambia, V. Masciullo, G. Ferrandina, P. B. Panici, S. Mancuso, G. Neri, J. R. Testa, *Int.J.Cancer* **1995,** *64*, 280-285.

[20.] S. Grünert, M. Jechlinger, H. Beug, *Nat.Rev.Mol.Cell.Bio.* **2003,** *4*, 657-665.

[21.] J. P. Thiery, *Curr.Opin.Cell Biol.* **2003,** *15*, 740-746.

[22.] C. Cordon-Cardo, C. Privee, *J.Exp.Med.* **1999,** *190*, 1367-1370.

[23.] E. Janda, K. Lehmann, I. Killisch, M. Jechlinger, M. Herzig, J. Downward, H. Beug, S. Grünert, *J.Cell.Bio.* **2002,** *156*, 299-313.

[24.] E. Janda, K. Lehmann, I. Killisch, M. Jechlinger, M. Herzig, J. Downward, H. Beug, S. Grünert, *J.Cell.Biol.* **2002,** *156*, 299-313.

[25.] W. J. Nelson, R. Nusse, *Science* **2004,** *303*, 1483-1487.

[26.] E. Janda, G. Litos, S. Grünert, J. Downward, H. Beug, *Oncogene* **2002,** *21*, 5148-5159.

[27.] International Human Genome Sequencing Consortium, *Nature* **2001,** *409*, 860-921.

[28.] L. Bialy, H. Waldmann, *Angew.Chem.Int.Ed.* **2005,** *44*, 3814-3839.

[29.] M. A. Lyon, A. P. Ducruet, P. Wipf, J. S. Lazo, *Nat.Rev.Drug Discovery* **2002,** *1*, 961-976.

[30.] J. M. Denu, J. A. Stuckey, M. A. Saper, J. E. Dixon, *Cell* **1996,** *87*, 361-364.

[31.] H. Ceulemans, M. Bollen, *Physiol.Rev.* **2004,** *84*, 1-39.

[32.] M. P. Egloff, P. T. Cohen, P. Reinemer, D. Barford, *J.Mol.Biol.* **1995,** *254*, 942-959.

[33.] J. Goldberg, H. B. Huang, Y. G. Kwon, P. Greengard, A. C. Nairn, J. Kuriyan, *Nature* **1995,** *376*, 745-753.

[34.] N. K. Tonks, *FEBS Lett.* **2003,** *546*, 140-148.

[35.] J. D. Bjorge, A. Pang, D. J. Fujuta, *J.Biol.Chem.* **2000,** *275*, 41439-41446.

[36.] M. Larsen, M. L. Tremblay, K. M. Yamada, *Nat.Rev.Mol.Cell Biol.* **2003,** *4*, 700-711.

[37.] B. A. Seeley, P. A. Staubs, D. R. Reichhart, P. Berhanu, K. L. Milarski, A. R. Saltiel, J. Kusari, *Diabetes* **1996,** *45*, 1379-1385.

[38.] A. Salmeen, J. N. Andersen, M. P. Myers, N. K. Tonks, D. Barford, *Cell* **2000,** *6*, 1401-1412.

[39.] R. DeVinney, O. Steele-Mortimer, B. B. Finlay, *Trends Microbiol.* **2006,** *8*, 29-32.

[40.] A. Koul, A. Choidas, M. Treder, A. K. Tyagi, K. Drlica, Y. Singh, A. Ullrich, *J.Bacteriol.* **2000,** *182*, 5425-5432.

[41.] U. Strausfeld, J. C. Labbé, D. Fesquet, J. C. Cavadore, A. Picard, K. Sadhu, P. Russell, M. Dorée, *Nature* **1991,** *351*, 242-245.

[42.] I. Vincent, B. Bu, K. Hudson, J. Husseman, D. Nochlin, L. W. Jin, *Neuroscience* **2001,** *105*, 633-650.

[43.] J. Yuvaniyama, J. M. Denu, J. E. Dixon, M. A. Saper, *Science* **1996,** *272*, 1328-1331.

[44.] M. Sodeoka, M. Sampe, S. Kojima, Y. Baba, T. Usui, K. Ueda, H. Osada, *J.Med.Chem.* **2001,** *44*, 3216-3222.

[45.] Y. A. Puius, Y. Zhao, M. Sullivan, D. S. Lawrence, S. C. Almo, Z. Y. Zhang, *Proc.Natl.Acad.Sci.USA* **1997,** *94*, 13420-13425.

[46.] B. G. Szczepankiewicz, G. Lui, P. J. Hadjuk, C. Abad-Zapatero, Z. Pei, Z. Xin, T. H. Lubben, J. M. Trevillyan, M. A. Stashko, S. J. Ballaron, H. Liang, F. Huang, C. W. Hutchins, S. W. Fesik, M. R. Jirousek, *J.Am.Chem.Soc.* **2003,** *125*, 4087-4096.

[47.] H. Zhao, G. Liu, Z. Xin, M. D. Serby, Z. Pei, B. G. Szczepankiewicz, P. J. Hadjuk, C. Abad-Zapatero, C. W. Hutchins, T. H. Lubben, S. J. Ballaron, D. L. Haasch, W. Kaszubska, C. M. Rondinone, J. M. Trevillyan, M. R. Jirousek, *Bioorg.Med.Chem.Lett.* **2004,** *14*, 5543-5546.

[48.] R. Srinivasan, M. Uttamchandani, S. Q. Yao, *Org.Lett.* **2006,** *8*, 713-716.

[49.] C. T. Walsh, *Antibiotics: Actions, Origins, Resistance.*, ASM Press, Washington DC, USA **2003**.

[50.] B. E. Evans, K. E. Rittle, M. G. Bock, R. M. DiPardo, R. M. Freidinger, W. L. Whitter, G. F. Lundell, D. F. Veber, P. S. Anderson, R. S. L. Chang, V. J. Lotti, D. J. Cerino, T. B. Chen, P. J. Kling, K. A. Kunkel, J. P. Springer, J. Hirshfield, *J.Med.Chem.* **1988,** *31*, 2235-2246.

[51.] S. L. Schreiber, *Science* **2000,** *287*, 1964-1969.

[52.] A. N. Koehler, A. F. Shamji, S. L. Schreiber, *J.Am.Chem.Soc.* **2003,** *105*, 8420-8421.

[53.] M. A. Koch, L.-O. Wittenberg, S. Basu, D. A. Jeyeraj, E. Gourzoulidou, K. Reineke, A. Odermatt, H. Waldmann, *Proc.Natl.Acad.Sci.USA* **2004,** *101*, 16721-16726.

[54.] K. C. Nicolaou, J. A. Pfefferkorn, A. J. Roeker, G. Q. Cao, S. Barluenga, H. J. Mitchell, *J.Am.Chem.Soc.* **2000,** *122*, 9939-9953.

[55.] K. C. Nicolaou, J. A. Pfefferkorn, H. J. Mitchell, A. J. Roeker, S. Barluenga, G. Q. Cao, R. L. Affleck, J. E. Lillig, *J.Am.Chem.Soc.* **2000,** *122*, 9954-9967.

[56.] K. C. Nicolaou, J. A. Pfefferkorn, F. Schuler, A. J. Roeker, G. Q. Cao, J. E. Casida, *Chem.Biol.* **2000,** *7*, 979-992.

[57.] K. C. Nicolaou, A. J. Roeker, S. Barluenga, J. A. Pfefferkorn, G. Q. Cao, *ChemBioChem* **2001,** *2*, 460-465.

[58.] K. C. Nicolaou, R. M. Evans, A. J. Roeker, R. Hughes, M. Downes, J. A. Pfefferkorn, *Org.Biomol.Chem.* **2003,** *1*, 908-920.

[59.] M. A. Koch, A. Schuffenhauer, M. Scheck, S. Wetzel, M. Casaulta, A. Odermatt, P. Ertl, H. Waldmann, *Proc.Natl.Acad.Sci.USA* **2005,** *102*, 17272-17277.

[60.] S. Tuske, S. G. Sarafiano, X. Wang, B. Hudson, E. Sineva, J. Mukhopadhyay, J. Birktoft, O. Leroy, S. Ismail, A. D. Clark, C. Dharia, A. Napoli, O. Laptenko, J. Lee, S. Borukov, R. Ebright, E. Arnold, *Cell* **2005,** *122*, 541-552.

[61.] C. W. Holzapel, *Tetrahedron* **1968,** *24*, 2103.

[62.] N. W. Siedler, I. Jona, M. Vegh, A. Martonsi, *J.Biol.Chem.* **1989,** *264*, 17816-17823.

[63.] B. J. Fennell, S. Carolan, G. R. Pettit, A. Bell, *J.Antimicrob.Chemother.* **2003,** *51*, 833-841.

[64.] S. Aoki, K. Higuchi, Y. Ye, R. Satari, M. Kobayashi, *Tetrahedron.Lett.* **2000,** *56*, 1833-1836.

[65.] R. Fischer, S. Lehr, D. Feucht, P. Loesel, O. Malsam, G. Bojak, T. Auler, M. J. Hills, H. Kehne, C. H. Rosinger, *WO 2005048710* **2005**.

[66.] M. A. Dekeyser, *Pest.Manag.Sci.* **2005,** *61*, 103-110.

[67.] J. W. Sims, J. P. Fillmore, D. D. Warner, E. W. Schmidt, *Chem.Commun.* **2004,** 186-188.

[68.] C. W. Holzapel, D. C. Wilkins, *Phytochemistry* **1971,** *10*, 351-358.

[69.] A. A. Chalmers, C. P. Gorst-Almann, P. S. Steyn, *J.Chem.Soc., Chem.Commun.* **1982,** 1377.

[70.] H. Chen, P. M. Harrison, *Org.Lett.* **2004,** *6*, 4033-4036.

[71.] G. F. Kaufmann, R. Sartorio, S. H. Lee, C. Rogers, M. M. Meijler, J. A. Moss, B. Clapham, A. P. Brogan, T. J. Dickserson, K. D. Janda, *Proc.Natl.Acad.Sci.USA* **2005,** *102*, 309-314.

[72.] C.-Y. Wang, B.-G. Wang, S. Wiryowidagdo, V. Wray, R. van Soest, K. G. Steube, H.-S. Guan, P. Proksch, R. Ebel, *J.Nat.Prod.* **2003,** *66*, 51-56.

[73.] C. Hopmann, M. Kurz, M. Brönstrup, J. Wink, D. LeBeller, *Tetrahedron Lett.* **2002,** *43*, 435-438.

[74.] R. N. Lacey, *J.Chem.Soc.* **1954,** 850-854.

[75.] Y. Iwata, N. Maekawara, K. Tanino, M. Miyashita, *Angew.Chem.Int.Ed.* **2005,** *117*, 1556-1560.

[76.] l. Burke, D. Dixon, S. Ley, F. Rodríguez, *Org.Lett.* **2000,** *2*, 3611-3613.

[77.] A. C. Hart, A. J. Phillips, *J.Am.Chem.Soc.* **2006,** *128*, 1094-1095.

[78.] R. Böhme, G. Jung, E. Breitmaier, *Helv.Chem.Acta.* **2005,** *88*, 2837-2841.

[79.] J. Poncet, P. Jouin, B. Castro, L. Nicolas, M. Boutar, A. Gaudemer, *J.Chem.Soc.Perkin Trans.I* **1990,** 611-616.

[80.] R. Schobert, C. Jagusch, *Tetrahedron* **2005,** *61*, 2301-2307.

[81.] P. Jouin, B. Castro, D. Nisato, *J.Chem.Soc.Perkin Trans.I* **1987,** 1177-1182.

[82.] S. Fustero, M. García de la Torre, J. F. Sanz-Cervera, C. Ramírez de Arellano, J. Piera, A. Simón, *Org.Lett.* **2002,** *4*, 3651-3654.

[83.] J. Matthews, R. Rivero, *J.Org.Chem.* **1998,** *63*, 4808-4810.

[84.] B. Kulkarni, A. Ganesan, *Tetrahedron Lett.* **1998,** *39*, 4369-4372.

[85.] L. Weber, P. Iazia, G. Biringer, P. Barbier, *Synlett* **1998,** 1156-1158.

[86.] T. Romoff, L. Ma, Y. Wang, D. Campbell, *Synlett* **1998,** 1341-1342.

[87.] Z. Liu, X. Ruan, Y. Huang, *Bioorg.Med.Chem.Lett.* **2003,** *13*, 2505-2507.

[88.] J. Shi, Z. Xiao, M. Ihnat, C. Kamat, B. Pandit, Z. Hu, P. Ki, *Biorg.Med.Chem.Lett.* **2003,** *13*, 1187-1189.

[89.] K. Tsuji, G. W. Spears, K. Nakamura, T. Tojo, N. Seki, A. Sugiyama, M. Matsuo, *Bioorg.Med.Chem.Lett.* **2002,** *12*, 85-88.

[90.] K. Schmidt, U. Riese, Z. Li, M. Hamburger, *J.Nat.Prod.* **2003,** *66*, 378-383.

[91.] T. Lambert, S. J. Danishefsky, *J.Am.Chem.Soc.* **2006,** *128*, 426-427.

[92.] T. Agatsuma, T. Akama, S. Nara, S. Matsumiya, R. Nakai, H. Ogawa, S. Otaki, S. Ikeda, Y. Saitoh, Y. Kanda, *Org.Lett.* **2002,** *4*, 4387-4390.

[93.] T. R. Hoye, V. Dvornikovs, *J.Am.Chem.Soc.* **2006,** *128*, 2550-2551.

[94.] B. Neises, W. Steglich, *Angew.Chem.Int.Ed.* **1978,** *17*, 522-524.

[95.] E. Atherton, R. C. Sheppard, *Solid Phase Peptide Synthesis*, IRL Press, Oxford **1989,** pp. 112-117.

[96.] L. G. Beholz, P. Benovsky, D. L. Ward, N. S. Barta, J. R. Stille, *J.Org.Chem.* **1997,** *62*, 1033-1042.

[97.] S. Raillard, G. Ji, A. Mann, T. Baer, *Org.Proc.Res.Dev.* **1999,** *3*, 177-183.

[98.] S. R. Chhabra, C. Harty, D. S. W. Hooi, M. Daykin, P. Williams, G. Telford, D. I. Pritchard, B. W. Bycroft, *J.Med.Chem.* **2003,** *46*, 97-104.

[99.] Y. Honma, Y. Sekine, S. Nomura, K. Naito, H. Narita, *JP 1994-31110* **1994,** *JP 06312927*.

[100.] Y. Honma, Y. Sekine, S. Nomura, K. Naito, H. Narita, *EP 92-114987* **1994,** *EP 531876*.

[101.] M. Matsuda, T. Kobayashi, S. Nagao, T. Ohta, S. Nozoe, *Heterocycles* **1996,** *43*, 685-690.

[102.] B. Neises, W. Steglich, *Angew.Chem.Int.Ed.* **1978,** *17*, 522-524.

[103.] M. C. Pirrung, M. Wedel, Y. Zhao, *Synlett* **2001,** 143-145.

[104.] J. Sohn, B. Kiburz, Z. Li, L. Deng, A. Safi, M. C. Pirrung, J. Rudolph, *J.Med.Chem.* **2003,** *46*, 2580-2588.

[105.] M. G. Gänzle, R. Vogel, *Appl.Envirom.Microbiol.* **2003,** *69*, 1305-1307.

[106.] E. Fischer, F. Jourdan, *Dtsch.Chem.Ges.* **1883,** *16*, 2241-2245.

[107.] W. Madelung, *Chem.Ber.* **1912,** *45*, 1128.

[108.] G. W. Gribble, *J.Chem.Soc., Perkin Trans.1* **2000,** 1045-1075.

[109.] G. Bartoli, G. Palmieri, M. Bosco, R. Dalpozzo, *Tetrahedron Lett.* **1989,** *30*, 2129-2132.

[110.] R. Dalpozzo, G. Bartoli, *Curr.Org.Chem.* **2005,** *9*, 163-178.

[111.] R. Tapia, G. Torres, J. Valderrama, *Synth.Commun.* **1986,** *16*, 681-687.

[112.] D. A. Nugiel, K. Jacobs, L. Cornelius, C.-H. Chang, P. K. Jadhav, E. R. Holler, R. M. Klabe, L. T. Bacheler, B. Cordova, S. Garber, C. Reide, K. A. Logue, L. J. Gory-Feret, G. N. Lam, S. Erikson-Viitanen, S. P. Seitz, *J.Med.Chem.* **1997,** *40*, 1465-1474.

[113.] N. K. Garg, R. Sarpong, B. M. Stoltz, *J.Am.Chem.Soc.* **2002,** *124*, 13179-13184.

[114.] M. Vlachou, A. Tsotinis, L. R. Kelland, D. E. Thurston, *Eur.J.Pharm.Sci.* **2002,** *17*, 139-143.

[115.] H. R. Snyder, J. A. MacDonald, *J.Am.Chem.Soc.* **1955,** *77*, 1257-1259.

[116.] Y. Yokoyama, H. Hikawa, M. Mitsuhashi, A. Uyama, Y. Murakami, *Tetrahedron Lett.* **1999,** *40*, 7803-7806.

[117.] H. K. Chenault, J. Dahmer, G. Whitesides, *Journal of the American Chemical Society* **1989,** *111*, 6354-6364.

[118.] Y. Yokoyama, H. Hikawa, M. Mitsuhashi, A. Uyama, Y. Hiroki, Y. Murakami, *Eur.J.Org.Chem.* **2004,** 1244-1253.

[119.] T. Sekiya, M. Fushimi, H. Hori, S. Hirohashi, S. Nishimura, T. Sugimura, *Proc.Natl.Acad.Sci.USA* **1984,** *81*, 4771-4775.

[120.] J. Behrens, M. M. Mareel, F. M. Van Roy, W. Birchmeier, *J.Cell Biol.* **1989,** *108*, 2435-2447.

[121.] I. M. Karaguni, P. Herter, P. Debruyne, S. Chtarbova, A. Kasprzynski, U. Herbrand, M.-R. Ahmadian, K.-H. Glüsenkamp, G. Winde, M. M. Mareel, T. Möröy, O. Müller, *Cancer Res.* **2002,** *62*, 1718-1723.

[122.] O. Müller, E. Gourzoulidou, M. Carpintero, I. M. Karaguni, A. Langerak, C. Herrmann, T. Möröy, R. Klein-Hitpaß, H. Waldmann, *Angew.Chem.Int.Ed.* **2004,** *43*, 450-454.

[123.] M. V. Berridge, A. S. Tan, *Arch.Biochem.Biophys.* **1993,** *303*, 474.

[124.] M. V. Berridge, A. S. Tan, K. D. McCoy, R. Wang, *Biochemica* **1996,** *4*, 14-19.

[125.] D. Dudley, L. Pang, S. J. Decker, A. J. Bridges, A. R. Saltiel, *Proc.Natl.Acad.Sci.USA* **1995,** *92*, 7686-7689.

[126.] R. Hoshino, *Oncogene* **1999,** *18*, 813-822.

[127.] D. R. Alessi, A. Cuenda, P. Cohen, D. T. Dudley, A. R. Saltiel, *J.Biol.Chem.* **1995,** *270*, 27489-27494.

[128.] B. J. Gates, M. DeLuca, *Arch.Biochem.Biophys.* **1975,** *169*, 616-621.

[129.] B. Bitler, W. D. McElroy, *Arch.Biochem.Biophys.* **1957,** *72*, 358-368.

[130.] D. N. Jackson, D. A. Foster, *FASEB Journal* **2004,** *18*, 627-636.

[131.] N. Brose, C. Rosenmund, *J.Cell Sci.* **2002,** *115*, 4399-4411.

[132.] C. Y. Logan, R. Nusse, *Ann.Rev.Cell.Dev.Biol.* **2004,** *20*, 781-810.

[133.] E. Janda, G. Litos, S. Grünert, J. Downward, H. Beug, *Oncogene* **2002,** *21*, 5128-5159.

[134.] J. P. Thiery, *Curr.Opin.Cell Biol.* **2003,** *15*, 740-746.

[135.] M. Sodeoka, M. Sampe, T. Kagamizono, H. Osada, *Tetrahedron Lett.* **1996,** *37*, 8775-8778.

[136.] E. Black, J. Breed, A. L. Breeze, K. Embrey, R. Garcia, T. W. Gero, L. Godfrey, P. W. Kenny, A. D. Morley, C. A. Minshull, A. D. Pannifer, J. Read, A. Rees, D. J. Russell, D. Toader, J. Tucker, *Bioorg.Med.Chem.Lett.* **2005,** *15*, 2503-2507.

[137.] S. P. Gunasekera, P. J. McCarthy, M. Kelly-Borges, E. Lobkovsky, J. Clardy, *J.Am.Chem.Soc.* **1996,** *118*, 8759-8760.

[138.] R. Shimazawa, T. Suzuki, K. Dodo, R. Shirai, *Bioorg.Med.Chem.Lett.* **2004,** *14*, 3291-3294.

[139.] M. Takahashi, K. Dodo, Y. Sugimoto, Y. Aoyagi, Y. Yamada, Y. Hashimoto, R. Shirai, *Bioorg.Med.Chem.Lett.* **2000,** *10*, 2571-2574.

[140.] W.-R. Li, S. T. Lin, M.-S. Chern, *J.Org.Chem.* **2002,** *67*, 4702-4706.

[141.] A. Höltzel, M. G. Gänzle, G. J. Nicholson, W. P. Hammes, G. Jung, *Angew.Chem.Int.Ed.* **2000,** *39*, 2766-2768.

[142.] C. P. Hart, *Drug Disc.Today Targets* **2005,** *10*, 513-519.

[143.] W. C. Still, M. Kahn, A. Mitra, *J.Org.Chem.* **1978,** *43*, 2923-2925.

[144.] D. D. Perrin, W. L. F. Armstrong, *Purification of Laboratory Chemicals*, Pergamon Press, Oxford **1988**.

[145.] D. A. Nugiel, K. Jacobs, L. Cornelius, C.-H. Chang, P. Jadhav, E. R. Holler, R. M. Klabe, L. T. Bcheler, B. Cordova, S. Garber, C. Reid, K. A. Logue, L. J. Gorey-Feret, G. N. Lam, S. Erickson-Viitanen, S. P. Seitz, *J.Med.Chem.* **1997,** *40*, 1465-1474.

[146.] W. S. Blair, M. Deshpand, H. Fnag, P. Lin, T. P. Spicer, O. B. Wallace, T. Wang, T. Wang, Z. Zhang, K. S. Yeung, *WO2000076521* **2000**.

[147.] Y. Yabe, C. Miura, H. Horikoshi, H. Miyagawa, Y. Baba, *Chem.Pharm.Bull.* **1979,** *27*, 1907-1911.

[148.] Z. Jia, A. N. Dinaut, Wang.Q., D. Waddleton, P. Payette, C. Ramachandran, B. Kennedy, G. Hum, S. D. Taylor, *J.Med.Chem.* **2001,** *44*, 4584-4594.

[149.] The OpenEye Tools were generously supplied by OpenEye Scientific Software for free. See also www.eyesopen.com.

Appendix A: Abbreviations
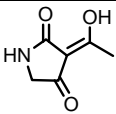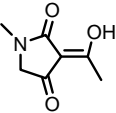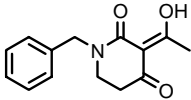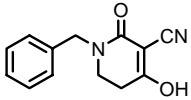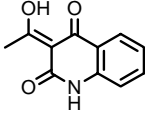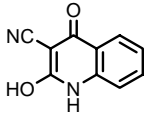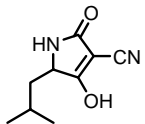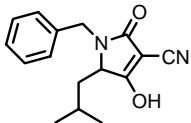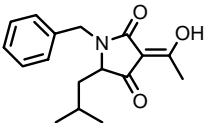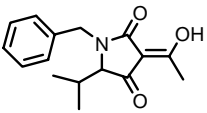
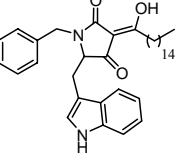|	
11-β-HSD-1	11-β-Hydroxysteroid dihydrogenase type 1
11-β-HSD-2	11-β-Hydroxysteroid dihydrogenase type 2
AchE	Acetyl cholinesterase
AcOH	Acetic acid
Ac$_2$O	Acetic anhydride
Boc	*Tert*-butyl carboxycarbonyl
Cdc25A	Cell cycle-dependant kinase A
CDK	Cyclin-dependant kinase
CDI	Carbonyldiimidazole
CH	Cyclohexane
DCC	*N, N'*-Dicyclohexylcarbodiimide
DAG	Diacylglycerol
DHB	2,5-Dihydroxybenzoic acid
DIC	*N,N'*-Di-*iso*-propylcarbodiimide
DIPEA	*N,N*-Diisopropylethylamine
DMAP	4-Dimethylaminopyridine
DMB	Dimethoxybenzyl
DMF	*N,N*-Dimethylformamide
DMSO	Dimethyl sulfoxide
EA, EtOAC	Ethyl acetate
EI	Electron impact
EGF	Epidermal growth factor
EGFR	Epidermal growth factor receptor
EMT	Epithelial mesenchymal transition
ESI	Electron spray ionization
FAB	Fast atom bombardment
Fmoc	9-Fluorenylmethyloxycarbonyl
GAP	GTPase activating protein
GEF	Guanine nucleotide exchange factor
GRB	Growth factor binding
HLR	HeLa luciferase reporter
HOBt	1-Hydroxy-1H-benzotriazole
HPLC	High Performance Liquid Chromatography
IC$_{50}$	50% inhibitory concentration
LCMS	Liquid Chromatography Mass Spectrometry
MALDI	Matrix assisted laser desorption ionization
MAP	Mitogen activated protein
MDCK	Madine-Darby canine kidney cell
MDCK-f3	Ras-transformed Madine-Darby canine kidney cell
MEK	Mitogen activating protein kinase kinase

_____
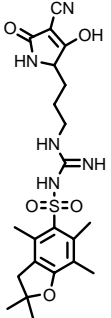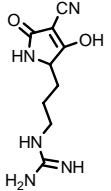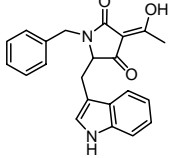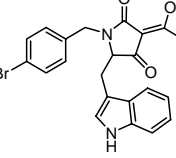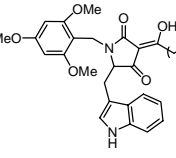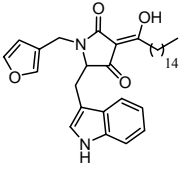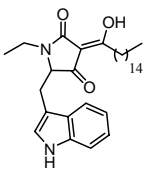
|	
MeOH	Methanol
MIC	Minimal inhibitory concentration
MS	Mass spectrum
NaOEt	Sodium ethoxide
NaOMe	Sodium methoxide
NMR	Nuclear magnetic resonance
Pbf	Pentamethyldihydrobenzofuran
PE	Petroleum ether
PKC	Protein kinase C
PMA	Phorbol 12-myristate 13-acetate
PS	Polystyrene
PP	Serine/threonine phosphatase
PP1	Protein Phosphatase-1
PTP	Protein tyrosine phosphatase
rac.	Racemic
R_f	Retention factor
R_t	Retention time
RNAP	RNA polymerase
RT	Room temperature
RTK	Receptor-tyrosine kinase
SAR	Structure activity relationship
Sat.	Saturated
Sos	Son of sevenless
TBAF	Tetrabutylammonium fluoride
TBDPS	Tert-butyl-diphenylsilyl
TCF/LEF	T cell factor/lymphocyte enhancer factor
TEA	Triethyl amine
TFA	Trifluoro acetic acid
TGF-β	Transforming growth-factor β
THF	Tetrahydrofuran
TOF	Time of flight
VHR	Vaccinia virus H1-related phosphatase
WST-1	4-[3-(4-Iodophenyl)-2-(4-nitrophenyl)-2H-5-tetrazolio]-1,3-benzene disulfonate

_____

_____

Appendix B: Biological Properties of Tetramic Acids

Entry	Cpd. Nr.	Structure	Phenotypical assay	WST-1 assay	Phosphatase assay	Antibiotics assay
1	**113**		no effect	not toxic	no inhibition	no effect
2	**114**		no effect	not toxic	no inhibition	no effect
3	**89**		no effect	not toxic	no inhibition	no effect
4	**112**		no effect	not toxic	no inhibition	no effect
5	**81**		no effect	not toxic	no inhibition	no effect
6	**110**		**reversal**	not toxic	no inhibition	no effect
7	**107**		no effect	not toxic	no inhibition	no effect
8	**116**		no effect	not toxic	no inhibition	no effect
9	**117**		no effect	not toxic	no inhibition	no effect
10	**115**		no effect	not toxic	no inhibition	no effect

_____ 124

_____

Entry	Cpd. Nr.	Structure	Phenotypical assay	WST assay	Phosphatase assay	Antibiotics assay
11	**118**		no effect	**toxic**	**Cdc25A: 92 µM MptpB: >100 µM**	**B. subtilisis >250 mg/l**
13	**119**		no effect	**toxic**	no inhibition	no effect
14	**19**		**reversal**	**toxic**	**Cdc25A: 60 µM PTP1B: 37 µM MptpB: 83 µM**	**B. subtilisis 70.3 mg/l**
15	**120**		no effect	**toxic**	no inhibition	no effect
16	**111**		no effect	not toxic	no inhibition	**B. subtilisis >250 mg/l**
17	**74**		no effect	not toxic	no inhibition	no effect
18	**128**		no effect	not toxic	no inhibition	no effect
19	**129**		no effect	not toxic	no inhibition	no effect

_____

Entry	Cpd. Nr.	Structure	Phenotypical assay	WST assay	Phosphatase assay	Antibiotics assay
20	**108**		no effect	not toxic	no inhibition	no effect
21	**130**		no effect	not toxic	no inhibition	no effect
22	**126**		no effect	not toxic	no inhibition	no effect
23	**123**		no effect	not toxic	no inhibition	no effect
24	**121**		no effect	not toxic	no inhibition	no effect
25	**122**		no effect	not toxic	**MptpB: 70 μM**	no effect

Entry	Cpd. Nr.	Structure	Phenotypical assay	WST assay	Phosphatase assays	Antibiotics assay
27	**127**		no effect	not toxic	**Cdc25A: 95 µM PTP1B: 10µM MptpB: 68 µM**	no effect
28	**125**		no effect	not toxic	**MptpB: 93 µM**	no effect

Appendix C: Tetramic Acid ^{1}H NMR Spectra

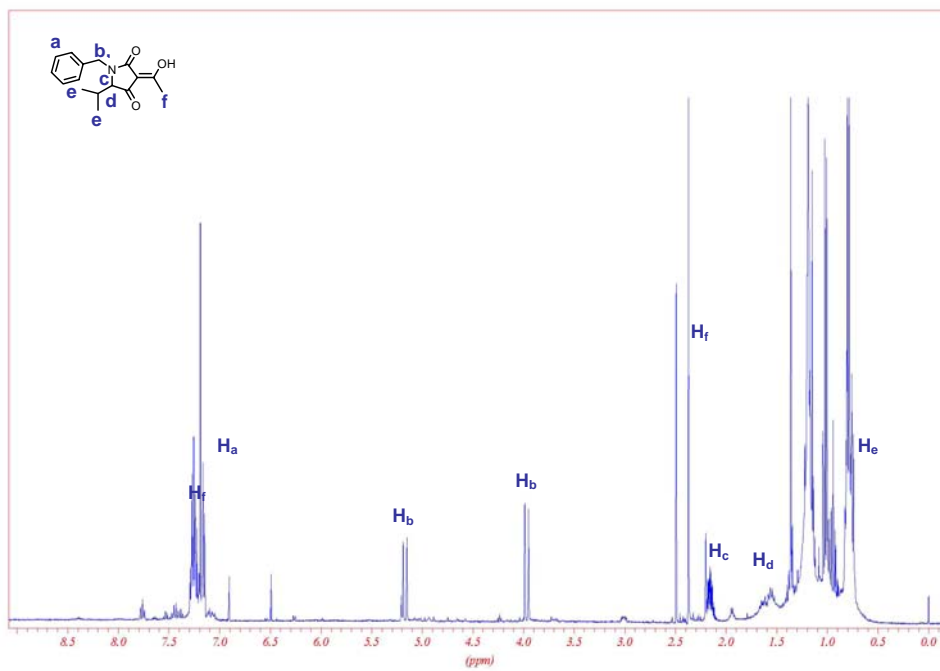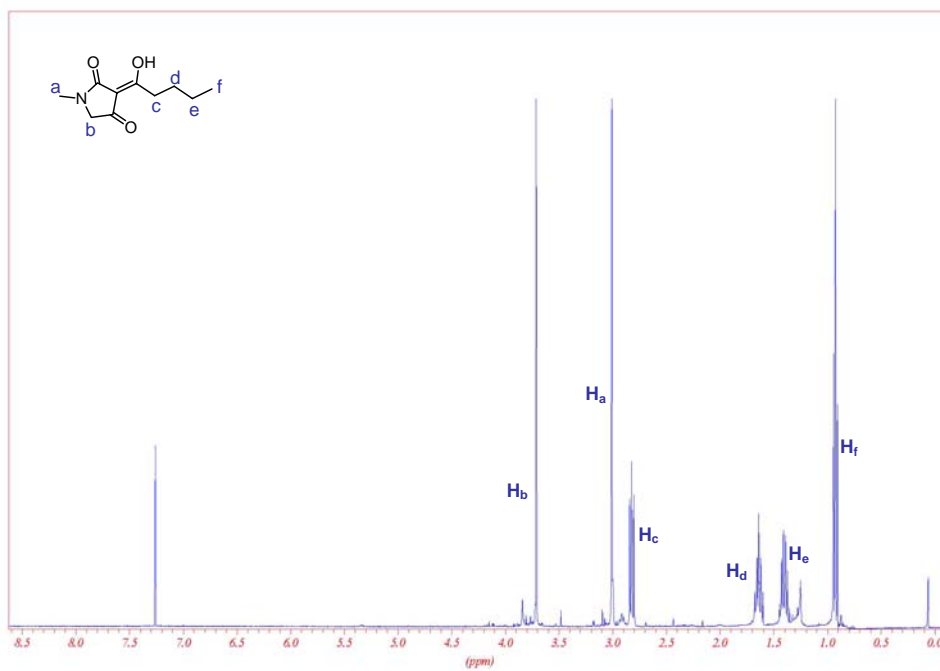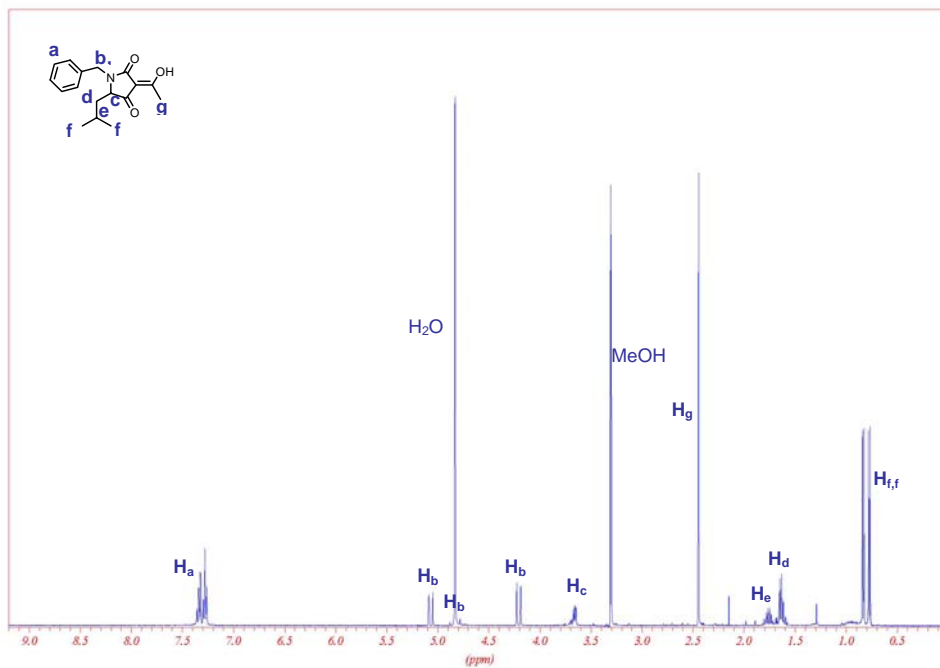_____

_____

_____

_____
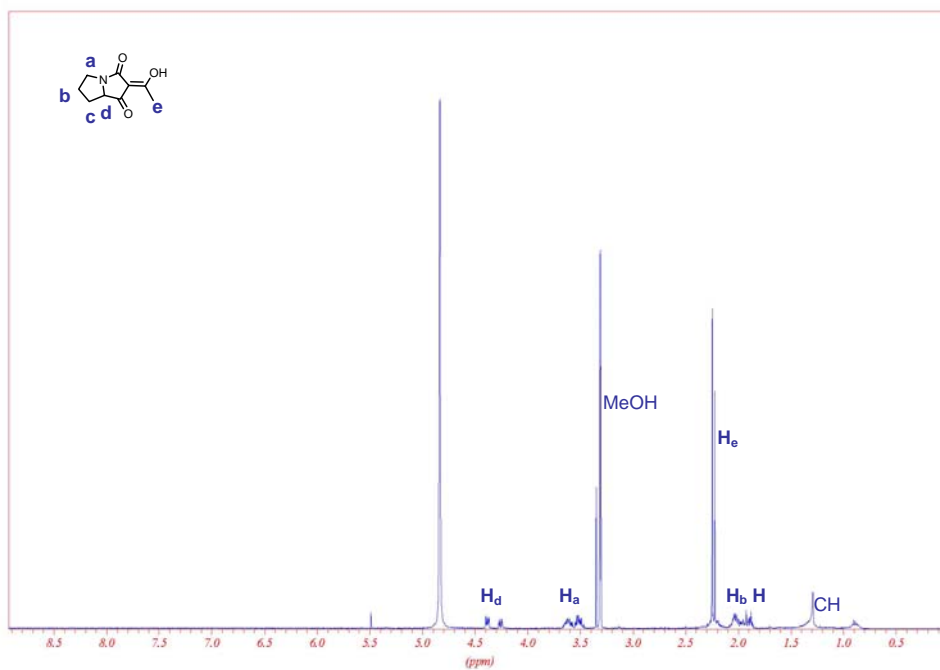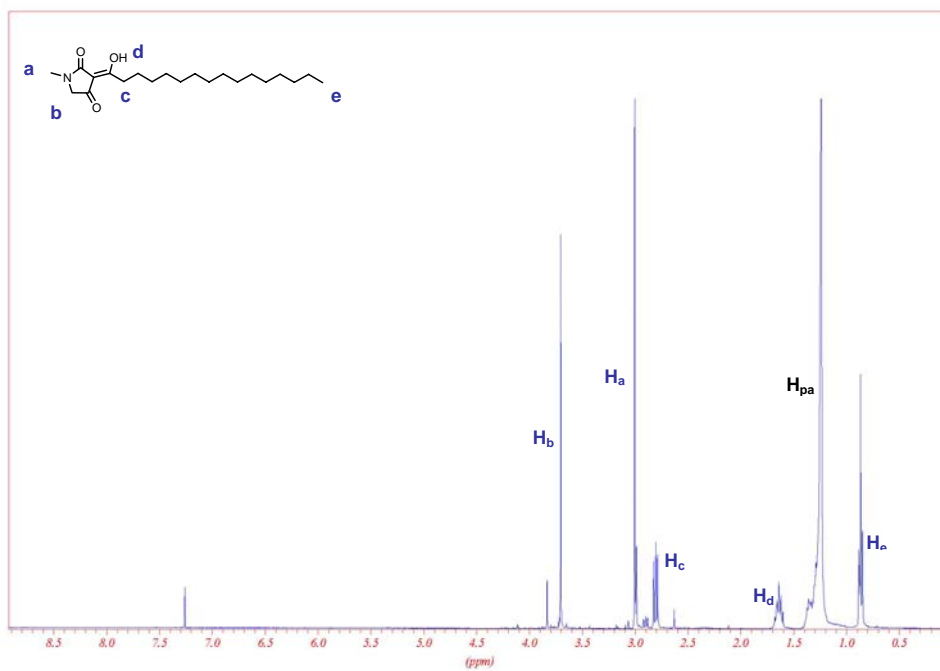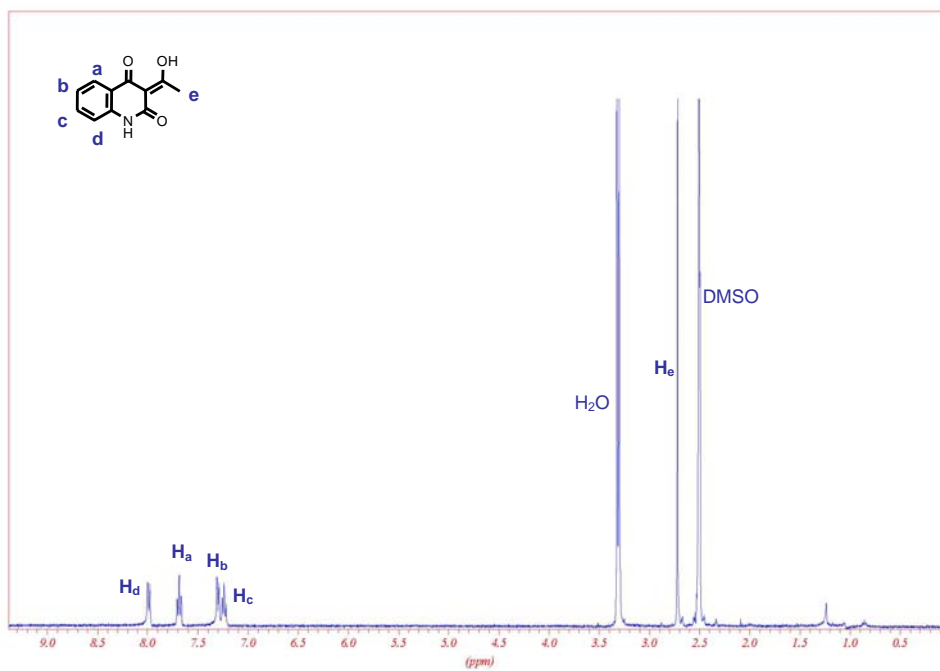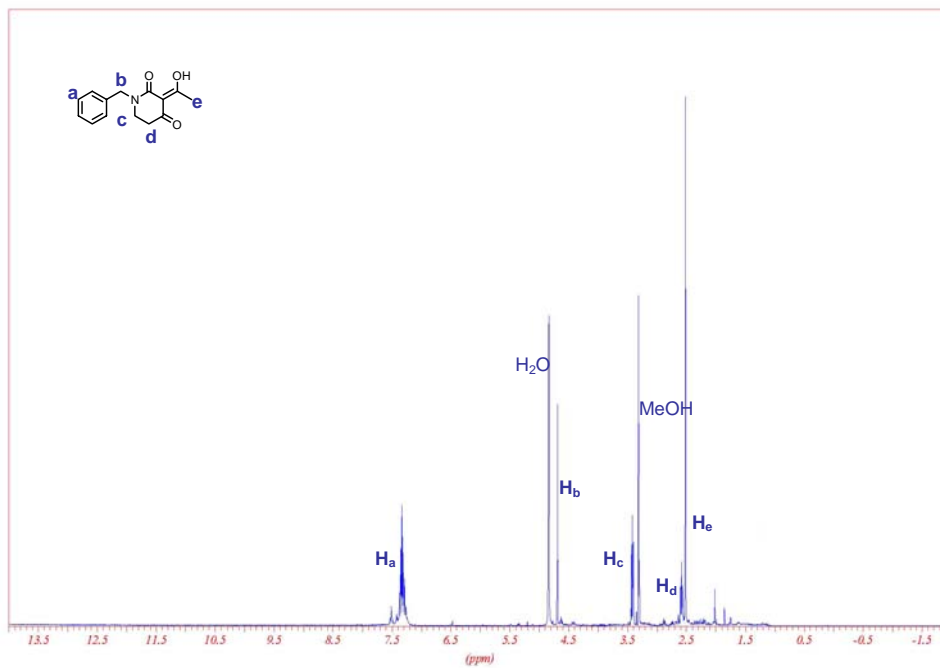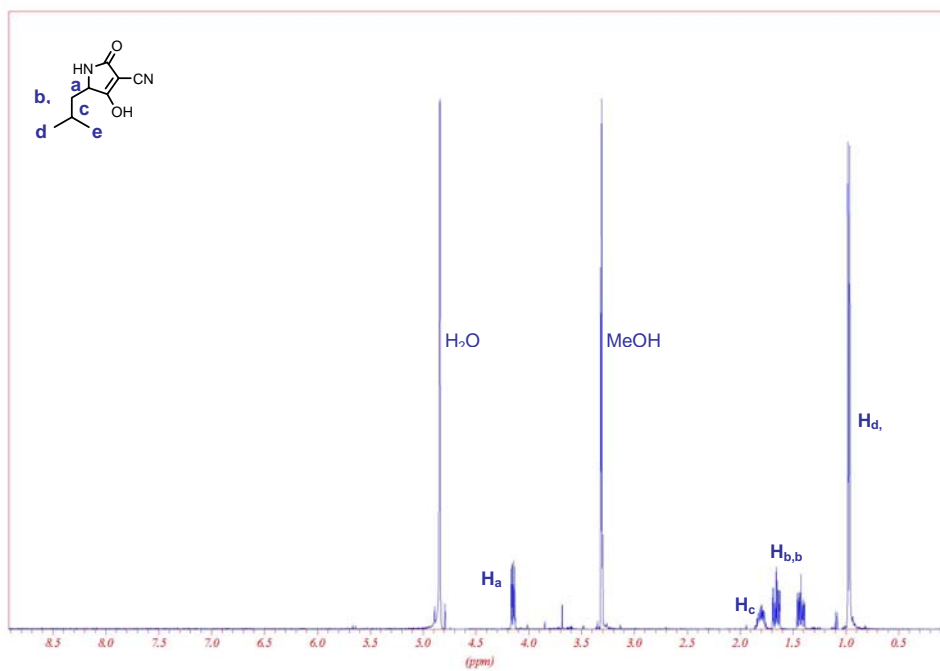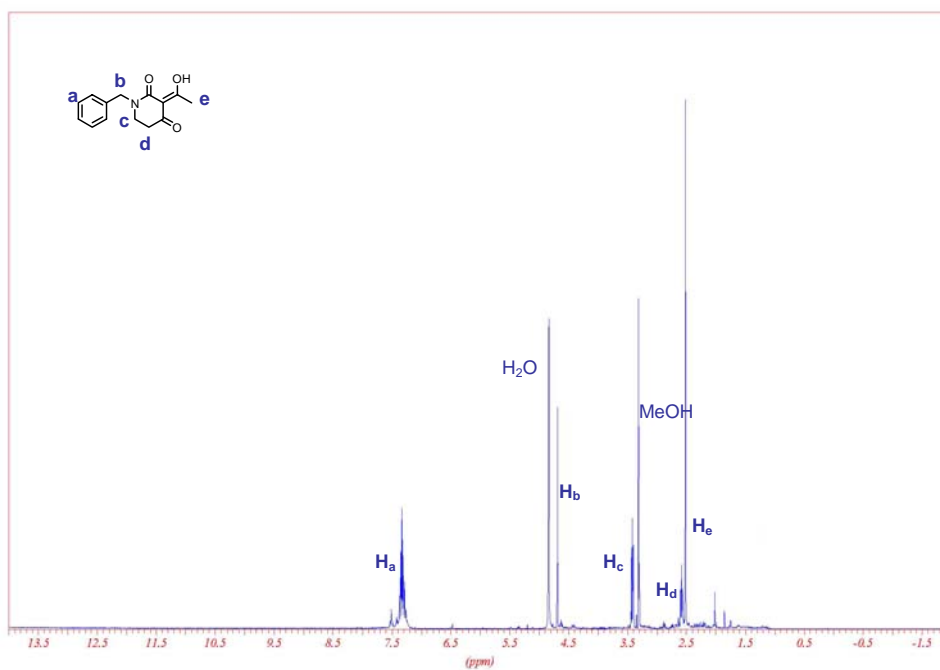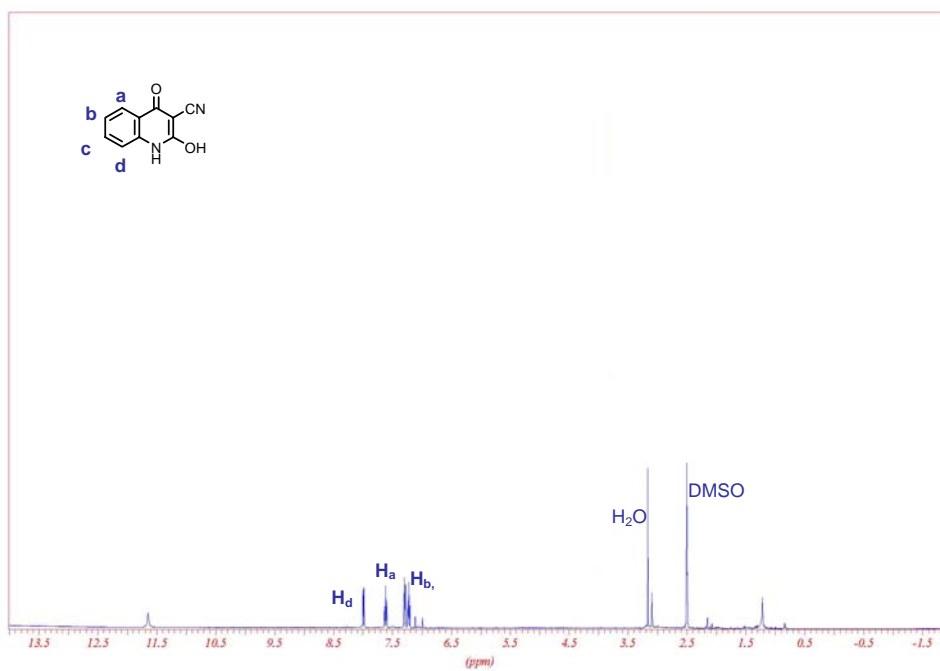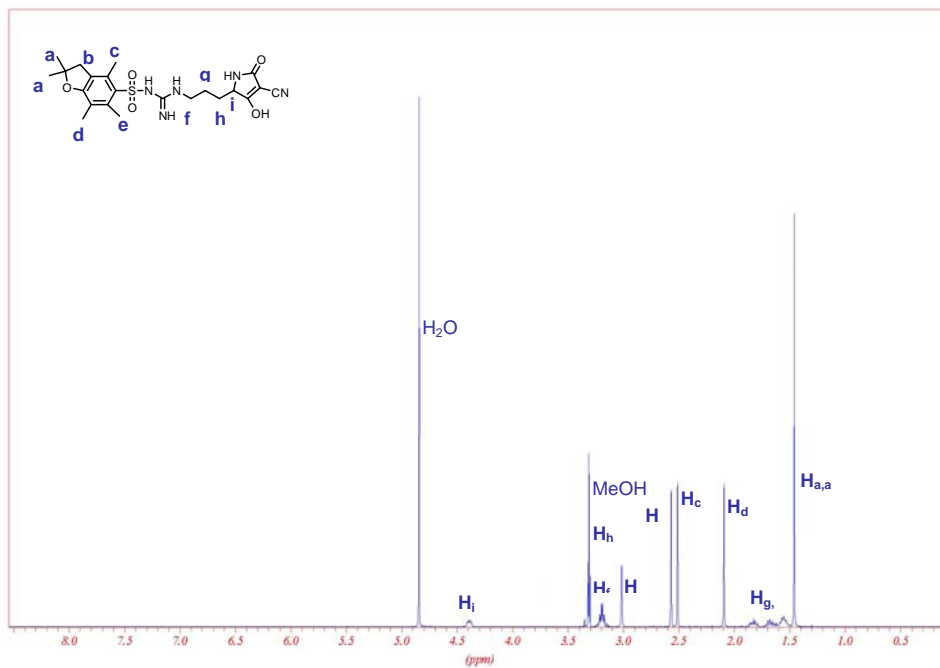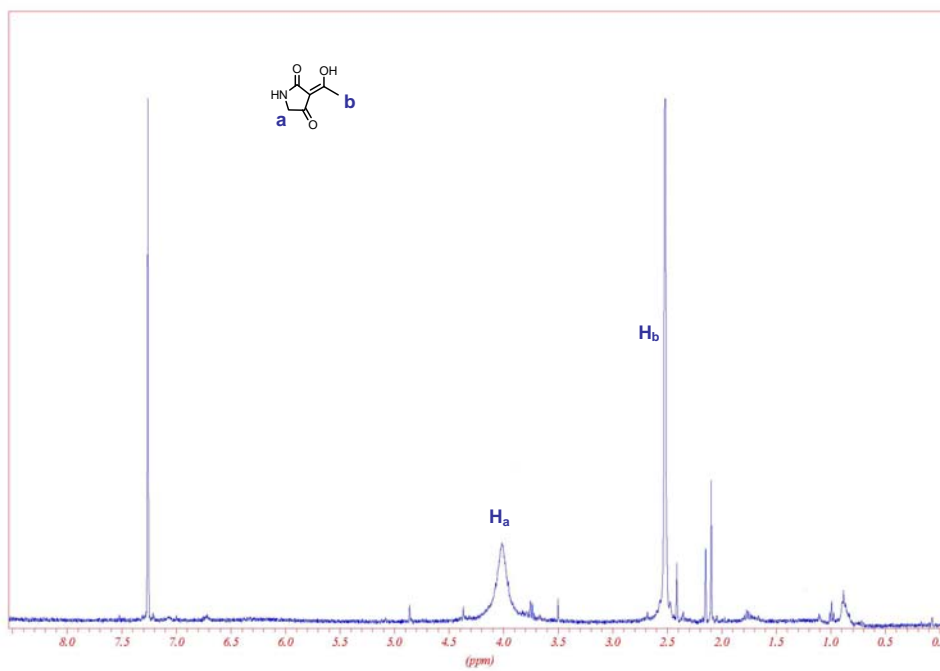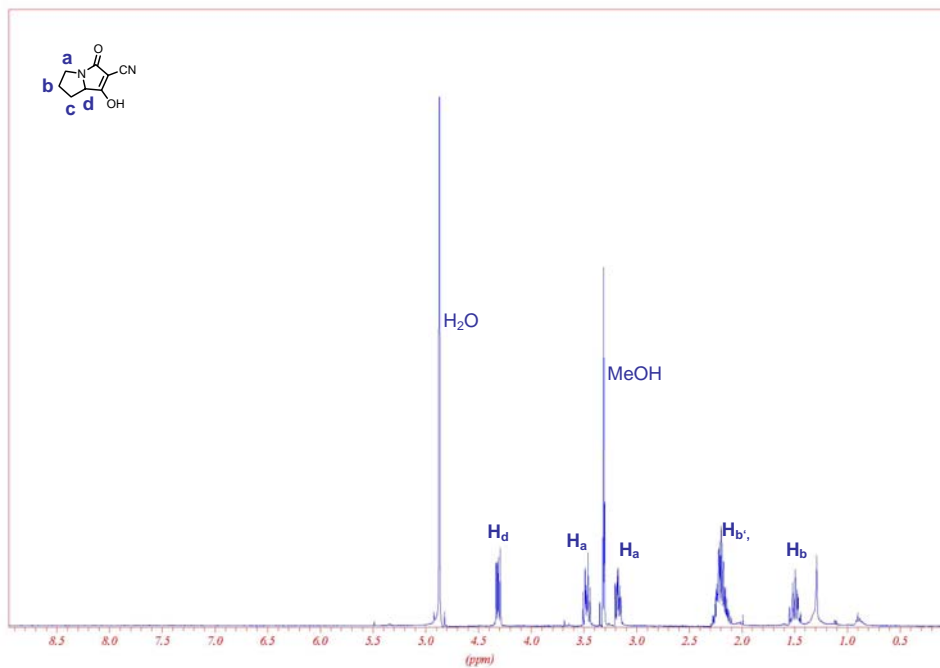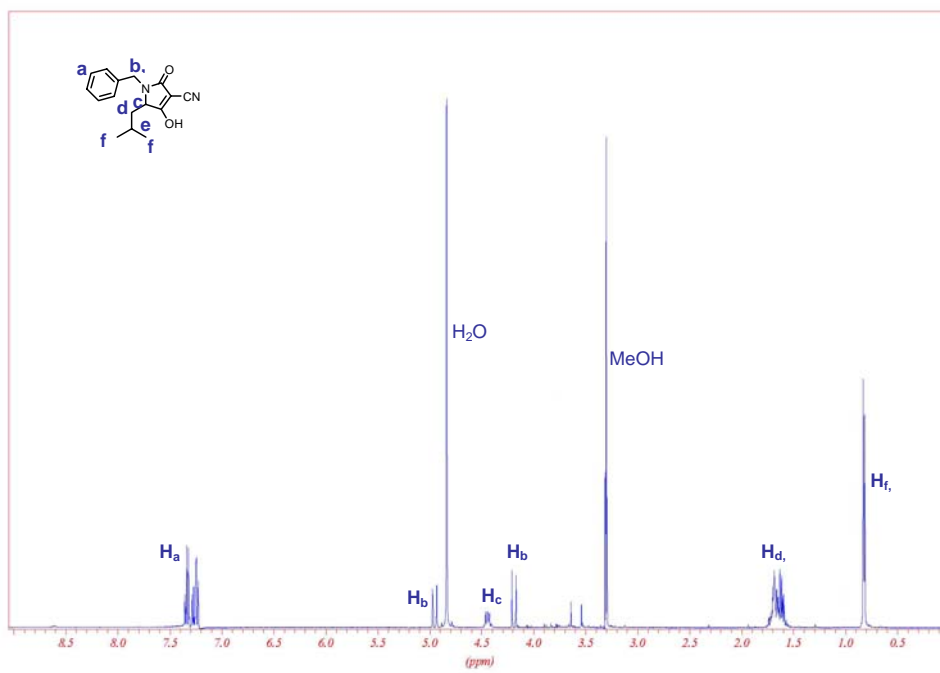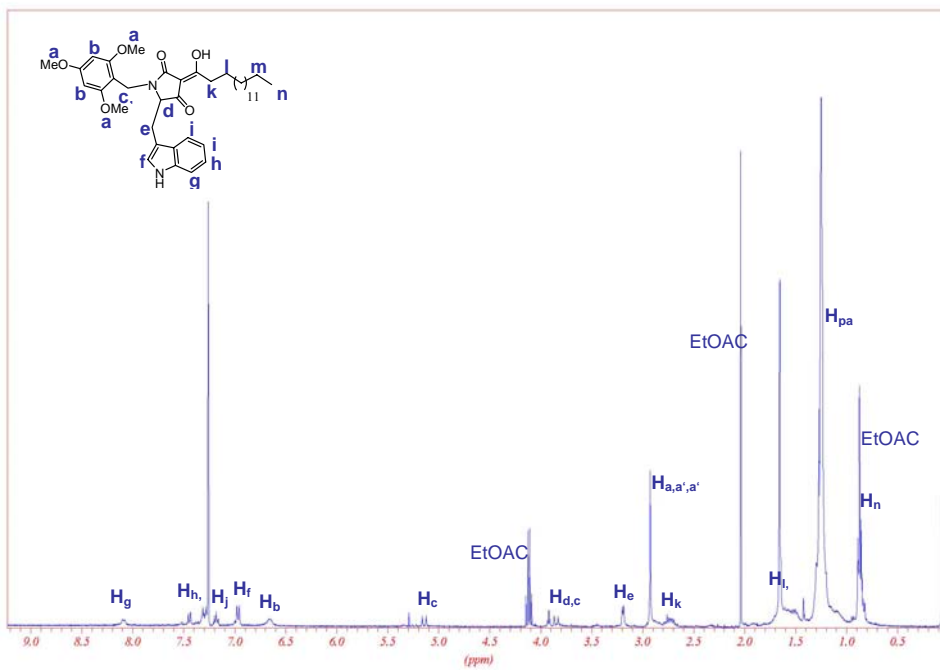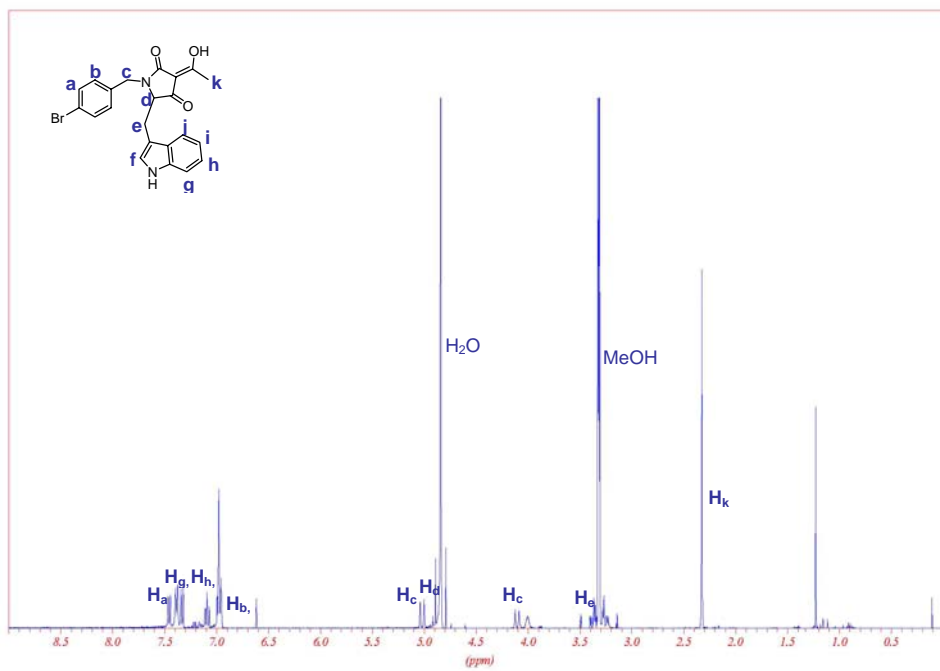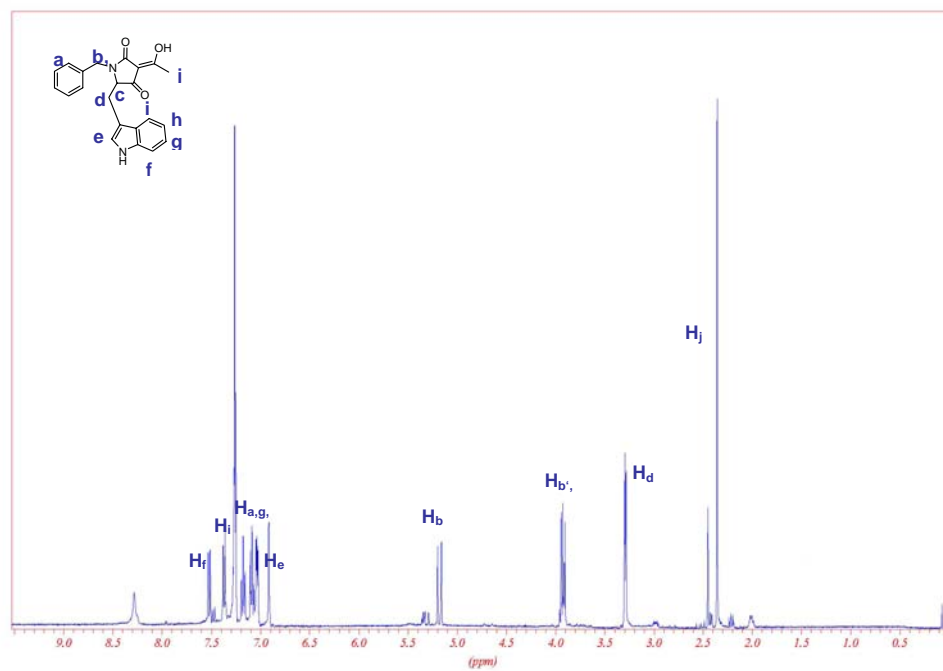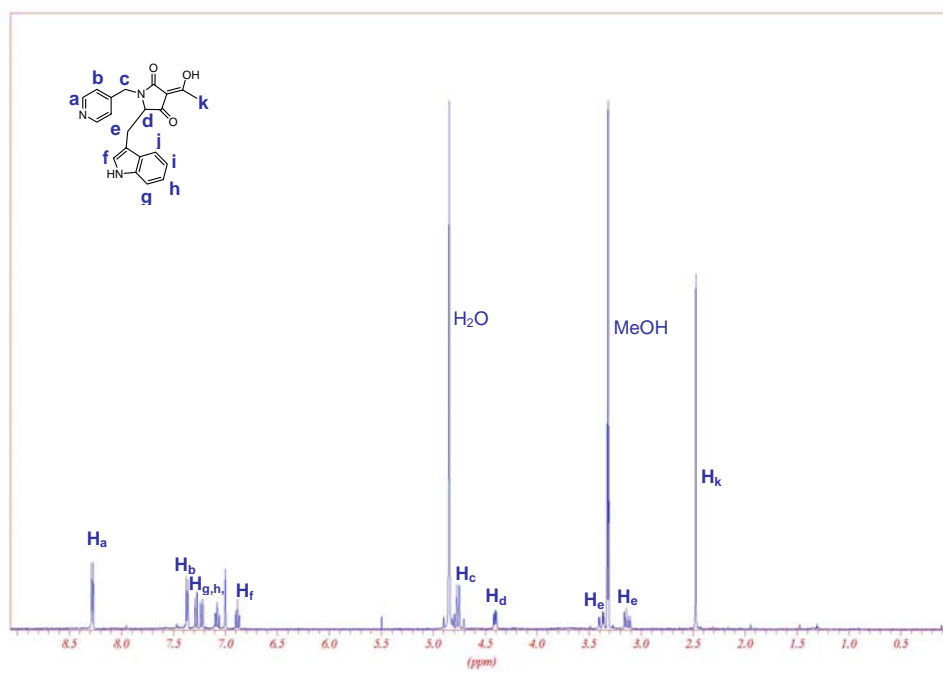
Zusammenfassung

der Dissertation von

Catherine P. Katzka

aus Mountain View, Californien

„Synthesis of Tetramic Acids and Investigation of
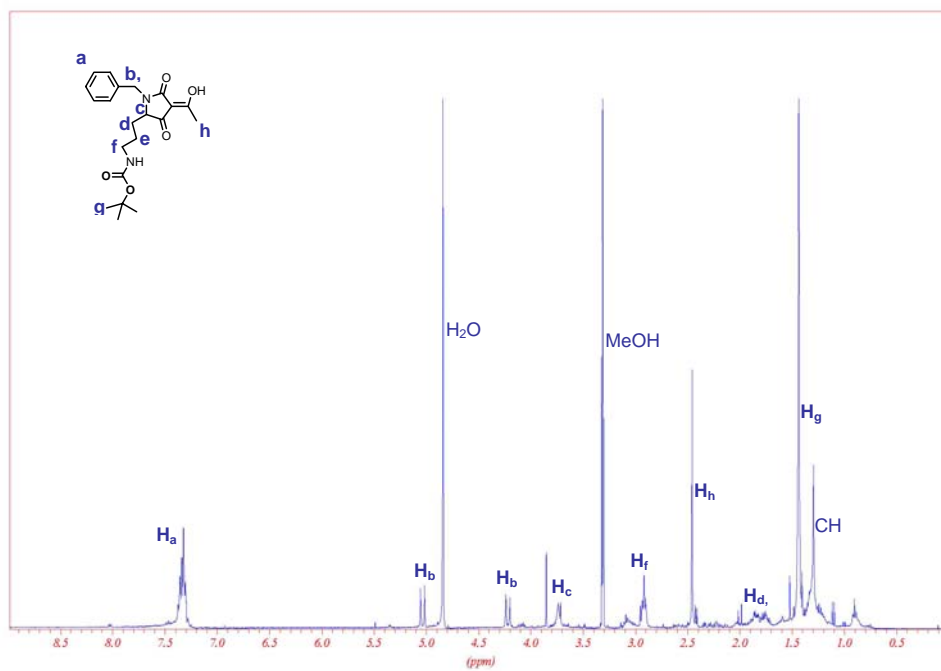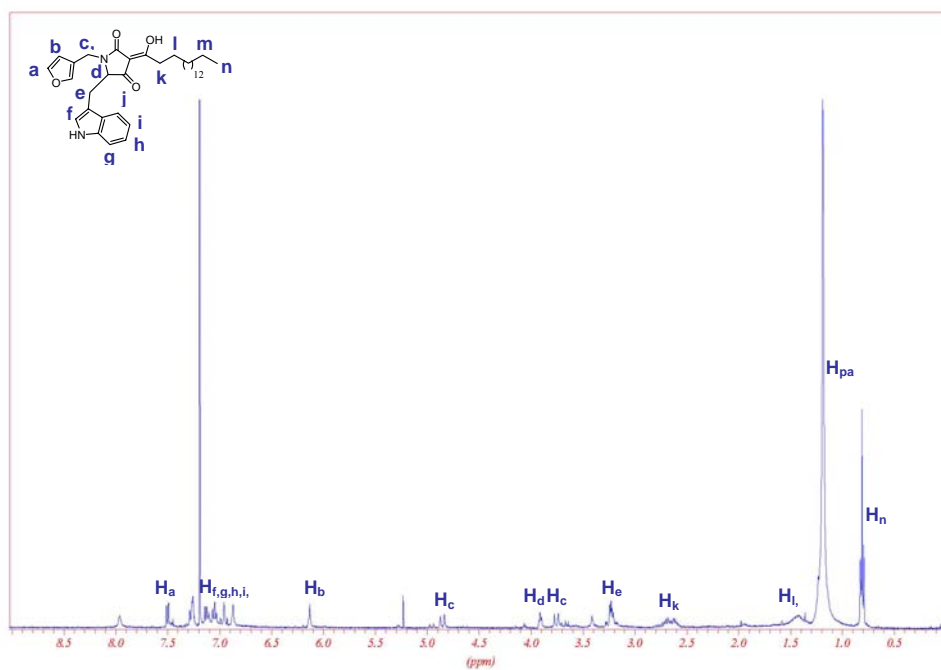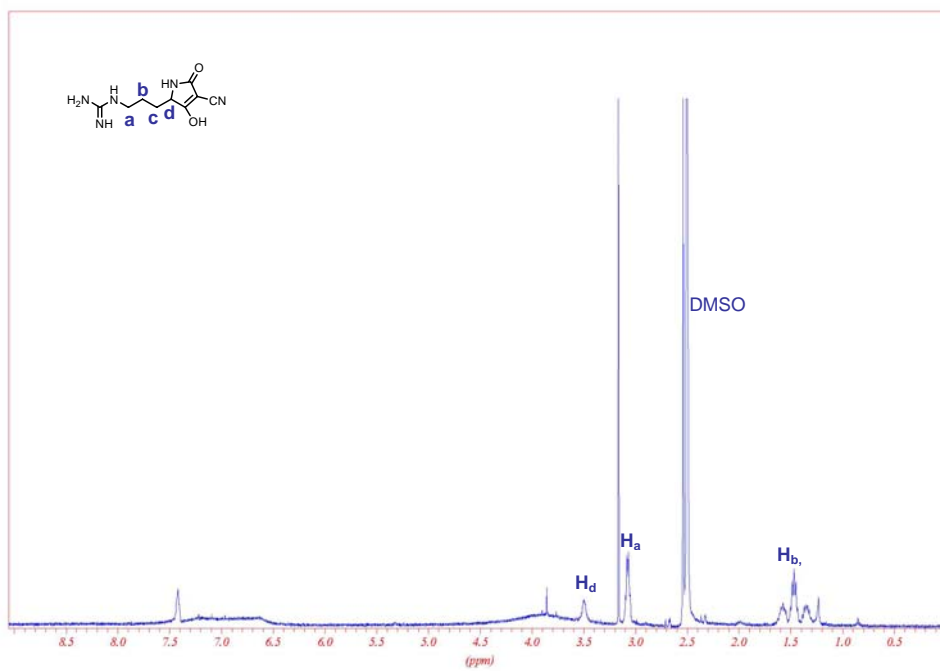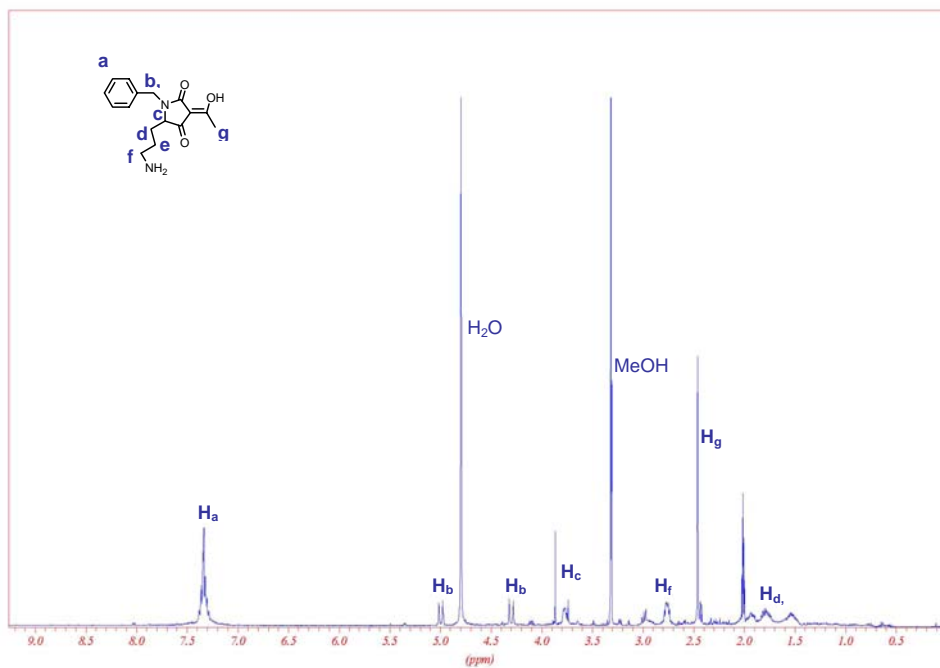
their Biological Properties"

Auf der Struktur der Tetramsäuren basierende Naturstoffe zeigen vielfältige biologische Aktivitäten.[1] Dies macht Pyrrolidin-2,4-dione (**1**, Abb.1) zu geeigneten Molekülen für die Synthese einer kleinen Substanzbibliothek und zur Untersuchung ihrer aktivierenden bzw. inhibierenden Eigenschaften in pharmazeutisch relevanten zellulären Signalwegen.
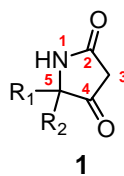
Abb. 1: Struktur der Pyrrolidin-2,4-dione (Tetramsäure) Einheit.

Im Rahmen dieser Dissertationsarbeit wurde eine kurze und effiziente Festphasensynthese zum Aufbau einer Tetramsäuren-Bibliothek entwickelt (Abb. 2). Der erste Schritt der Synthese ist die Beladung von Wang-Harz mit einer Fmoc-geschützten Aminosäure. Im Folgenden wird die Aminofunktion entschützt und das resultierende primäre Amin durch reduktive Alkylierung mit verschiedenen Aldehyden und Natriumtriacetoxyborhydrid alkyliert. Nach Acylierung mit einem β-Ketoäquivalent und Abspaltung unter basischen Bedingungen erhält man die gewünschte Tetramsäure.

_____ 139

Abb. 2: Exemplarische Festphasen-Synthese zur Darstellung von Tetramsäuren.

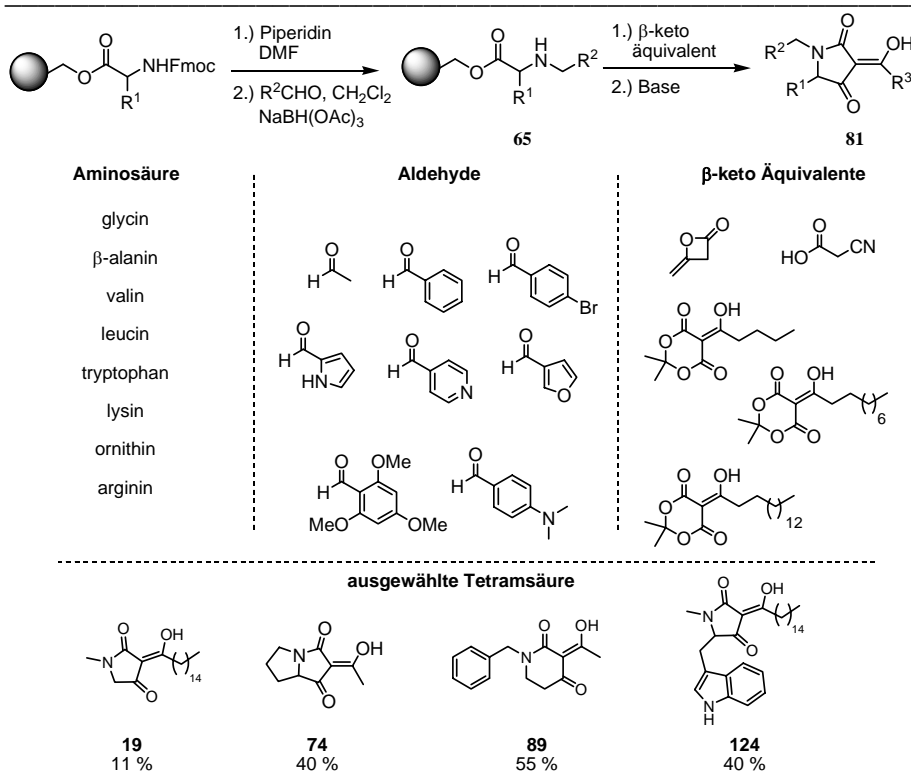In der Synthese wurden verschiedene Aminosäuren sowie Aldehyde und β-Ketoäquivalente eingesetzt. Die Synthesesequenz ermöglicht nicht nur die Darstellung von Pyrrolidin-2,4-dionen, sondern durch Einsatz von β-Alanin als Aminosäure auch die von Piperidin-2,4-dionen (**89**).

Des Weiteren ermöglicht der Einsatz von festphasengebundener Anthranilsäure den Zugang zu Quinolin-3-carboxamiden.

Weiterhin wurde die Synthesestrategie zur Darstellung des Naturstoffes Laccarin eingesetzt.

Um den Zugang zu Indol-basierten Tetramsäuren zu ermöglichen wurde eine Strategie zur Synthese von in Position sieben substituierten Tryptophanen aus Indol-Derivaten und Serin entwickelt. Die Indole wurden mittels einer Bartoli-Indolsynthese aus *o*-Nitroarenen und Vinyl-Grignardverbindungen hergestellt (Abb.3). Auf diesem Wege wurden insgesamt acht verschiedene Derivate mit Ausbeuten zwischen sechs und 61% erzeugt.
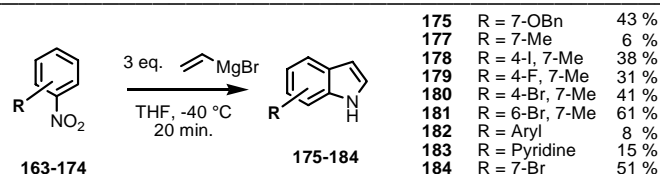
175	R = 7-OBn	43 %
177	R = 7-Me	6 %
178	R = 4-I, 7-Me	38 %
179	R = 4-F, 7-Me	31 %
180	R = 4-Br, 7-Me	41 %
181	R = 6-Br, 7-Me	61 %
182	R = Aryl	8 %
183	R = Pyridine	15 %
184	R = 7-Br	51 %

Reaktion: **163-174** + 3 eq. $\text{CH}_2\text{=CH-MgBr}$, THF, -40 °C, 20 min. → **175-184**

Abb. 3: Schematische Darstellung der Bartoli-Indolsynthese.

Die Synthese der Tryptophan-Analoga wurde durch eine biomimetische Reaktion aus Indol und Serin in Essigsäure mittels Essigsäureanhydrid realisiert (Abb. 4). So konnten sechs verschiedene Tryptophanderivate mit Ausbeuten zwischen sechs und 42% dargestellt werden.
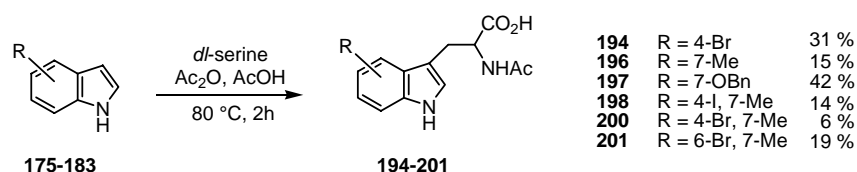
Reaktion: **175-183** + *dl*-serine, Ac_2O, AcOH, 80 °C, 2h → **194-201**

194	R = 4-Br	31 %
196	R = 7-Me	15 %
197	R = 7-OBn	42 %
198	R = 4-I, 7-Me	14 %
200	R = 4-Br, 7-Me	6 %
201	R = 6-Br, 7-Me	19 %

Abb. 4: Schematische Darstellung der Tryptophansynthese.

Zur Evaluierung ihrer biologischen Aktivität wurden die synthetisierten Tetramsäuren in verschiedenen biologischen Tests untersucht. Die Ergebnisse dieser Untersuchungen sind in Tabelle 1 zusammengefasst.

In der ersten Studie wurden die Tetramsäuren auf ihre Cytotoxizität sowie ihre Fähigkeit zur Rücktransformation der Morphologie von Ras-transformierten MDCK Zellen untersucht. In diesem zellbasierten Assay zeigten sich zwei Verbindungen, Melophlin A (**19**) und **110** in der Lage den Phänotyp der transformierten Zellen in den des Wildtyps zu revertieren. Diese Wirkung war für Melophlin A schon bekannt, [2] dennoch konnte sie für keines der synthetisierten Melophlin-Derivate gefunden werden. Weiterhin konnte gezeigt werden, dass diese Verbindungen ab einer Konzentration von 50 µM cytotoxisch sind.

Um die beobachteten Effekte besser verstehen zu können, wurden die Verbindungen in MAPK/PKC spezifischen Luciferase Reportergen-Assays untersucht. Hier zeigte sich, dass Melophlin A einen Abfall der Luciferase-Aktivität von 75% bei Aktivierung mit PMA und 54% nach Aktivierung mit EGF induziert. Dies könnte bedeuten, dass sich das makromolekulare Ziel von Melophlin A im Ras/MAPK Signalweg befindet. Dagegen konnte keine durch **110** induzierte Änderung der Luciferase-Aktivität festgestellt werden. Dies deutet an, dass die beobachtete Änderung im Phänotyp nach Behandlung der Zellen mit **110** nicht auf einer
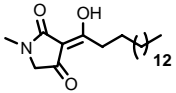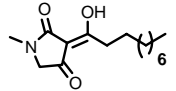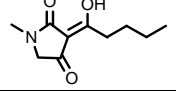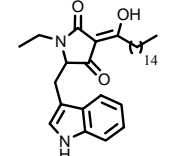
_____
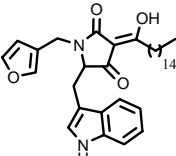
Inhibierung eines Proteins des Ras/MAPK-Signalwegs beruht. Zur Aufklärung könnte es helfen mittels eines biotinylierten Moleküls **110** die Zielproteine zu isolieren und deren Wirkmechanismus zu untersuchen.

Des Weiteren wurde die Aktivität der Tetramsäuren in Phosphatase-Assays untersucht. Hier zeigten sich fünf Tetramsäuren (**125**, **127**, **122**, **118** und **19**) mäßig aktiv gegen MTP1B, PTP1B und Cdc25A. Es wurde beobachtet, dass eine lange Lipidseitenkette ein wichtiges Strukturelement für die Aktivität in den Phosphatase-Assays ist. Die Tryptophan-basierten Tetramsäuren zeigen selektive Inh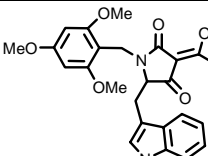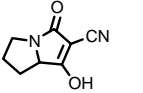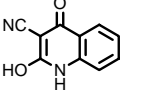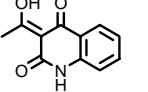ibierung der PTPs. Für die weitere Untersuchung wurden erste Berechnungen zur Energieminimierung der Wechselwirkungen zwischen Wirksubstanz und Kinase durchgeführt.

Als letztes wurde getestet, ob die Tetramsäuren Aktivität in antibakteriellen Assays gegen Gram-positive und Gram–negative Bakterien zeigen. Einige der getesteten Substanzen inhibieren das Wachstum Gram-positiver Bakterien (siehe Tabelle 1), während kein Einfluss auf Gram-negative Bakterien beobachtet werden konnte. Diese Ergebnisse unterstützen die vom Arbeitskreis Janda veröffentlichte Hypothese,[3] dass Tetramsäuren Quorumsensoren sind. Vier der getesteten Verbindungen zeigten sich als mäßig aktiv gegen Gram-positive Bakterien und könnten somit für die Isolierung von Zielproteinen und die Untersuchung des Wirkmechanismus genutzt werden.

Tabelle 1: Zusammenfassung der Ergebnisse der biologischen Untersuchungen von Tetramsäuren.

Struktur	Nr.	Phänotypische Assay	WST-1 Assay	Phosphatase Assay	Anti-Bakterielle Assay
	19	**Rück-transformation**	**toxisch**	**Cdc25A: 60 µM** **PTP1B: 37 µM** **MptpB: 83 µM**	kein Effekt
	119	kein Effekt	**toxisch**	n.d.	**B.Subtilisis (70 mg/l)**
	118	kein Effekt	**toxisch**	**Cdc25A: 92 µM**	**B.Subtilisis (>250 mg/l)**
	125	kein Effekt	nicht toxisch	**MptpB: 93 µM**	kein Effekt
	127	kein Effekt	nicht toxisch	**Cdc25A: 95 µM** **PTP1B: 10 µM** **MptpB: 68 µM**	kein Effekt
	122	kein Effekt	nicht toxisch	**MptpB: 70 µM**	kein Effekt
	111	kein Effekt	nicht toxisch	MptpB: >100 µM	**B.subtilisis (>250 mg/l)**
	110	**Rück-transformation**	nicht toxisch	MptpB: >100 µM	kein Effekt
	81	kein Effekt	nicht toxisch	Cdc25A:>100 µM	**B.Subtilisis (MIC n.d.)**

Referenzen

[1.] B. Royles, _Chem.Rev._ **1996,** _95_, 1981-2001.

[2.] S. Aoki, K. Higuchi, Y. Ye, R. Satari, M. Kobayashi, _Tetrahedron.Lett._ **2000,** _56_, 1833-1836.

[3.] G. F. Kaufmann, R. Sartorio, S. H. Lee, C. Rogers, M. M. Meijler, J. A. Moss, B. Clapham, A. P. Brogan, T. J. Dickserson, K. D. Janda, _Proc.Natl.Acad.Sci.USA_ **2005,** _102_, 309-314.

Acknowledgements

I would like to thank Prof. Dr. Herbert Waldmann for his support and constructive guidance and for providing all the necessary tools for the development of this work.

I wish to express my gratitude to Sandra Eichhorn, C. Vorneweg for measuring mass spectra, Dr. P. Janning for most helpful assistance in maintaining and fixing essential instruments, H. Rimpel and PD. Dr. H. Prinz for running the phosphatase assays.

Thousands of thanks go to Dirk Pendzialek, Sascha Menninger, Bernhard Ellinger, Annette Langerak and PD. Dr. O. Müller who demonstrated unbelievable patience while teaching me the essentials of cell biology and were great partners in stimulating discussions. Many thanks to Stefan Wetzel for performing the molecular modeling experiments.

I benefited from a set of great lab colleagues: Drs. Michael Scheck and Michael Manger were responsible for teaching me the basics of Badisch; Nicola Bisek, Drs. Claudia Rosenbaum and Maria Lumbierres were responsible for assuring that I still speak Hochdeutsch, if not Pott and for insuperable support; Tobias Voigt was responsible for finding the Achilles heel(s) of any instrument (and of course fixing the problem) and providing musical entertainment; Matthias 'Pommes' Riedrich and Torben 'Turtle' Lessmann (the usual suspects) for always lending an ear and making sure that the day ends with a light head and a few laughs. I would also like to particularly thank Claudia Seifert for skillful assistance in the laboratory. Many thanks to all of my colleagues, that are too numerous and dear to be all mentioned here, who have contributed less directly but not less vitally to this thesis.

I am especially grateful to Nicola Bisek, Torben Lessmann, Matthias Riedrich, Drs. Rolf-Peter Breinbauer, Daniel Gottlieb, and Swen Hölder for their proof-reading and for the critical discussions and suggestions over the *nth* version of this manuscript.

Finally, I especially grateful for the unconditional support from my family, far and close.

_____

Curriculum Vitae

Name: Catherine Pravinee Katzka

Date of Birth: 07.02.1977

Place of Birth: Mountain View, California

Nationalities: French, U.S. American

Education

09/1981 – 06/1987   École Franco-Américaine de la Péninsule, Palo Alto, California

09/1987 – 06/1994   Lycée Francais International Lapérouse, San Francisco, California

06/1994   High School Diploma: Baccalauréat, Série A1

University Education

01/1995 – 12/1999   University of California, Berkeley, Major in Chemistry

12/1999   Bachelor of Science, Chemistry

01/2000 – 01/2002   Universität Dortmund, Diploma studies in Chemistry

06/2001 – 01/2002   Diploma thesis under the supervision of Prof. Dr. H. Waldmann, Max Planck Institute of Molecular Physiology, Dortmund, on the „Synthesis of modified, lipidated N-Ras C-terminus Peptides"

01/2002   Diploma, Chemistry

02/2002 – 06/2006   Ph.D. thesis under the supervision of Prof. Dr. H. Waldmann, Max Planck Institute of Molecular Physiology, Dortmund, on the „Synthesis of Tetramic Acids and Investigation of their Biological Activities"

Dortmund, May 2006

_____